2004

Geochemical evolution of flooding mine waters in a zoned sulfide -hosted ore deposit Summit Valley mining district Butte Montana

John J. Metesh
The University of Montana

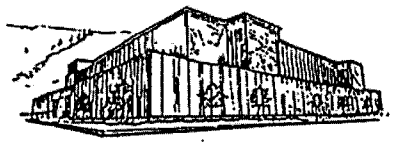

GEOCHEMICAL EVOLUTION OF FLOODING MINE WATERS IN A ZONED, SULFIDE-HOSTED ORE DEPOSIT, SUMMIT VALLEY MINING DISTRICT, BUTTE, MONTANA

by

John J. Metesh

B.S. Montana State University, 1986

M.S. Montana College of Mineral Science and Technology, 1990

presented in partial fulfilment of the requirements

for the degree of

Doctorate of Philosophy

The University of Montana

December, 2003

Approved by:

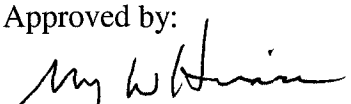

Chair

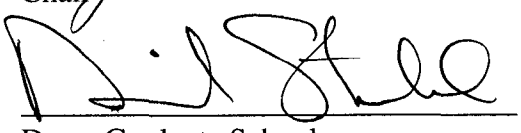

Dean, Graduate School

5-26-04

Date

Metesh, John J., Ph.D., December 2003 Geology

Geochemical evolution of flooding mine waters in a zoned, sulfide-hosted ore deposit, Summit Valley Mining District, Butte, Montana

Director: Nancy W. Hinman

The chemistry of ground water is a function of several variables including the composition of the recharge water, the hydrogeologic properties of the aquifer, and the mineralogic composition of the aquifer material. The chemistry of water depends, in part, on the history of that water; each component of the hydrologic cycle imparts a change, permanent or temporary, on the chemistry and is carried with the water as it moves through the hydrologic cycle. This study evaluates the evolution of water chemistry through a zoned sulfide deposit. Atmospheric oxygen and carbon dioxide provide the source and sink for near-surface waters and mineral assemblages for various components of the sulfide deposit. Each of the four groups of minerals (sulfides, alteration minerals, secondary minerals, and carbonate minerals) interact with water with varying degrees as influence by other processes such as oxidation/reduction, buffering, dissolution, and precipitation. While it is possible to determine the concentration and nature of complexes through analytical techniques, the large number of complex species makes it impractical, particularly at low concentrations. Geochemical modeling provides a means of accounting for the dominant species possible for most solutions.

This investigation considered the influence of local mineralogy, mine geometry, and the mine-flooding water-balance to evaluate the variation in water chemistry within the mines of the Summit Valley mining district in Butte, Montana. The mines in this are have been active at various times over the past 130 years; underground mining ceased in 1982 and ground water was allowed to flood the workings; water levels in the workings are still rising at present. Each mine, and in some cases, each set of workings within the zoned porphyry-copper orebody has unique mineralogy. Mineralogic information was examined to construct a general model of mineral assemblages for each mine. Detailed maps of the underground workings were used to determine mine volumes, connections between mines, and to give weight to the potential influence of minerals from difference parts of the mine. The mine geometry and its position in the flooding system were used to identify potential sources and the likely chemistry of water entering each mine. Mines that represented different positions within the ore body and for which sufficient information could be obtained where selected to construct the models.

The results of the geochemical modeling were used to determine flow paths during the early and late period of flooding as well as identify sources of water entering the underground workings. The early period of flooding was marked by a considerable volume of surface water entering the workings via a nearby open pit. The source of this water, an acid leaching operation, was identified through modeling the mass balance of iron and copper in the receiving waters. The evolution of water chemistry became more stable and predictable after the initial effects of this surface water and flow paths were identified through geochemical modeling.

Table of Contents

List of Figures iv

List of Tables vi

List of Minerals vii

Introduction 1
Geochemical evolution of ground water 1
Modeling geochemical evolution 8
Limitations of Geochemical Models 11
Summit Valley Mining District 12
Hypothesis Statement 21
Experimental Approach 22
Equilibrium modeling 23
Model Calibration and Uncertainty 26
Sequence of Geochemical Modeling 27

Travona mine 30
Background 30
Mineralogy 34
Water quality 34
Equilibrium Modeling: Travona Shaft 35
Early Flooding (1984 to 1986) 37
Period of 1st Transition (1986 - 1987) 42
Period of 2nd Transition (1987 to present) 48

Summary of Travona Mine 48

Anselmo Mine 49
Background 49
Mineralogy 50
Water Quality 53
Equilibrium Modeling - Anselmo shaft 55
Oxidation of chalcopyrite and sphalerite 59

Summary of Anslemo mine 69

Steward and Kelley mines 70
Background 70
Mineralogy 72
Mine-flooding Water-balance 75

Summary of water balance 86
Water Quality 89
Equilibrium Modeling - Kelley shaft 99
Equilibrium Modeling of the Steward - Kelley system 103

Summary of the Steward - Kelley mines 110

Summary and Conclusions 112

References 117

Appendix I: Bioassay of Selected Mine shafts in the Butte area 125

Appendix II: Annotated listing of model input files for Travona simulations 129

Appendix III: Annotated listing of model input files for Anselmo simulations 135

Appendix IV: Annotated listing of model input files for Kelley simulations 144

List of Figures

Figure 1. The hydrologic cycle 2
Figure 2. Geochemical evolution in a mine environment 7
Figure 3. Butte area map of mining features 13
Figure 4. Mineral zones of the Summit Valley mining district 16
Figure 5. Potentiometric map of the flooding mines 29
Figure 6. West Camp workings 31
Figure 7. Travona hydrograph 33
Figure 8. Travona chemistry 36
Figure 9. Oxidation model results 39
Figure 10. Modeling results for Travona simulation 41
Figure 11. Iron concentrations related to water level 43
Figure 12. Solubility of iron versus H_2S 44
Figure 13. Solubility of zinc versus H_2S 44
Figure 14. Comparison of model data and sample data for the Travona shaft. 47
Figure 15. Anselmo mine workings 51

Figure 16. Anselmo hydrograph 52
Figure 17. Anselmo water quality 54
Figure 18. Comparison of model data with sample data from the Anselmo shaft. 58
Figure 19. Modeling results with high CO_2 60
Figure 20. Modeling results with low CO_2 61
Figure 21. Comparison of mixing model data with Anselmo shaft data. 66
Figure 22. Comparison of the equilibration model results with Anselmo shaft data. . . . 68
Figure 23. Mine workings of the East Camp. 71
Figure 24. Cross-section of mineral zones 74
Figure 25. Map of features related to mine flooding 76
Figure 26. Hydrograph for the Kelley shaft 78
Figure 27. Volume of mine workings with depth 82
Figure 28. Water-level differences in the East Camp mines 87
Figure 29. Connections between mines of the East Camp. 88
Figure 30. Total iron and iron-speciation for the Kelley shaft 90
Figure 31. Copper concentrations for the Kelley and Belmont shafts. 92
Figure 32. Zinc concentrations for the Kelley and Belmont shafts 93
Figure 33. Iron and zinc concentrations for the Steward shaft 94
Figure 34. MBMG data for the East Camp shafts 97
Figure 35. MBMG data for the East Camp shafts 98
Figure 36. Mixing model results compared to 1983 data for the Kelley shaft. 101
Figure 37. Molal concentrations for the Anselmo, Steward, and Kelley shafts 102
Figure 38. Comparison of Steward shaft sample data to model results. 106
Figure 39. Comparison of shallow and deep water quality in the Kelley shaft 107
Figure 40. Comparison of Kelley shaft sample (1997) data to model results. 109
Figure 41. Conceptual model for the early period of flooding 113
Figure 42. Conceptual model for the later period of flooding 116

List of Tables

Table 1. Examples of surface-water chemistry 1
Table 2. Mineral phases used in the Travona simulation 35
Table 3. Comparison of model results with sample collected in the early period of flooding (1984) of the Travona shaft 40
Table 4. Comparison of model results to a sample collected in mid-1987 from the Travona shaft 46
Table 5. Mineral phases used in the Anselmo simulation 55
Table 6. Comparison of model results with sample collected in the early period of flooding (1984) of the Anselmo shaft 57
Table 7. Oxidation of chalcopyrite and sphalerite at various concentrations of CO_2 and O_2 62
Table 8. Results of mixing deep and shallow waters compared to data from the Anselmo shaft 65
Table 9. Results of deep waters equilibrated with shallow minerals in the Anselmo shaft 67
Table 10. Annual cumulative volumes for the Berkeley Pit 81
Table 11. Water balance for the period from 1984 to 2000. 83
Table 12. A comparison of the mixing model with sample results from the Kelley shaft 100
Table 13. Mineral phases used in the Steward simulation 103
Table 14. Comparison of Steward shaft sample data to model results 104
Table 15. Comparison of Kelley shaft sample data to model results 108
Table 16. Bacteria counts for mines shafts in the Butte area 126
Table 17. Identified species and locations 127

List of Minerals

arsenolite	As_2O_3
bornite	Cu_5FeS_4
chalcocite	Cu_2S
chalcopyrite	$CuFeS_2$
covellite	CuS
cryptomelane	KMn_8O_{16}
goslarite	$ZnSO_4 : 7H_2O$
greenockite	CdS
kaolinite	$Al_2Si_2O_5(OH)_4$
montmorillonite	$(Al,Mg)_8(Si_4O_{10})_3(OH)_{10} - 12H_2O$
muscovite	$KAl_2(AlSi_3O_{10})(OH)_2$
pyrite	FeS_2
pyrolusite	MnO_2
quartz	SiO_2
rhodochrosite	$MnCO_3$
sphalerite	ZnS

Introduction

Geochemical evolution of ground water

The natural hydrologic cycle is comprised of transfers between water reserviors such as precipitation, continental surface water, soil water, ground water, and ocean water (figure 1). The physical characteristics (solid, liquid, or vapor) of natural water depends on its position in the hydrologic cycle. Processes such as precipitation, evaporation, or transpiration transfer water between reservoirs. The chemistry of water depends, in part, on the history of that water; reactions between water, gases, geologic, and biological materials impart chemical changes, permanent or temporary, in the water.

The chemistry of ground water is a function of several variables including 1) the composition of the *recharge water*, 2) the *hydrogeologic properties* of the aquifer, and 3) the *mineralogic composition* of the aquifer material.

Recharge waters, either precipitation, storm or snow-melt runoff, or surface water exhibit a wide variation in chemistry; table 1 provides some examples of the range of concentrations of several constituents.

Table 1. Examples of water chemistry for rain water, river water, and storm runoff water (all values are μg/L) .

Constituent	Global mean rain[1]	Kalyan, India rain water [2]	Mississippi River[3]	Baseflow/stormflow for Shoshone River[3]
Na	1,976	3,400	20,000	5,300 / 5,600
K	312	390	2,900	640 / 710
Mg	291	580	1,000	1,540 / 1,580
Ca	80	2,600	38,000	4,900 / 5,000
Cl	3,793	4,750	24,000	not reported
SO_4	193	5,300	51,000	not reported

(1: after Languir, 1997, p. 278; 2: Naik and others, 2002; 3: after Hem, 1992, p. 9; 3: after Drever, 1997, p. 267)

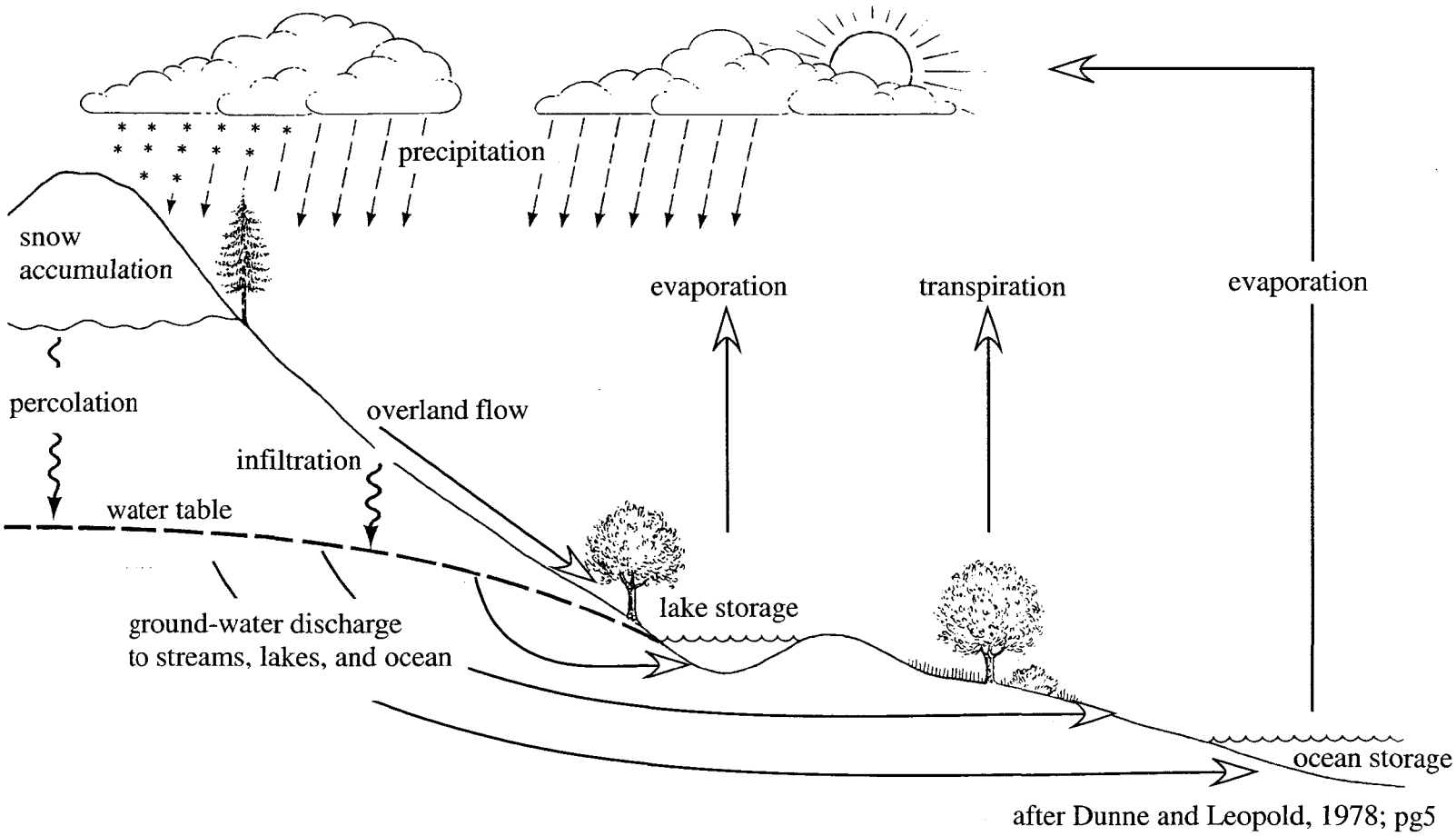

Figure 1. The natural hydrologic cycle.

It has long been recognized that organic and inorganic constituents are most often introduced in the local rainwater (Naik, 2002) or at the ground surface and entrained in the ground-water recharge.

Ground-water flow velocity is a function of *hydrogeologic properties* including hydraulic conductivity, porosity, and gradient; these properties determine the residence time or the duration of time in which the water is in contact with the aquifer material. The higher the flow velocity, the lower the residence time and the less rock-water interaction; the water has less time in which to interact with the aquifer material to dissolve or precipitate solids. Ground-water residence times range from a few days to more than 10,000 years (Clark and Fritz, 1997).

The *mineralogic composition* of the aquifer material constrains the chemical character of the water. The weathering rate and weathering products of the aquifer material impart a predictable quality to the water. Distinctive rock types (igneous, sedimentary, and metamorphic) produce distinctive water quality (Hem,1992). Although generalizations may be made between lithology and water quality, a precise prediction of the concentration of a given constituent requires knowledge of the potential geochemical processes at a scale commensurate with the size of the ground-water flow system. In addition, there are two general types of geochemical processes: 1) reversible reactions or reactions with high reaction rates relative to the ground-water flow velocity, and 2) irreversible reactions or reactions with low reaction rates relative to the ground-water flow velocity (Rubin, 1983).

Regional-scale investigations of geochemical evolution of ground water rely most often on the chemistry of major cations and anions. The complexity of the conceptual models depends, of course, on the number and type of rocks with which the ground water interacts. Large aquifers with a single or few similar lithologic units may exhibit a predictable change in chemistry along flow paths of many miles (Downey,1984) . Geochemical evolution of ground water in flow systems that are relatively simple with respect to flow path, lithology, and hydrologic properties can be described by simple mass action relationships. These investigations rely on irreversible reactions or slow reaction

rates combined with very long flow paths; as such, mass-action relationships are used to describe the change in ground-water chemistry from a surface source of contamination (Kelley, 1997) or by distinctive changes in lithology along the ground-water flow path Palmer and Cherry, 1984). The complexity of the model increases and the precision decreases as more lithologic units are considered; studies related to large regional aquifer systems (Gosselin and others, 2001, Eberts and George, 2000; MacFarlane and others, 1990) must rely on large differences in the concentration of a few constituents and can only make generalizations as to recharge sources and travel paths. Most often, the dominant water type is mapped to identify areas of similar water type in the hopes of identifying recharge areas and flow paths. Typically, sulfate-dominant waters are distinguished from bicarbonate-dominant waters and further classified based on the relative dominance of calcium, sodium, or magnesium. The dominant water type is compared to the likely lithologic unit from which the water originated. For example, calcium-magnesium sulfate waters are attributed to dolomite or calcite (Eberts and George, 2000). Sodium enrichment is attributed to interaction of ground water and clay minerals. Gosselin and others (2001) identified sources of ground water in the Dakota Aquifer to evaluate the potential impacts of ground-water extraction on a regional scale. The main focus of the investigation was to determine the final chemistry in a portion of a large aquifer where ground waters of two different chemistries mixed. A similar approach is used to describe the chemistry of water along the flow path from the ground-water recharge area to deep anoxic conditions under hydraulic gradients induced by mining of the aquifer (coal) or large-scale pumping of ground water (Clark, 1995; Davis,1984). Reconstructing the flow path from the recharge area to the point of observation relies on evaluating the geochemical processes within each lithologic unit and the ability to identify characteristics unique to each. Once accomplished, the proper order or most likely flow path through the various lithologic units can be described (Palmer and Cherry, 1984).

Although, geochemical processes and chemical reactions are certainly independent of scale, the ability to observe the contribution of a particular geochemical

process is dependent on scale. As the scale of observation becomes smaller, the number and complexity of geochemical processes becomes greater. Investigations of geochemical evolution in smaller, local aquifers present a different challenge where chemical processes, particularly the rates of chemical reactions relative to residence time, influence the observed water quality. The geochemical process is dominated by reversible reactions and/or reactions with high rates. The flow path is much shorter and consequently, the residence time may to short to allow chemical equilibrium; or, to put another way, the reaction rates involving the constituents of interest are too slow to achieve equilibrium. This is especially true for the evaluation of contaminated water generated by the interaction between solid/liquid waste material and ground water or surface water. Whether organic or inorganic, the rate of weathering/dissolution, subsequent reactions, oxidation/reduction, and precipitation of new solids controls the concentrations of constituents throughout the travel path of the contaminated water. Contaminants introduced at the surface or ground-water recharge area are common; the evolution of even the simplest contaminant, nitrate for example, can be observed along the ground-water flow path (Kelley, 1997). Many geochemical processes largely ignored in studies of regional aquifers are critical at the local scale. Ritchie (1994) lists several parameters critical to the evaluation of contaminant generation from a sulfidic waste pile; in addition to the characteristics of the waste material, oxygen diffusion rates, oxidation rates, mass of oxygen consumed, and bulk density are important components of the conceptual model. As with the regional-scale studies, multiple layers of distinguishable physical and mineralogical characteristics can greatly affect the final chemistry even at the small scale of a waste pile (Hartog and others, 2002), a shallow aquifer downgradient of a contamination source (Kent and others, 1987), or underground openings (Gi-Tak and others, 2001; Capo and others, 2001).

In essence, gross mineralogic information and mass action equations may suffice for describing large-scale, regional ground-water flow systems using major cation- and anion-concentrations. Describing smaller scale, local ground-water flow systems requires detailed information commensurate with the scale and the geochemical processes that

dominate that system. Ground-water flow systems comprised of layers or zones of distinct mineralogy favor a unique solution about the direction, length, and chemical characteristics of the flow path.

Figure 2 presents a summary of the general geochemical processes in a zoned sulfide deposit. Carbon dioxide and oxygen dissolve or exsolve near the air - water interface based on partial pressures in the atmosphere immediately above the water and on chemical reactions in the water. Each of the four groups of minerals interact with water with varying degrees as influence by other processes such as oxidation/reduction, buffering, dissolution, and precipitation. Dissolution reactions of sulfide and aluminosilicate minerals generally have slow reaction rates under near surface, low-temperature conditions; the reactions are most commonly irreversible. Secondary minerals that precipitate in one part of the flow path may re-dissolve as conditions change or as the water moves through another layer or mineral zone; the reactions are commonly reversible. Primary carbonate minerals are most often dissolved irreversibly; precipitation and subsequent dissolution of secondary carbonate minerals is also common.

The physical scale of figure 2 is largely independent of the geochemical processes; the zone of mixing and/or equilibration can be the pore space in a waste dump, a mine opening, or a tailings impoundment. The number of individual minerals in each group can be numerous and each contributes to the final water chemistry depending on the conditions present. Moreover, chemical processes (precipitation/dissolution, oxidation/reduction) and properties (pH, redox) determine number and nature of complexes, as well as adsorption and cation exchange. While it is possible to determine the identity and concentration of complexes through analytical techniques, the large number of aqueous species makes it impractical, particularly for those complexes in low concentrations. Geochemical modeling provides a means of accounting for the likely dominant species produced during the geochemical evolution of ground water.

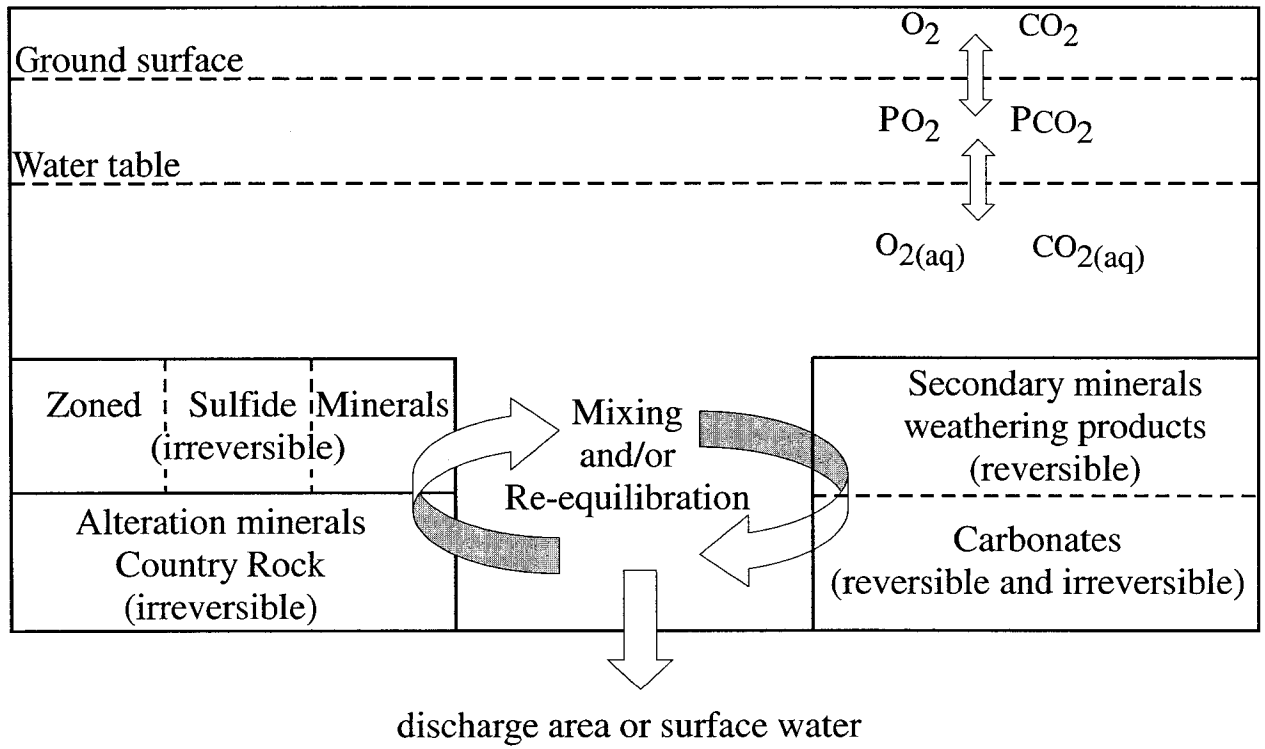

Figure 2. Geochemical evolution in a mine environment includes sulfides, country rock, secondary minerals, and carbonates. Some reactions are reversible while others irreversible. The chemistry of water along any flow path is determined, in part, on its relationship with the ore body.

Modeling geochemical evolution

The term "geochemical model" has come to mean either a conceptual model of geochemical processes such as that presented in figure 2 or a computer code designed to calculate the type and concentration of constituents within the conceptual model; the distinction is most often made in the context. Herein, geochemical modeling follows the latter definition. Modeling geochemical systems was introduced as early as 1962 to determine the chemical species in seawater (Garrels and Thompson, 1962). The introduction of computer-generated calculations led to a plethora of models in the 1980's. Later efforts were focused on the development of thermodynamic databases and computer-code improvement (Bassett and Melchior, 1990). There are generally three types of geochemical models: 1) *speciation* 2) *mass balance*, and 3) *mass transfer* or reaction path models (Bassett and Melchior,1990; Langmuir, 1997, p. 558); and most operate on the assumption that all chemical constituents in an aqueous solution exist as free ions or as complexes. Chemical *speciation* models calculate the equilibrium activities of components and complexes in solution. Most models of this type include the distribution of the components and complexes in solid, aqueous, and gas phases. *Speciation* models assume that the modeled system is in equilibrium and rely on a database of thermodynamic properties of a fixed number of species. *Mass balance* models are used to define the net mass of solid, aqueous, or gas that is dissolved or precipitated under specified, equilibrium conditions. Speciation models are commonly coupled with mass balance and *mass transfer* models to determine the species resulting from dissolution/precipitation reactions, gas exchange/reactions, ion exchange/adsorption, and mixing. As noted, geochemical models are constrained by the completeness and inclusiveness of the thermodynamic database on which the calculations rely. The type, number, and thermodynamic constants for mineral/solid phases, chemical/redox equilibrium reactions, and species vary between databases and thermodynamic data for new minerals and complexes are published often (for example, Hemingway and others, 2002). The almost constant expansion of the databases and improvement of the computer codes has led to wide application of the geochemical

models. Although most include all three of the aforementioned types, some models expand concepts related to multiple reservoirs for mixing or equilibration (Choi and others, 2000), kinetically controlled reactions (Friedly and Rubin, 1992), and three-dimensional transport reactions (Goode and Konicow, 1991; Rubin, 1992). Geochemical models have been integral to geochemical evolution studies and enable modeling of complex ground-water flow systems.

The scale independence of computer-based models lends itself well to the scale dependence of studies related to geochemical evolution. That is, the models calculate activities, molalities, and partial pressures suitable for consideration in either regional-scale geochemical systems or within the pore space of a waste dump. In any case, assuming proper selection of the model code, the limitations lie with the detail of information with which to compare model results and data. As with the application of basic geochemical concepts to geochemical evolution studies, the application of geochemical models reflects the scale. In a manner that reflects the scale of geochemical evolution, the application of geochemical models can be grouped as either *regional-scale models* or *local-scale models*. The advances in both analytical chemistry and computers have prompted considerable work at the mineralogic scale.

Geochemical models, particularly those using mass balance and mass transfer, are widely used in regional-scale studies. *Regional-scale models* are used with analytical data for major cations and ions to distinguish source areas for ground-water and the possible mixing of different types of waters (Gosselin and others, 2001). Similarly, geochemical models are often employed to evaluate alternative ground-water flow paths through multi-layered aquifers units (Palmer and Cherry, 1984).

As noted, local-scale studies are often related to contaminant transport; *local-scale* geochemical models are used to simultaneously evaluate a multitude of geochemical processes that must be considered (Balistreiri and others, 2003; Kawano and Tomita, 2001; Ball and others, 1999). Reactive transport of contaminants combines ground-water flow with geochemical processes; again modeling is used to evaluate the behavior of contaminants under varying conditions (Parkhurst and others, 2003; Benner

and others, 1999). Evaluation of reclamation alternatives for organic or inorganic contamination commonly relies on geochemical modeling (Paulson and Balistreiri, 1999; Runkel and Kimball, 2002; Brown and others, 2000). Although all of the aforementioned applications utilize geochemical reactions, local-scale models can be used to evaluate reactions related to specific minerals or reaction products. Many studies focus on specific contaminants (Kawano and Tomika, 2001) and the treatment thereof (Benner and others, 1999; Tonkin and others, 2002). The basic approach uses the model to reproduce conditions found in the field and then extend the model to time periods or physical areas where data is lacking. The models are used to evaluate the effect of removing the contaminant source on water quality down-gradient of the source and provide an estimate of how long the changes will take. The effect of the change caused by source removal is modeled over time (recovery) and over the volume of affected aquifer (plume movement). Thus, alternative treatment strategies can be compared for their effectiveness in reducing contamination of ground water.

The system depicted in figure 2 would be best modeled at a local-scale. The ground-water flow path or paths would determine the sequence of oxidation, dissolution, reaction(s), and precipitation for each rock type. The flow path(s) would also determine relationship of each rock type to the other rock types; for example a flow path that begins with the ground-water recharge area and flows through country rock into the zoned sulfides. The sequence of the rock types along the flow path in this example would be reflected in the initial conditions of either near-surface conditions (surface water recharge or infiltration) for CO_2 and O_2, then equilibration with the country rock or as lateral ground-water inflow (background water quality), and then re-equilibration with the minerals in the sulfide zone. The size, flow rate, and influence of other waters entering the mixing/equilibration zone, which can be a pore space or mine opening, will determine the nature of mixing of two or more waters from other flow paths, changes in the gas phases, or the dissolution/precipitation of secondary minerals resulting from previous (up-gradient) reactions.

Limitations of Geochemical Models

There are several limitations in the use of computer-based geochemical models to represent natural systems. The primary assumption is the same as that discussed for geochemical evolution: the assumption of equilibrium. That is, chemical reactions occur at a high rate relative to physical processes such as ground-water flow. The same assumption of equilibrium is made for redox potentials and can be particularly problematic for redox potentials measured by electrodes compared to those calculated using the concentrations of redox pairs. Conversely, chemical reactions that are slow relative to the physical processes (for example, the dissolution of quartz) and thus, the assumption of equilibrium is in error. As noted, development and improvement of the thermodynamic databases used by the model have improved over the past few years. The modeler assumes however, that the thermodynamic data is appropriate for the system being modeled. Most databases use equilibrium constants or Gibb's Free Energy values derived from experimental data at standard temperatures and pressures. The algorithms extrapolate for non-standard temperatures and pressures. Similarly, the complexes and minerals in the database are limited; species may well exist in the system being modeled, but may not exist in the database.

Summit Valley Mining District

Butte's history began with placer gold mining in the mid-1860's. As the gold played out, silver was discovered and underground mining began. Silver soon gave way to copper and zinc mining; the first copper ore was shipped from Butte as early as 1882 from what became known as the Summit Valley mining district. In a 92-year period (1882 - 1972), nearly one-half billion tons of ore were mined to produce over 30 billion pounds (14 billion kilograms) of copper, zinc, manganese, lead, and other base metals. Production from the underground mines was as much as 250 million pounds (114 million kilograms) of copper per annum during World War II. As mining technology changed, production of ore evolved from underground to surface mining. The annual production of copper from surface mines was as much as 250 million pounds (114 million kilograms) from the mid-1960's to the mid-1970's; during that same period, the underground mines produced between 50 and 100 million pounds (between 23 and 45 million kilograms) of copper per annum (Miller, 1973).

Safety concerns after a major underground fire, economics, and consolidation of the ownership of the major mines in Butte prompted the interconnection of workings throughout the district. A vast network of mine workings totals an estimated 10,000 miles (16,000 kilometers) of drifts, cross- cuts, shafts, and other workings associated with mining; underground and surface mining produced millions of cubic yards of waste rock and changed the landscape of 6 square miles (10 square kilometers) in the upper Clark Fork River (figure 3). In 1975, the Anaconda Mining Company, holder of all mining properties in Butte, sold all of its interest to the Atlantic Richfield Coal Company. On April 22, 1982, with no notice given, the order was given to shut down all underground mining; this decision was made irrevocable by shutting down the pumps that removed the water from the workings. The following year, all remaining surface mining operations in Butte were shut down. The ensuing economic and environmental impact is strongly evident 20 years later.

Although one of the largest, the Butte area mine system is not unique in its geologic and hydrogeologic setting. There are hundreds of mines in Montana and

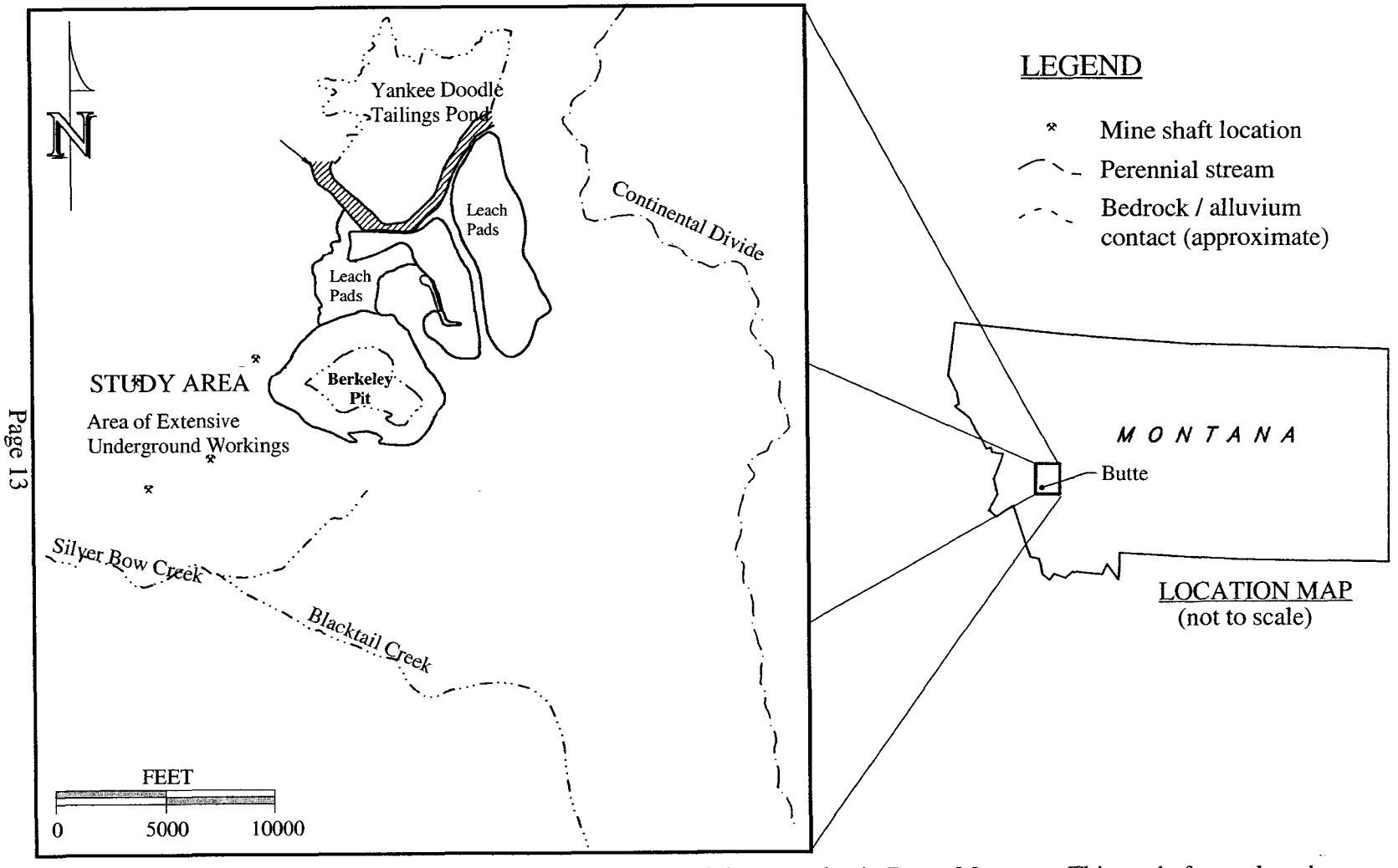

Figure 3. The Summit Valley mining district is an extensive mining complex in Butte, Montana. This study focused on the underground mines west of the Berkeley Pit.

throughout the western U.S. that exploited polymetalic, sulfide-hosted ore deposits; many of these exhibit acid mine drainage similar to that of the early mine flooding in Butte. Understanding what controls the chemical changes in Butte mine waters may provide information to design low-cost, passive, permanent solutions. The Summit Valley mining district provides a unique opportunity to evaluate the evolution of chemistry in a flooding mine and form a better understanding of the hydrgeologic and geochemical processes. Water-quality data have been collected annually and semi-annually from wells and shafts in and around the ore body over the past 22 years. These data demonstrate a dynamic process through both time and space. For example, in the early period of flooding, water chemistry is influenced by hydrogeologic and mineralogic conditions in the deeper portions of the mine. As flooding continued, water samples reflect conditions in the shallower portion of the ore body. Connections between mines also vary with depth; mines in the outer portions of the district were not as deep and had little influence on waters flowing into the mines during the early flooding. Each sample from each shaft reflects the variation of mineralogy, hydrogeology, and mine geometry.

Conceptual models related to the chemistry of water in mined areas often focus only on the mine outlet rather than consider the many components of the mine. Models presented in the literature treat the entire ore body and host rock within the hydrologic influence of the workings as one unit; this research is intended to demonstrate methods of treating the mine discharge as the sum of the parts. Similarly, models presented in the literature are 2-dimensional with respect to space and address water-quality changes along a flow path at a given time; this investigation considers the variation of water chemistry with respect to the vertical and horizontal position within the ore body through time.

Nearly all of the literature pertaining to porphyry copper deposits over the last 30 years includes the Butte deposit as an example; in fact, one of the earliest models of porphyry deposits, proposed by Lowel (1970), includes Butte. Although the rock is only barely porphyritic and the deposition of minerals only loosely resembles the model proposed by most workers, the zonal deposition of minerals in the Butte ore body was well documented even in the early 20th century by Sales (1914). Sales' original work first

proposed the concept of 3 distinct mineral zones based on ore-mineral assemblages:

- Central zone: the primary ore is from copper minerals such as chalcocite, bornite, covellite, and enargite. Zinc and manganese minerals are rare to non-existent. Veins are closely spaced and extensively pyritized. Most rocks exhibit pervasive sericitic alteration.
- Intermediate zone: the primary ore is still copper minerals, but are dominated by chalcopyrite, bornite, tennantite, and covellite. Sphalerite and galena occurrences increase with distance from the central zone. Rock alteration is primarily argillic (montmorilillonite or kaolinite) near the veins.
- Peripheral zone: ore minerals are predominantly sphalerite (shallow) and chalcopyrite near the boundary between the peripheral zone and the intermediate zone. The veins become predominantly rhodochrosite, sphalerite, and silver minerals with distance from the boundary. Rock alteration is mildly sericitic to argillic near the veins.

The earliest mines were developed based on the near-surface mineralogy, but often changed production as workings extended through the transition between these mineral zones. The Travona mine, for example, was originally developed as a silver mine in the 1880's. Although silver continued be important, manganese ores were its primary production in the 1940's. Similarly, the Anselmo mine was developed for silver, but soon became one the largest producers of zinc ores in Montana. Figure 4 presents the mineral zones defined by Sales (1914) and the larger mines of the Summit Valley mining district.

From the first post- mineflooding sample, water in the Butte mines was characterized as acid rock drainage. That is, the oxidation of pyrite in conjunction with the presence of water has produced acid and ferric iron which oxidizes more pyrite and other sulfides. The "poster child" for this process is the Berkeley Pit, a large open-pit mine in the center of the district. A detailed discussion of pyrite oxidation, however, would have to include artificial oxidation and acid generation for the extraction of copper

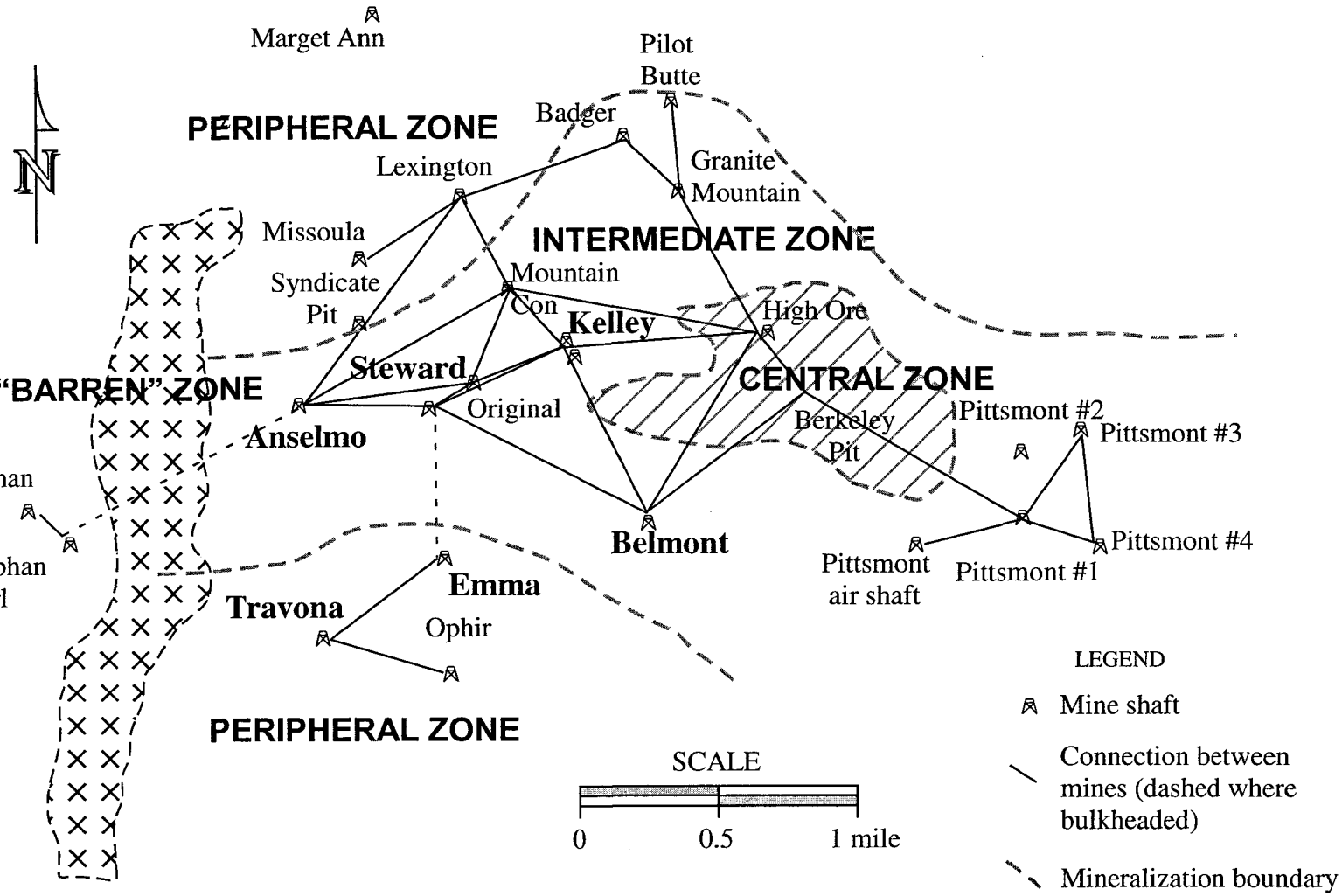

Figure 4. The Summit Valley mining district has three distinct zones of mineralization: the peripheral, intermediate, and central zones (after Sales, 1914). A fourth, barren zone, is a post-mineralization rhyolite on the western edge of the district. Mines included in this investigation are in bold.

from low-grade waste rock. Copper cementation or the removal of copper from solution through ion-exchange with iron has been practiced in Butte since 1886; production from mine discharge and leaching of large piles of waste rock produced over 50,000 pounds of copper in 1972 (Miller, 1973). Management of water during active operations and during the shut-down of mining played an important role in the chemistry of the waters flooding the underground mines and open pits and are discussed later.

Most discussions of water quality related to acid rock drainage tend to give the greatest importance to pyrite and place other sulfides in a subordinate role. The same agents: oxidation of pyrite, circulation of water, and the dissolution/transport of metals are responsible for the degradation of ground water, surface water, and soil at thousands of mine sites in the Western U.S. Literature describing the chemistry of acid mine drainage are varied and extensive, but workers generally agree that the process begins with the oxidation of pyrite and proceeds under two conditions: abiogenic and biogenic (Pohl, 1962; Nordstrom, 1985; Langmuir, 1997, p. 456).

Abiogenic oxidation of pyrite by $O_{2(gas)}$ at pH > 4 is generally slow, but the rate increases with increasing pH (Langmuir, 1997, p. 458). The initial reaction produces two protons and sulfate:

$$FeS_{2(s)} + 7/2\ O_{2(gas)} + H_2O = Fe^{2+} + 2SO_4^{2-} + 2H^+ \qquad (1)$$

Ferrous iron is oxidized to ferric iron and consumes 1 proton :

$$Fe^{2+} + ¼O_{2(gas)} + H^+ = Fe^{3+} + ½H_2O \qquad (2)$$

Ferric iron is hydrolized to precipitate insoluble ferric hydroxide and produce two protons:

$$Fe^{3+} + 3H_2O = Fe(OH)_{3(s)} + 3H^+ \qquad (3)$$

The overall reaction for abiogenic oxidation produces four moles of acid and two moles of sulfate for each mole of pyrite:

$$FeS_{2(s)} + 15/4\ O_{2(gas)} + 5/2\ H_2O = Fe(OH)_{3(s)} + 2SO_4^{2-} + 4H^+ \qquad (4)$$

The oxidation of pyrite by oxygen requires exposure to a replenished oxygen supply and a mineral surface area sufficient to sustain reactions (Ritchie, 1994). Oxidation is usually restricted to the surface of the mineral and rate of acid generation is limited by the rate of oxidation of ferrous iron by oxygen (Alpers and others, 1994).

Bacteria (particularly, Thiobacillus ferrooxidans) greatly increase the production of ferric iron (Harahuc and others, 2000a;) as much as 10 to 100 times that of abiotic processes (Olsen, 1991), by increasing the pH at the surface of the mineral (Fowler and others, 1999). Biogenic oxidation of pyrite occurs at pH> 4 where lithotrophic bacteria catalyze the oxidation of ferrous iron:

$$14Fe^{2+} + 7/2O_{2(gas)} + 14H^+ = 14Fe^{3+} + 7H_2O \qquad (5)$$

The oxidation of pyrite under these conditions becomes a "run away" reaction where pyrite is oxidized by the ferric iron produced from equation 5:

$$FeS_{2(s)} + 14Fe^{3+} + 8H_2O = 15Fe^{2+} + 2SO_4^{2-} + 16H^+ \qquad (6)$$

Although the impact of pyrite oxidation predominates the geochemical processes in mining impacted environments, it is not, of course, the only sulfide of importance. Copper ores such as chalcopyrite, chalcocite, and covelite and zinc ores such as sphalerite also oxidize under similar conditions to produce heavy-metal contamination in mine waters. Thiobaccillus ferrooxidans, does not, reportedly, play a role in the oxidation of other sulfides beyond the production of ferric iron (Fowler and Crundwell, 1998; 1999). Inhibition of microbial iron oxidation increases zinc and copper recovery from ores and

waste rock (Harahuc and others, 2000b). In the case of oxidation of copper minerals, however, ferric iron increases the rate of dissolution of covelite and chalcocite, but inhibits oxidation of chalcopyrite (Third and others, 2002); other bacteria, such as Acidianus brierleyi, affect a direct oxidation at a much greater rate than that of ferric iron (Konishi and others, 1999). Oxidation of chalcopyrite at the colloidal scale is augmented best by the oxidation of the sulfur rather than the iron component of the mineral (Silvester and others, 1992), but the rate of oxidation varies by several orders of magnitude between those predicted in small-scale laboratory studies and the field (Malstrom and others, 2000). Bacteria are certainly present in the waters of the Butte mines. Although no Thiobaccillus ferrooxidans or similar oxidizing bacteria have been reported, several types have been identified. The results of a simple assay of bacteria collected from several shafts in the Butte area are presented in Appendix I.

The solubility of individual constituents in environments similar to those found in the Butte mines has been the subject of several recent investigations. For example, the Travona mine water has high concentrations of dissolved iron and zinc; this mine also produces a notable quantity of hydrogen sulfide. The inverse relationship between hydrogen sulfide and iron concentrations (Langmiur,1997) is apparent in both the short-term and long-term trends in that shaft. Decreasing concentrations of iron coincide with increasing concentrations of hydrogen sulfide. Zinc concentrations are also controlled by hydrogen sulfide in reducing conditions (Dasklakis and Helz,1993). These relationships between metal solubility and hydrogen sulfide provide the basis for evaluating water quality changes in the Travona and Emma mines.

In the intermediate and central zones of the mining district, copper, zinc, and cadmium have shown considerable variation with time. Although copper concentrations can be controlled by bisulfide concentrations (Mountain and Seward,1999), the redox conditions of these shafts are not considered reducing. More likely, direct oxidation of such minerals as chalcopyrite and other copper minerals (for example, Welham, 2001) controls concentrations. Dissolution of zinc minerals, particularly sphalerite, may produce several complexes under a range of conditions (Roberts and others, 2002).

Cadmium concentrations vary considerably throughout the area; the solubility of greenockite, the only cadmium mineral identified, likely controls cadmium concentrations (Wang and Tessier,1999). These experimental data can provide the basis for evaluating the dominant geochemical processes within the mine workings.

As the mine workings flood with water, the basic components of the acid generation are altered. Primarily, oxygen is decreased as the mine openings filled with water which may lead to an abiogenic decrease in ORP. When the mines were operating, the chemistry of the water flowing through the workings was similar to the chemistry of surface water. As the mines continue to flood, the ORP may eventually reflect the chemistry of ground water. It is also possible that the billions of board feet of timber used in the mines and the oils associated with machinery have provided conditions for biogenic reduction of iron and/or sulfate. Both iron bacteria and sulfate reducing bacteria are anaerobic heterotrophs that use iron (Sokolov and others, 2001) or sulfate (Widell, 1988; Postgate, 1984) as an electron acceptor . Sulfate is reduced to for bisulfide and bicarbonate:

$$CH_3COO^- + SO_4^{2-} ==> \ 2HCO_3^- + HS^- \qquad (7)$$

bicarbonate consumes acid to increase the pH:

$$2HCO_3^- + 2H^+ ==> 2H_2CO_3 \qquad (8)$$

bisulfide consumes acid to produce hydrogen sulfide gas and reacts with metal ions to precipitate metal sulfides:

$$HS^- + H^+ ==> \ H_2S \qquad (9)$$

$$HS^- + Me^{2+} ==> H^+ + MeS \qquad (10)$$

Additional precipitation of metals sulfides may occur on the surface of existing sulfides such as pyrite as is common in supergene ore deposits (Podda and others, 2000). Ferric iron consumes the bisulfide equation 10 at a much higher rate than most other metals and, if ferric iron concentrations are high, precipitation of other metal sulfides is limited (dos Santos Afonso and Stumm, 1992; Cantrell and others, 2003).

Although pyrite is common through the district, especially in the central zone, it was far from ubiquitous in the mines of the intermediate and peripheral zones which are the focus of this study. This investigation evaluates water quality relative to the original mineralogy to determine the path by which water chemistry developed. Such an approach is commonly called "inverse" modeling. The porphyry ore deposit at Butte, Montana exhibits distinctive, well defined zonation of mineralization. Underground and surface mining and the subsequent flooding of the mine workings have created observable, albeit complex, ground-water flow paths through this zoned deposit.

Hypothesis Statement

Water chemistry and ground-water flow gradients can be used to determine and demonstrate the evolution of water quality with respect to time and space in a zoned orebody. Evaluating each component and each flow path described in figure 2 as it relates to the Summit Valley Mining District in Butte, Montana can be used to define surface-water and ground-water flow paths, water chemistry along those flow paths, and water chemistry through time.

Experimental Approach

This investigation considered the influence of local mineralogy, mine geometry, and the mine-flooding water-balance to evaluate the variation in water chemistry within the mines with respect to time and space. Each mine, and in some cases, each set of workings within the zoned porphyry-copper orebody has unique mineralogy. Mineralogic information available from many published works related to Butte, unpublished MBMG data, and specimens/records of the Anaconda Mineral Collection of minerals maintained by the MBMG were examined to construct a general model of mineral assemblages for each mine.

Detailed maps of the underground workings were used to determine mine volumes, connections between mines, and to give weight to the potential influence of minerals from difference parts of the mine. Similarly, the mine geometry and its position in the flooding system were used to identify potential sources and the likely chemistry of water entering each mine. Mines that represented different positions within the ore body and for which sufficient information could be obtained were selected to construct the model:

- Travona — location: peripheral zone
  water source: peripheral zone, barren zone (west)
- Anselmo — location: peripheral zone
  water source: barren zone (west), peripheral zone
- Steward — location: intermediate zone
  water source: Anselmo mine, intermediate zone
- Belmont — location: intermediate zone,
  water source: Travona mine, intermediate zone rocks
- Kelley — location: intermediate zone / central zone
  water source: Steward, Lexington/Missoula, Belmont, intermediate zone, central zone

Equilibrium modeling

Geochemical modeling was used to explore the relative influence of the various known minerals within each mine selected. A list of "equilibrium phases" or minerals were equilibrated with inflow waters under the conditions found in the mines. Dominant (controlling) equilibrium phases (minerals, $P_{CO2,}$, etc.) for each mine, important sources of water, and the relative amount of each source-water flowing into each mine were determined from this modeling. A detailed description of the input and the constraints used, as well as comparison to observed chemistry are presented for each mine. Annotated input files and flow charts for each model are presented in the appendixes.

Although several computer codes were used, modeling results using PHREEQCI (Charlton and others, 1997) are presented. The code is capable of several types of calculations including solid solution, ion-exchange, kinetics of reactions, and 1-dimensional transport. The application of PHREEQCI (Charlton and others, 1997) for this investigation was used for its capability for mole-balance (balanced reactions that occur simultaneously) and mass-action equations (equilibrium equations). The code was used to simulate batch-reactions with mineral phase equilibrium and batch-reactions resulting from the mixing of two or more waters. This particular model code was chosen over similar codes based simply on familiarity, ease of use, and compatibility with graphics software for post-processing.

The concentration of various dissolved constituents changed over time in several of the shafts. The set of initial conditions determined in the first part of the modeling were used to simulate the possible changes that occurred as the mines flooded. Parameters such as field ORP (or Fe^{2+}/Fe^{3+} and As^{3+}/As^{5+} concentrations where available), P_{CO2} availability (open vs closed), hydrogen sulfide, and dissolved oxygen were varied within observed or expected ranges to produce the change in water chemistry. The primary use of the modeling effort was to demonstrate the balance of multiple reactions known to occur in a given shaft at a given time. The goal was not so much to produce a computer simulation of chemistry, but to describe the evolution of water chemistry as the mines flooded and to identify flow paths based on the chemistry in the shaft.

Mineral phases

The fundamental approach to modeling conditions in the mine openings was to equilibrate mineral phases with water. In PHREEQCI, equilibrium phases are specified along with the target saturation index and the maximum molar amount that can be dissolved. The saturation index (log[ion activity product / equilibrium constant]) is most often set to zero to achieve equilibrium between the mineral and the solution. Similarly, if equilibrium is the objective, the maximum molar amount to be dissolved is set at a value higher than the amount that is actually dissolved. In all simulations, the saturation index for the selected minerals was set to zero and the maximum mole amount that could be dissolved far exceeded final amount dissolved. There was, however, one exception to this approach: where the primary mineral phase did not exist in the thermodynamic database, but an intermediate, highly soluble phase did. Enargite is the likely mineral responsible for dissolved arsenic in much of the Butte area, but does not exist in the database. Welham (2001) identified arsenolite as a soluble mid-member oxidation product of enargite; thus, arsenolite, in limited amounts was used to establish arsenic concentrations in several of the simulations.

Gas phases

The PHREEQECI software allows the equilibration of gases in four ways: 1) as an equilibrium phase similar to that of minerals (the log partial pressure is given in place of the saturation index), 2) as a fixed partial pressure for an open system, 3) a fixed volume for a closed system, and 4) as a titrant that is added in steps for an open or closed system. Modeling the conditions in the shafts was best accomplished by using a fixed partial pressure which was adjusted as needed to achieve calibration.

Modeling conditions in the shafts required constraints on the concentration or partial pressure of gases in solution. In addition to exchange with atmospheric oxygen and carbon dioxide (figure 2), subaqueous generation of gases by organic and/or inorganic reactions was considered. Several of the shafts in the Butte area exhibit effervescence when sampled; the relative intensity of the effervescence varies over time

and sometimes with the depth the sample. The East Camp sites (Anselmo, Steward, and Kelley) exhibit a gas that is odorless, but has been identified as predominantly carbon dioxide. The West Camp sites (Travona, Emma, and Ophir) exhibit a strong odor of hydrogen sulfide gas. These conditions were used to define the upper and lower limits used in the modeling.

Oxygen in generally considered to be 21% of the total atmospheric gases; at a total pressure of 1 atmosphere, the partial pressure of oxygen is 0.21 atmospheres (atm). In surface waters, dissolved oxygen ranges from a maximum of about 8.25 mg/L (at 0.21 atm) to the detection limit of about 0.005 mg/L and ground waters have an average of 0.7 mg/L dissolved oxygen (Langmuir, 1997, p. 409). A dissolved oxygen value of 0.7 mg/L was used to simulate ground-water flowing into the workings and a value of 8.25 mg/L was used to simulate oxidation near the water surface for modeling conditions in the mine shafts. Carbon dioxide in surface waters in equilibrium with atmospheric conditions is generally reported as $10^{-3.5}$ atm; values for deep surface waters and ground waters is often higher (Langmuir, 1997, p. 156). Measured values of dissolved carbon dioxide have been reported as high as 0.1 atm in deep mine waters (Capo and others, 2001). As noted, several shafts in the Butte area exhibit effervescence; the composition of the gas is likely to be nitrogen, carbon dioxide, and possibly methane. Assuming a total gas composition of carbon dioxide, the maximum content would be 1 atmosphere to cause effervescence. A range of $10^{-3.5}$ to 1 atmospheres was considered in the modeling of conditions in the shafts, but the maximum was much less than 1 atmosphere to achieve reasonable results. Hydrogen sulfide has been noted in the waters of the West Camp since sampling began; measurements of the gas concentration have been made periodically and ranged from <0.1 to 1.6 mg/L in the waters. In all of the model simulations, the values of gas phases for oxygen, carbon dioxide, and hydrogen sulfide used in the model were well within the ranges discussed.

Model Calibration and Uncertainty

Calibration of each simulation was done by comparing the analytical results for the shaft and/or time period in question. As with any chemical analysis, there is uncertainty in the data; whenever possible, the quality of the sample data was obtained and only those data meeting the requirements of the quality assurance plan were used. The sources of water-quality data used in this investigation include the Montana Bureau of Mines and Geology (MBMG) who collected and analyzed the samples, the Anaconda Company who collected and analyzed the samples, and from published reports. Data quality standards for most water analyses require a 20% relative percent difference (RPD) between duplicate samples:

$$RPD = \frac{(C_1 - C_2)}{\frac{(C_1 + C_2)}{2}} * 100$$

where:

RPD:	Relative Percent Difference
C_1:	larger of the two observed values
C_2:	smaller of the two observed values

This same method was used to compare the results of each simulation to that of the appropriate sample data. In the strictest sense, the model could be considered calibrated with a relative percent difference of 40% assuming the maximum error for both sample and model results, and in the same direction.

Uncertainty in the data used in the model creates a minimum uncertainty in the model results. The potential for a high degree of uncertainty in the analytical results can be quite large, especially under the conditions in which many of the samples were collected. Sampling of the shafts was done by means of a bailer, open-top or point source, sent down the shaft. The earliest samples were collected a depths over 3,000 feet (900 meters) below the surface; the latest samples are collected at 400 to 500 feet (120 to 150 meters) below the surface. Debris in the water, obstructions in the shaft, and equipment failure can contribute to contamination of the sample. Data "outliers" should be expected, but are not difficult to identify. Evaluation of trends and events in this

investigation gave weight to multiple samples in a short period of time and samples collected under conditions known to the author as acceptable. In all cases, data meeting minimum quality as established by the U.S. EPA were used. Indeed, all of the sampling and analyses were conducted under a quality assurance plans, sampling and analysis plans, and laboratory analysis plans approved by the U.S. EPA and all data were qualified.

Sequence of Geochemical Modeling

As noted, water chemistry in the shafts have changed over time; there is also a notable difference in water chemistry from one shaft to the next. The modeling then, must include both aspects: the changing conditions as the mines flood and the changing conditions as the water flows from one mine to the next.

As noted, water-quality data were collected soon after flooding of the mines began in 1982. The change in chemistry as the mines flooded is well documented and of sufficient detail for modeling. Modeling of the chemical changes over time rely on the observed chemistry over time and a comparison of water level with the mineralogy within that mine and interconnection to up-gradient mines.

Figure 5 presents the potentiometric surface of the flooding mines based on water-level elevations in the shafts measured in December of 2002. Based strictly on water-level differences, ground water flows from the outer margins of the mined area inward toward the Berkeley Pit. Ground water can potentially flow from the Travona and Emma mines of the West Camp northward toward the Anselmo mine or northeastward toward the Belmont. Ground water in the area of the Orphan Girl and Orphan Boy mines on the western extreme can potentially flow toward the Anselmo mine, then toward the Steward and Kelley mines. Thus, the sequence of modeling the changes in the mines along the flow path, as limited by the available data, would be: 1) Travona, 2) Anselmo, 3) Steward, and 4) Kelley. The chemistry of the ground-water inflow into the Travona would be based on shallow bedrock wells area that are not directly connected to the mine. In addition to potential flow from the Travona, ground-water flow into the Anslemo

might include water from the Orphan Girl / Orphan Boy mines or the nearby unmined bedrock.

In several cases, there were alternative approaches to modeling for the unique solution; the approach that gave the best comparison between the sample results and the model output was selected. A modeling flow diagram and annotated input files for each mine shaft modeled is presented in Appendixes II through IV.

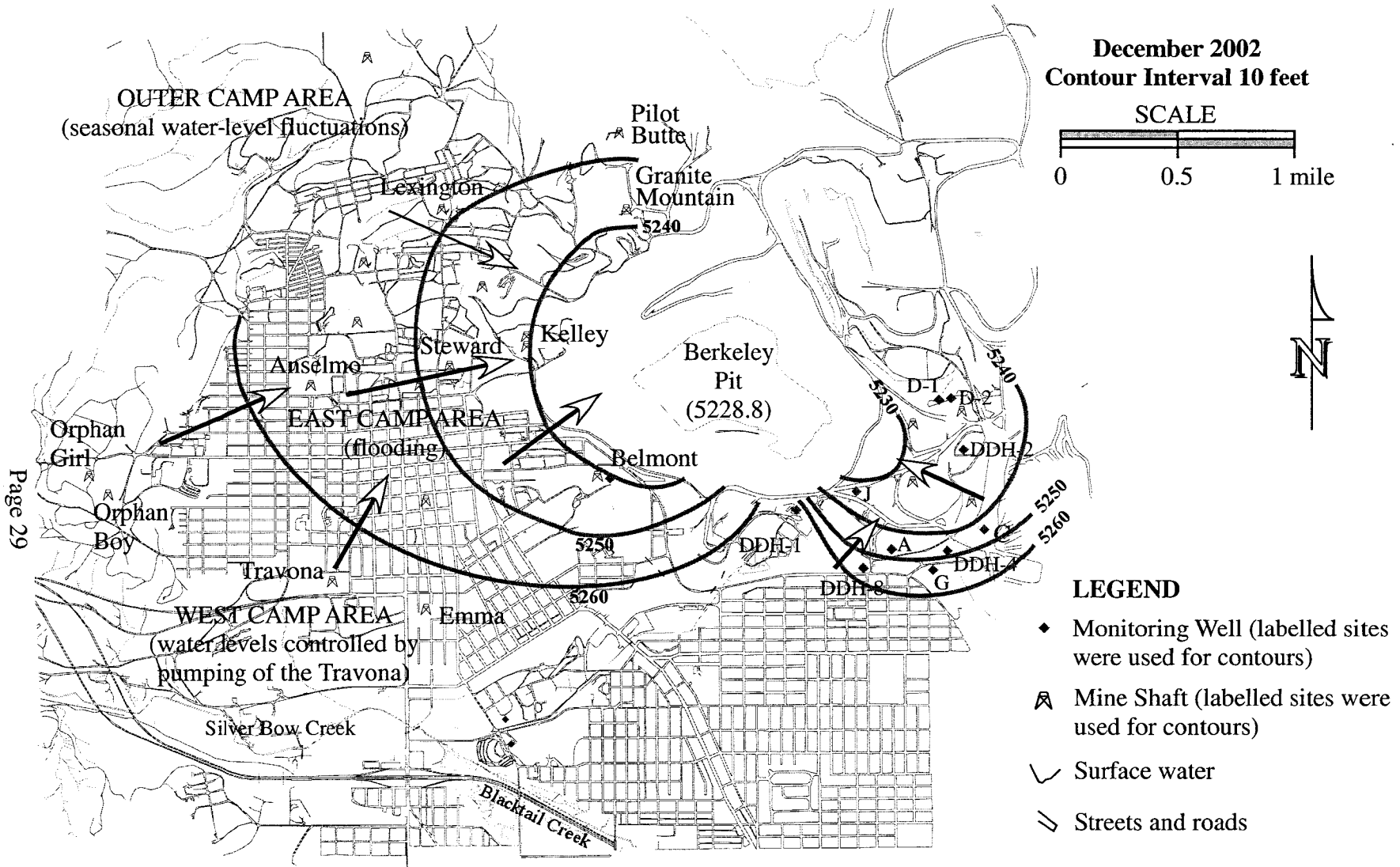

Figure 5. Potentiometric map of the flooding mines based on December 2002 water levels; arrows indicate direction of potential ground-water flow.

Travona mine

Water levels in the Travona mine indicate a potential for ground-water flow to other mines with little or no potential for flow from any other mine (figure 5). Thus, as the most up-gradient mine and its potential to be a substantial source of water to other mines, the Travona is the first site considered for modeling the chemical changes.

Background

The Travona mine is reportedly the oldest hardrock mine in the Summit Valley mining district. A major silver discovery in 1875 led to about 18 years of silver production from the area. After several years of inactivity, the mine was re-opened for its wealth of "zinc-free" manganese ore (rhodochrosite) as well as minor reserves of silver. As the mine expanded, many of the workings of the Travona intersected those of the Emma and Ophir mines to the east and were commonly referred to as the West Camp mines. When mine ownership in the Butte District was consolidated, several of the workings were extended to the East Camp mines including the Steward mine and Belmont mine north and east of the West Camp (figure 6).

Ore production from the West Camp had all but ceased by 1960; dewatering ended in 1965. The workings were separated from those of the East Camp (Steward and Belmont mines) by "water tight" bulkheads (figure 6); the intent was to reduce the amount of pumping that was required to keep the workings of the East Camp dry and allow flooding of the West Camp. Water levels in the West Camp rose until springs developed at the surface in residential areas downhill of the mines. A well was drilled into the workings in 1966 to drain the mine water directly to Silver Bow Creek; the initial discharge from the well was estimated to be 3,800 gpm. Flow from the well declined over several months and eventually stopped.

Although the workings of the West Camp were bulkheaded, there remains at least some hyrologic connection to the East Camp. This is evidenced by the response in water levels during the final flooding of the mines. When all pumping from the Butte mines

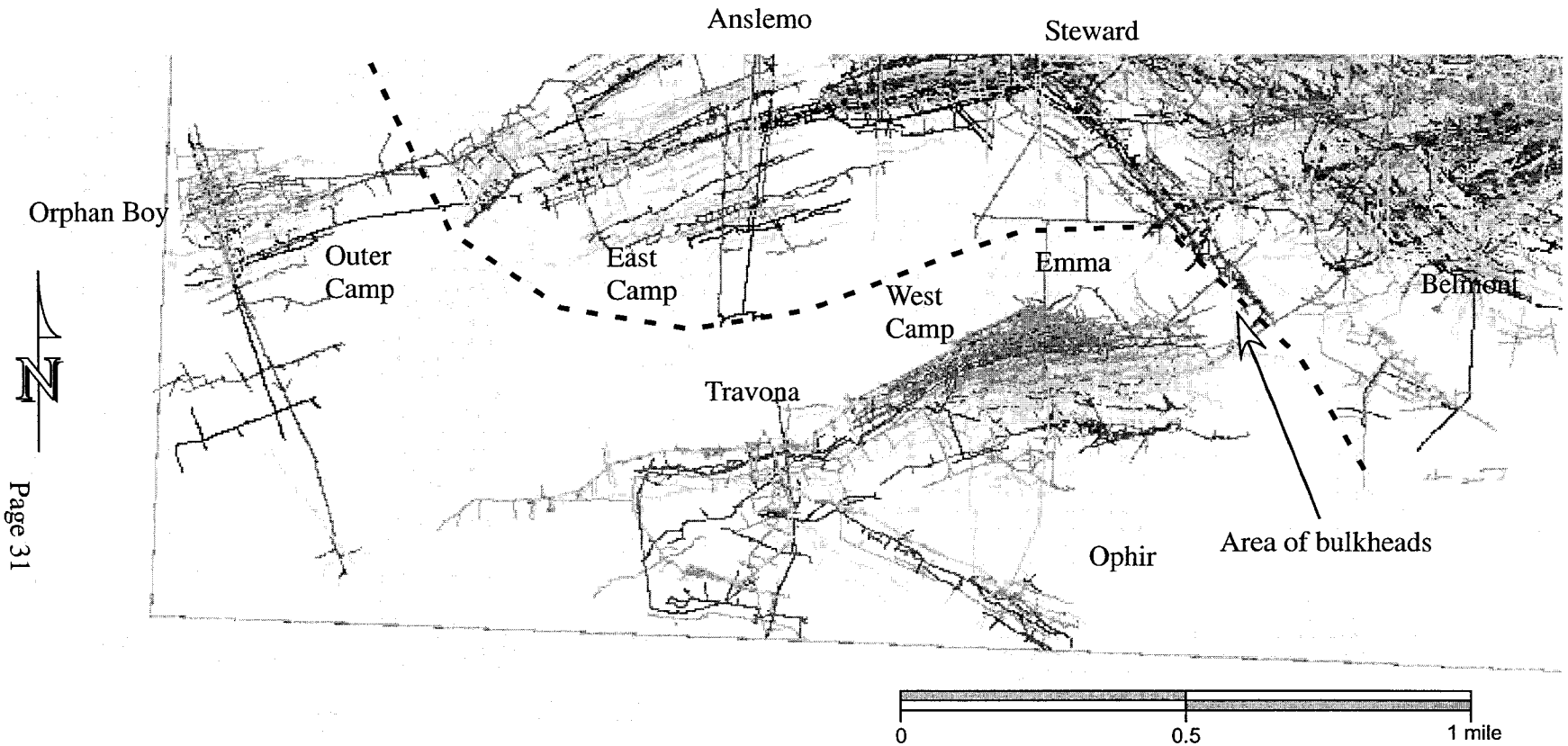

Figure 6. Composite map of mine workings in the West Camp (Travona, Emma, and Ophir mines) and East Camp (Belmont, Steward, and Anslemo mines); dashed line indicates approximate boundary. The Orphan Boy mine is considered part of the Outer Camp.

ceased in April of 1982, the initial data showed that there was little effect on water levels in the Travona shaft. However, about 15 months after the East Camp began to flood, water levels in the Travona shaft began to rise (figure 7); initially, the water level in the Travona was about 2,200 feet (670 meters) higher than mines of the East Camp. By 1985, there was an 850-foot (260 meter) difference in water levels between the West and East Camps; the rate of rise in the East Camp had slowed to about 10 feet (3 meters) per month and the rate of rise in the Travona was about 5 feet (1.5 meters) per month. Water levels in the West Camp have been controlled by pumping since 1989; concern for discharge to the surface and Silver Bow Creek prompted an "action level" elevation of 5,435 feet (1,656 meters) above mean sea level (amsl) above which the water level would not be allowed to rise.

Ground water and water within the workings of the Travona and Emma mines exhibit higher water levels than any of the other mines in the district. This is particularly true after 1965 when the mine was allowed to flood. Although the hydraulic gradient from the West Camp to the East Camp has decreased since flooding of the East Camp began in 1982, there was still over 200 feet (61 meters) of head difference in 2002. Thus, the West Camp mines represent a system that is hydrologically isolated with respect to other mines in the district and is a potential source of ground-water recharge to the East Camp mines.

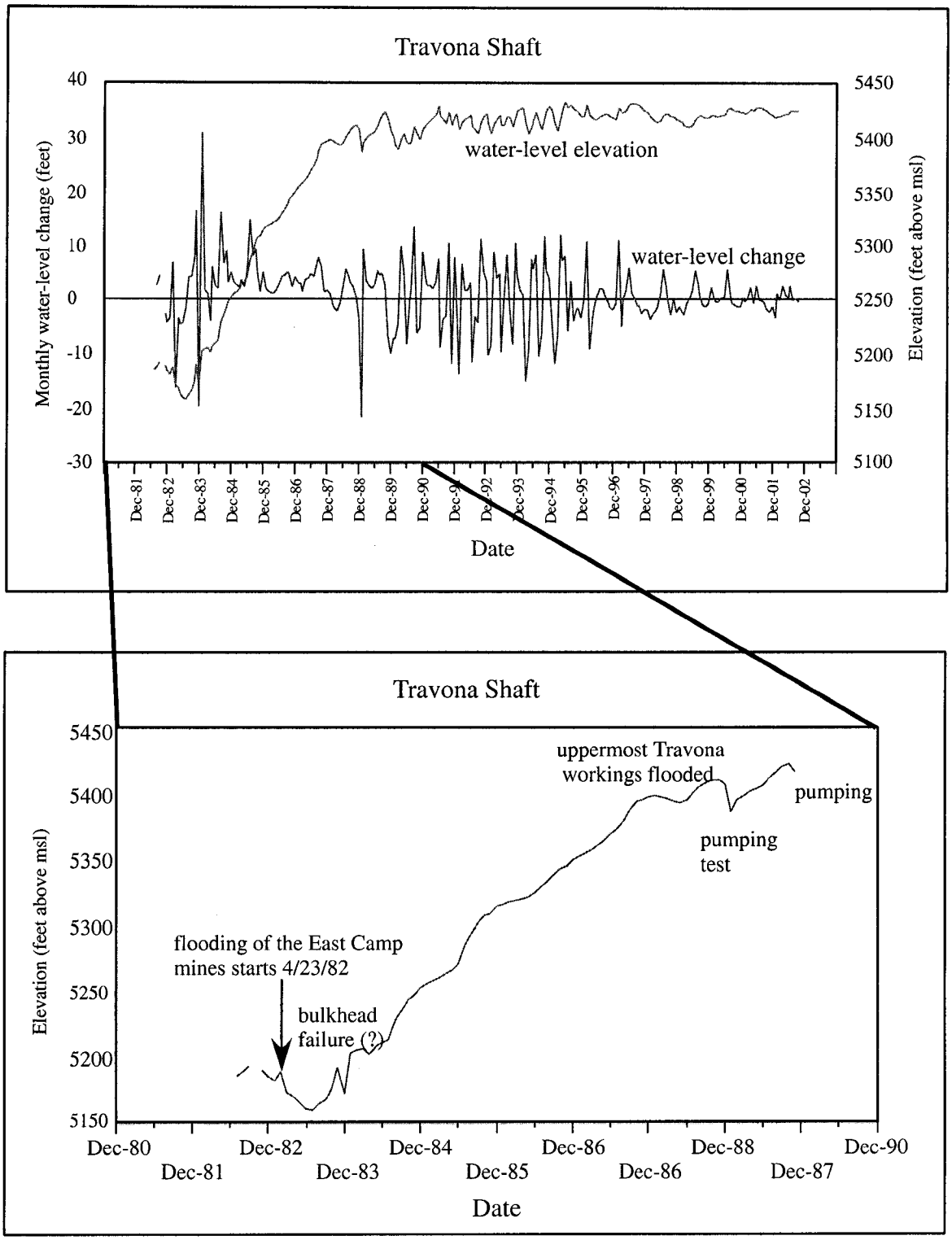

Fig 7. Water levels in the Travona shaft responded to flooding of the East Camp mines after a 15 month delay. Water levels have been controlled by pumping since 1989. The hydrograph for the early period of flooding is expanded to show the effects of various events.

Mineralogy

The Travona, Emma, and Ophir mines (West Camp) exploited the southwest-northeast Emma vein system which represents the southern extent of the large east-west vein system of the Summit Valley mining district. The vein mineralogy grades from oxide and carbonate ore minerals of the Peripheral Zone on the southwest end to sulfide minerals of the Intermediate Zone on the northeast end. The southwest end of the vein and mine workings is bounded on all levels by a post-mineralization rhyolite dike. Sales (1914) first described this area as being within the Peripheral Zone with rhodochrosite, sphalerite, and quartz. Ziehen (1986) revisited several of the mines in Butte and describes them in more detail: The upper levels of the Emma vein system contain rhodochrosite and quartz as well as minor pyrite and minor sphalerite. The lower levels and eastern levels (Ophir) exposed veins of more sphalerite (sometimes coated with Greenockite) and minor chalcopyrite. Oxidized zones contain silicious manganese oxides such as pyrolusite and cryptomelane. Alteration minerals in the Emma vein system are related to mild sericitic alteration (muscovite) as well as kaolinite- and montmorillonite - argillic alteration.

Water quality

Regular water-quality monitoring of Travona and Emma shafts began in 1982, just after flooding of the East Camp mines began. In the early period of monitoring, samples were obtained by means of a bailer lowered down the shaft. In January of 1989, the Montana Bureau of Mines and Geology conducted a 28-day pumping test during which both water levels and water quality were monitored; samples were collected from the pump discharge. As noted, water levels in the West Camp have been controlled by pumping since 1989; samples have been collected from the pump discharge since that time. Analyses of samples usually included major anions, cations and dissolved metals.

In the first 4 years of flooding (1982 to1986) there was little change in the concentration of dissolved constituents; the pH was near neutral and dissolved metals concentrations were generally low (water levels had risen about 180 feet (55 meters) over

that same period). In the year between July, 1986 and July, 1987 concentrations of several dissolved constituents including manganese, sulfate, and iron increased sharply (figure 8). After the peak in mid-1987, concentrations trend downward for the rest of the period of record interrupted only by the effects of a month-long pumping test conducted in early 1989 (figure 8).

Equilibrium Modeling: Travona Shaft

A geochemical equilibrium model, PHREEQECI (Charlton and others, 1997) was used to evaluate those processes responsible for the changes in chemistry during the flooding of the Travona mine. Minerals indigenous to the Travona, Emma, and Ophir mines (table 2) were equilibrated with water whose chemistry represented ground waters entering the mines. Although concentration data from shallow monitoring wells vary with time and space, the change has been small; therefore, water quality of the ground water recharging the mine were assumed to be constant. All of the mineral phases listed were used throughout the simulation.

Table 2. Mineral phases used in the Travona simulation.

Mineral Phase	comments
Arsenolite: As_2O_3	based on tennantite/enargite
Montmorillonite: $(Al,Mg)_8(Si_4O_{10})_3(OH)_{10} - 12H_2O$	alteration mineral
Quartz: SiO_2	country rock
Pyrite: FeS_2	gangue mineral
Rhodochrosite: $MnCO_3$	dominant ore mineral
Chalcopyrite: $CuFeS_2$	reported as "occurrences"

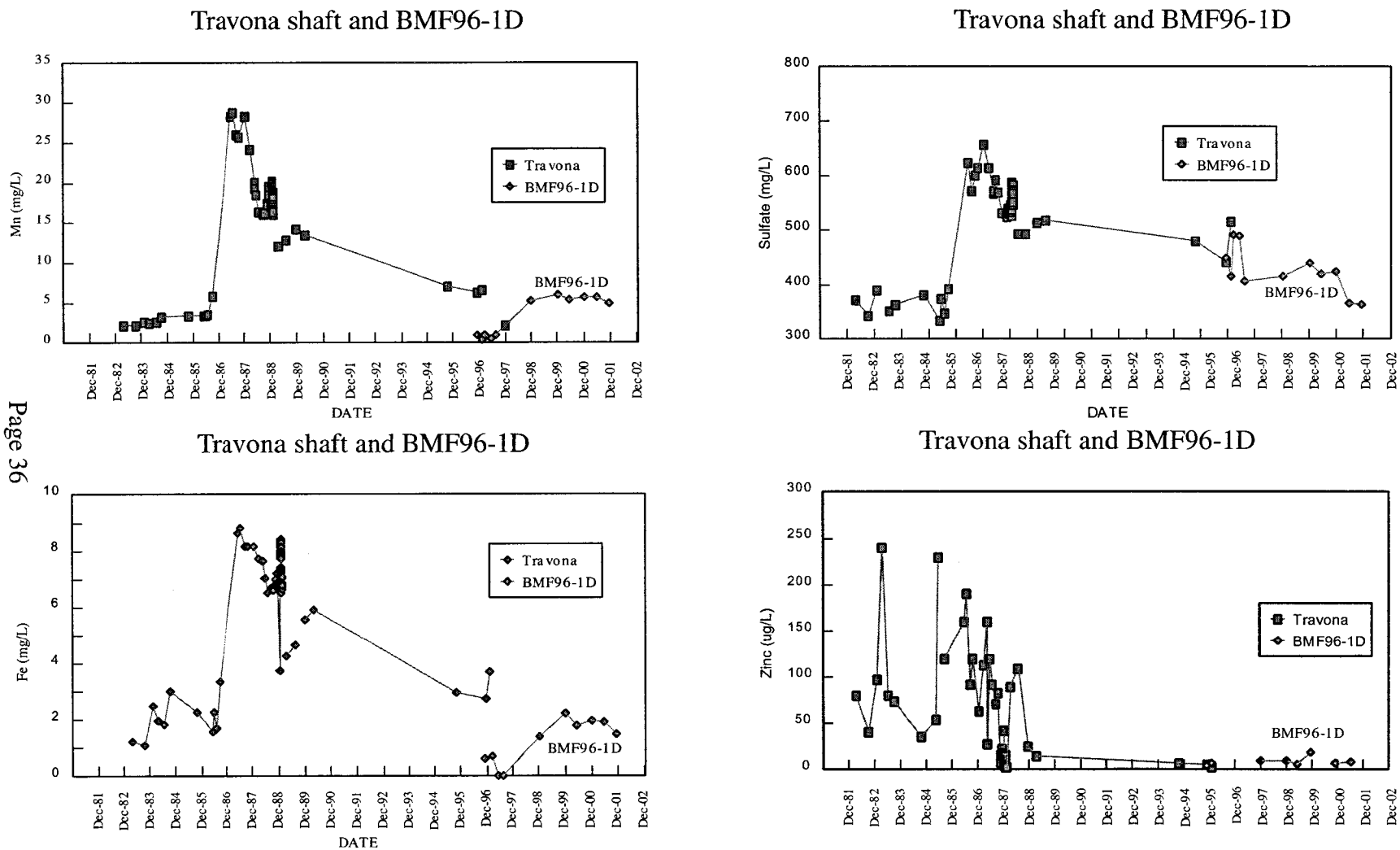

Figure 8. Selected chemistry from the Travona shaft. The concentration of manganese, sulfate, and iron increased dramatically in 1987 while that of zinc decreased. BMF96-1D is a well drilled into the workings of the Travona mine.

Modeling focused on three time-segments of the Travona flooding as related to the three significant changes in chemistry:

- early flooding (1984 to 1986),
- a period of rapid increase in concentrations of several dissolved constituents (1986 - 1987) and,
- the relatively gradual decrease in concentrations (1989 to 2002).

Early Flooding (1984 to 1986)

An inverse model of water-quality data from the early period of flooding indicated that the water was undersaturated with respect to all iron minerals in the database. In other words, all the available iron from ground-water flowing into the workings and all of the iron produced from dissolution of the available minerals (table 2) failed to produce sufficient iron in the final solution. Two alternative modeling approaches were considered. The first approach was to assume that abundant secondary, soluble, Fe-rich minerals (oxyhydroxides) formed after the mine began to flood. In this case, the identity of the minerals would be assumed and added to the list of minerals in table 2. The second approach was to consider that the conditions during active pumping of the mines were much different than those observed during the early period of flooding. That is, air was circulated throughout the mine and, with the abundant pyrite, acid rock drainage was likely produced. The oxidizing conditions changed to reducing conditions soon after air circulation was shut down and flooding of the mine began. Modeling could be used reproduce conditions found in the initial flooding of the workings using the same list of known minerals and inflow chemistry. The oxygen concentration would be decreased from atmospheric conditions (0.21 atm) to simulate a flooding mine. This approach provides the best opportunity for a unique solution by limiting the assumptions regarding mineralogy and redox conditions. Also, water chemistry data collection during initial flooding of other sites in the area provide a reliable basis for "pre-historic" (pre-1984) conditions in the Travona.

"Pre-historic" conditions in the Travona shaft were simulated by equilibrating the minerals listed in table 2 with water entering from the shallow "leached zone". The leached zone is the mineralized rock above the historic water level from which any sulfides have been leached through the natural weathering process. Each step of the model was considered a time step in the flooding of the mine. Oxygen was added to the system in increasing amounts until the solution became acidic; oxygen was then added to the system in decreasing amounts until no oxygen was being introduced. All other inputs to the model were held constant throughout the simulation.

Figure 9 presents the results of the oxidation model for total iron and pH; the input file is described in more detail in Appendix II. The maximum iron concentration of about 0.01 moles/L is in the lower range of concentrations observed at mines of the East Camp during initial flooding. The non-symmetrical nature of iron concentrations is evident when compared to pH (figure 9b). Iron concentration and pH coincide with observed values at only one point during the simulation: when oxygen has been "depleted" as the mine floods. These results further demonstrate that iron was stored as precipitates and provide additional iron as the system evolves from oxidizing to reducing conditions.

Table 3 compares model results for early period of flooding to those of a sample collected from the Travona shaft on 2/16/84; the input file is described in more detail in Appendix II. Figure 10 compares the model results with the sample data; there is generally good agreement, particularly for sulfate, sulfide, and iron.

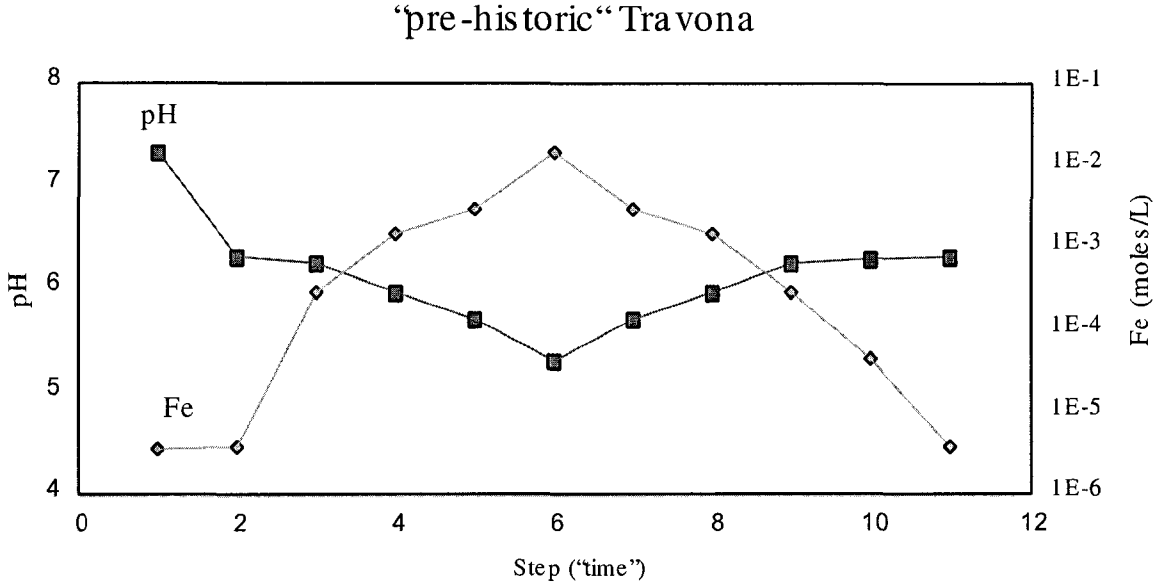

Figure 9a. Model results for iron and pH as a function increasing and then decreasing oxygen.

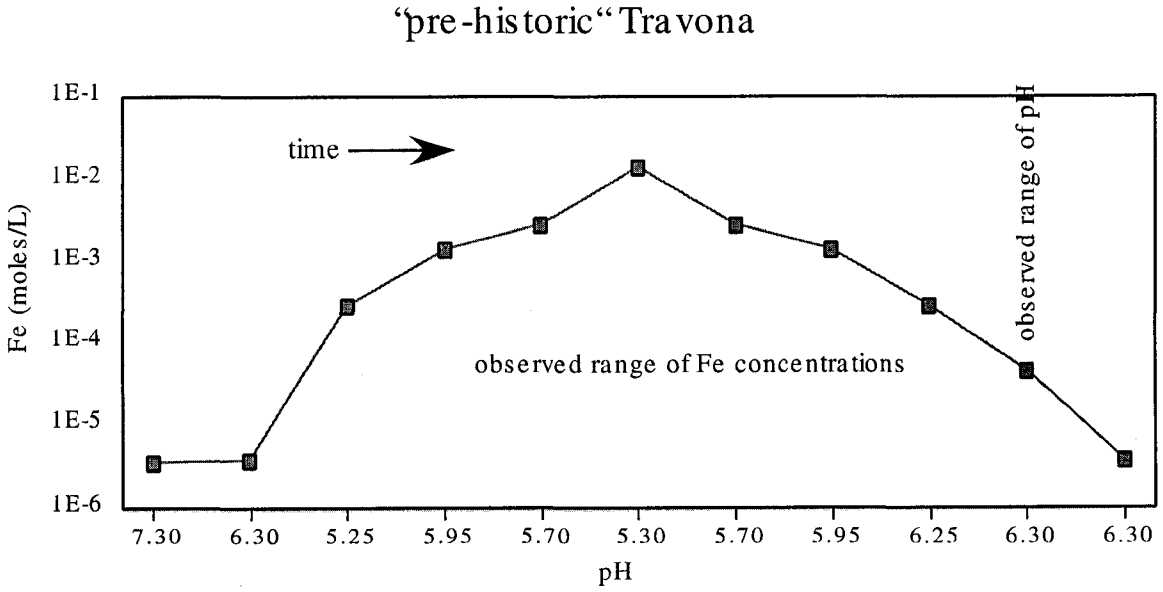

Figure 9b. Model results from figure 6a for iron as a function of pH.

Table 3. Comparison of model results with sample collected in the early period of flooding (1984) of the Travona shaft.

	Model		Travona		Difference		RPD*
Analyte	molality	mg/L	molality	mg/L	molality	mg/L	
Al	8.72e-07	0.02	1.48e-06	0.04	1.35e-06	0.04	87
As	1.66e-06	0.12	1.04e-06	0.08	-6.18e-07	-0.05	46
C	7.16e-03		7.52e-03		3.63e-04	4.36	5
HCO3-	4.24e-03		4.67e-03		4.30e-04	0.00	10
CO2	2.91e-03		2.69e-03		-2.17e-04	-0.00	8
Ca	5.15e-03	206.21	3.52e-03	141.12	-1.62e-03	-65.09	37
Cl	1.19e-03	42.15	1.01e-03	35.63	-1.84e-04	-6.52	17
Cu	8.48e-26	0.00	<IDL		-8.48e-26	-0.00	
F	3.48e-05	0.66	3.69e-05	0.70	2.10e-06	0.04	6
Fe	5.15e-05	2.88	4.50e-05	2.51	-6.49e-06	-0.36	13
K	1.43e-04	5.61	1.15e-04	4.50	-2.82e-05	-1.10	22
Mg	2.42e-03	58.85	1.71e-03	41.55	-7.12e-04	-17.31	34
Mn	5.08e-05	2.79	4.81e-05	2.64	-2.74e-06	-0.15	6
Na	1.37e-03	31.53	3.01e-03	69.15	1.64e-03	37.62	75
S(6)	5.46e-03	175.02	4.07e-03	130.61	-1.39e-03	-44.40	29
Zn	1.55e-06	0.10	1.50e-06	0.10	-4.60e-08	-0.00	3
S(-2)	4.15e-06	0.14	6.00e-06	0.20	1.85e-06	0.06	36

* relative percent difference

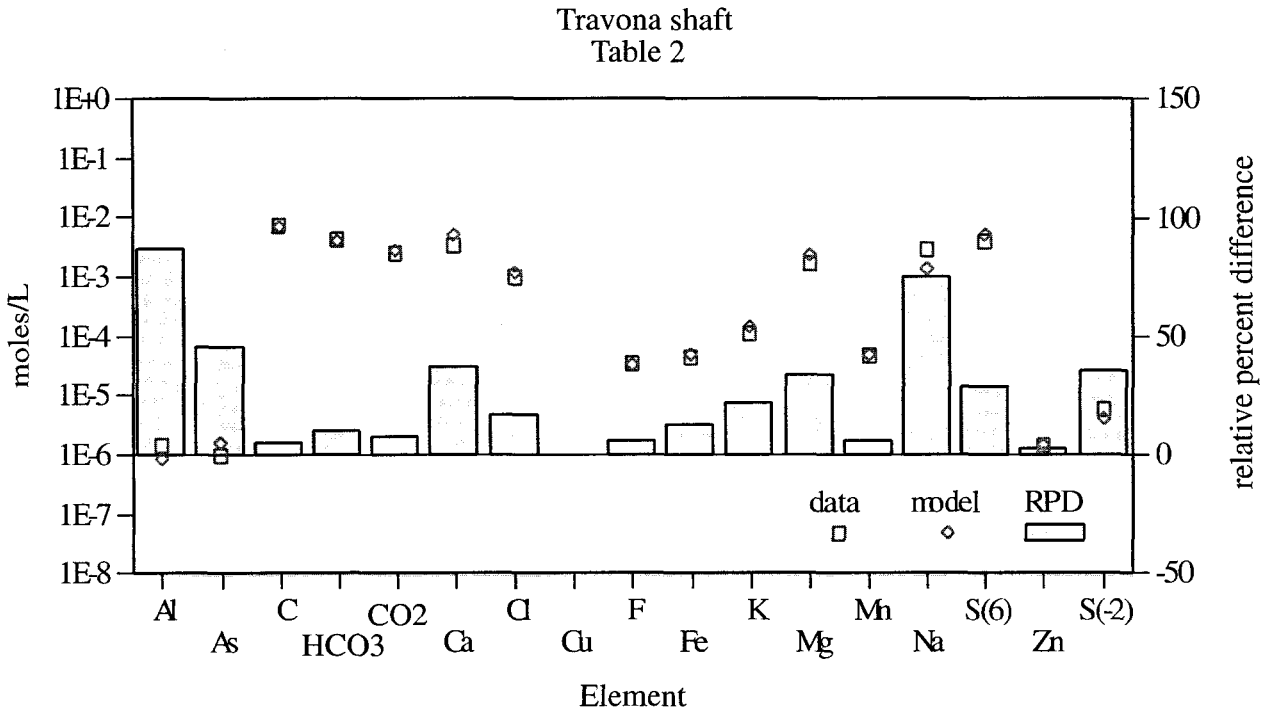

Figure 10. Comparison of concentrations of constituents between the model and data collected from the Travona shaft in the early period of flooding (1984). The relative percent difference (RPD) was not calculated for sample data below the detection limit.

Period of 1st Transition (1986 - 1987)

In the twelve-month period from mid-1986 to mid-1987 the iron concentration, as well as the concentration of several other constituents, increased sharply (figure 11). The concentration of several dissolved constituents, especially zinc changed from exhibiting wide fluctuations to more consistent, decreasing concentrations. Redox conditions (based on As III and AsV concentrations), pH, and temperature did not change appreciably during this period. Water levels during this period rose about 40 feet (12 meters) from an elevation of 5,329 to 5,369 feet (1624 to 1,636 meters) amsl; the uppermost mine workings of the Travona are near an elevation of 5,327 feet (1,623 meters) amsl (MBMG, unpublished records). It is likely that during this period, the last large opening of the mine was flooded.

Although the presence of H_2S gas has been reported throughout the period of record, only a few measurements have been made. A single measurement during the early period of flooding (1984) indicated an H_2S concentration of 1.6 mg/L; during the long-term pumping test, concentration values ranged from < 0.1 to 0.2 mg/L; recent measurements by Gammons and others (2003) range from 0.1 to 0.7 mg/L. This suggests a possible control of iron and zinc concentrations by H_2S.

The concentration of iron in the Travona shaft displays an inverse relationship with H_2S (increasing iron = decreasing H_2S) concentrations as suggested by:

$$Fe^{2+} + H_2S_{(aq)} = FeS_{(am)} + 2H^+ \quad \log K_{eq} = -2.69 \text{ (Langmuir, 1997, p. 427)} \qquad (11)$$

Figure 12 presents the solubility of Fe^{2+} with respect to H_2S over the range of total iron and H_2S observed in the Travona shaft. Although the inverse relationship holds, the values for H_2S and Fe^{2+} predicted by this equation are much lower than those observed. The concentration of zinc in the Travona shaft displays a proportional relationship with the concentration of H_2S (decreasing zinc = decreasing H_2S), but solubility is a function of both $Zn^{2+}$and zinc-bisulfide as described by:

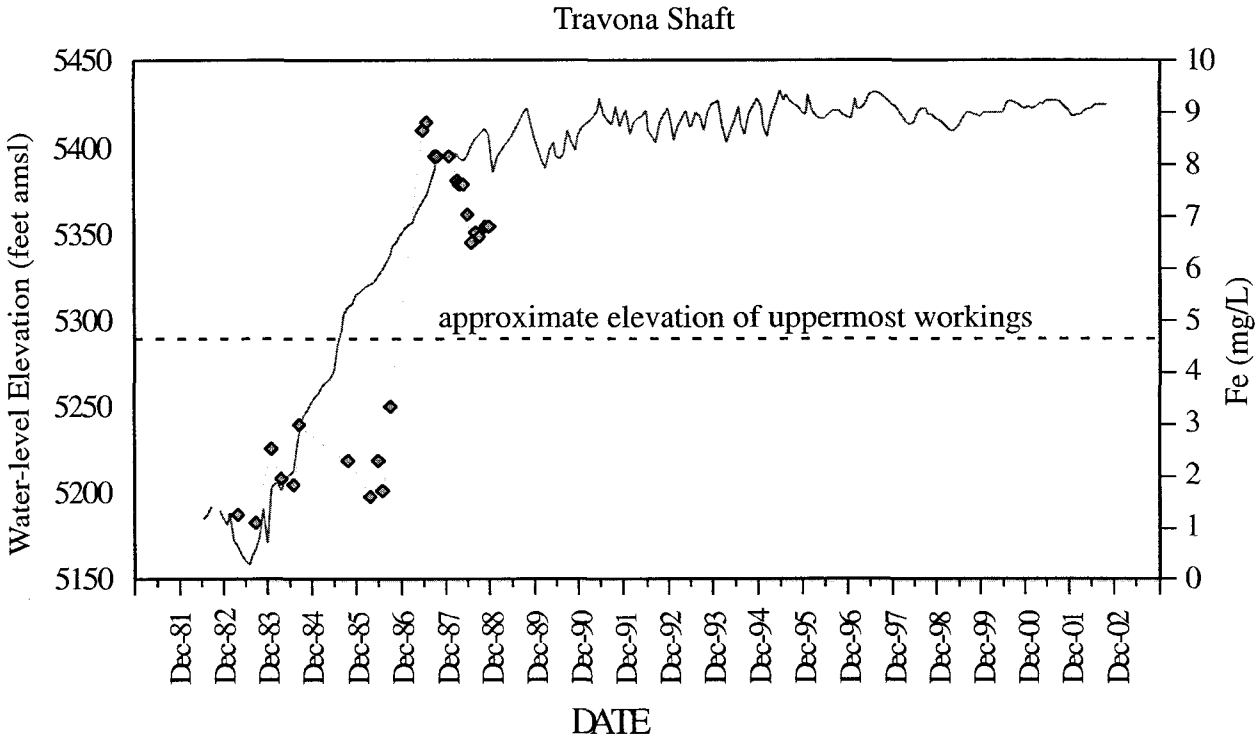

Figure 11. The concentration of iron compared to water levels in the Travona shaft. The largest increase in the concentrations of several dissolved constituents generally coincides with the flooding of the uppermost mine workings.

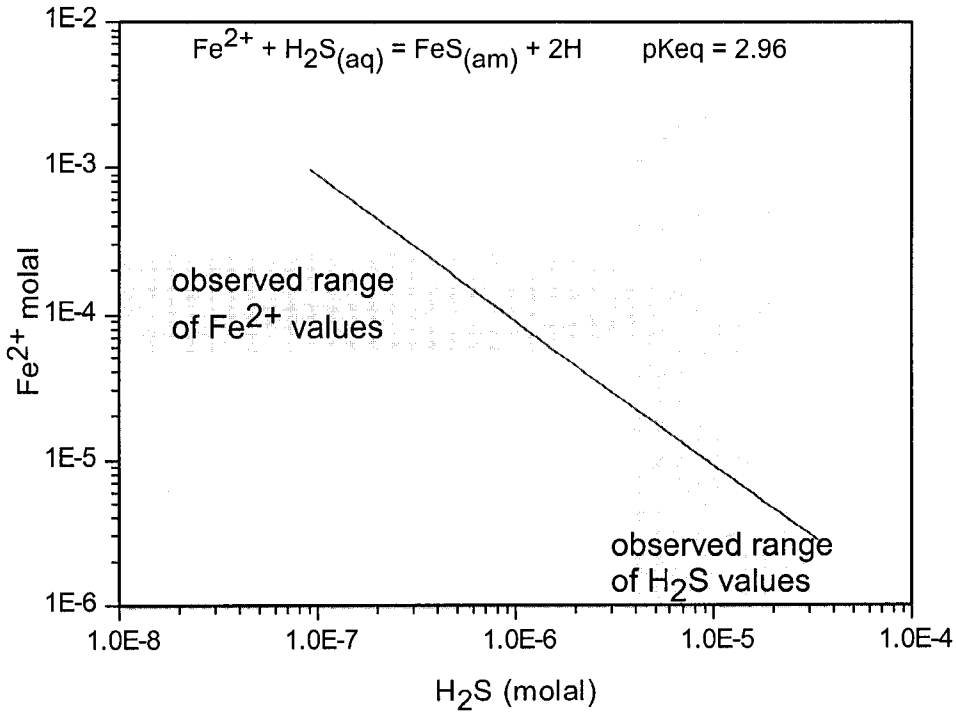

Figure 12. Solubility curve for Fe^{2+} at pH 6.5 based on Langmuir (1997, p. 427).

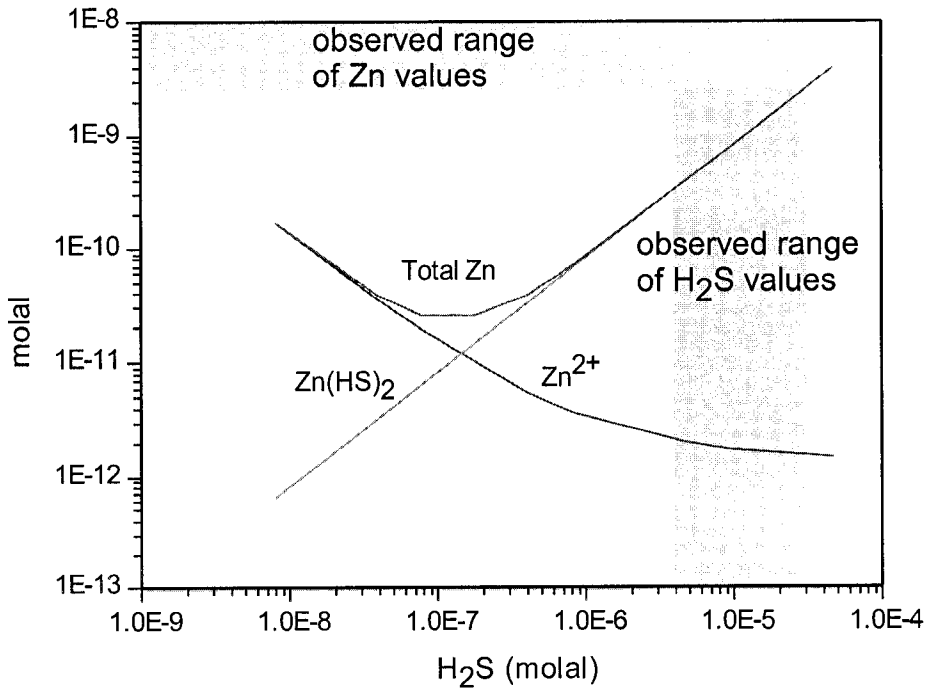

Figure 13. Solubility curve for sphalerite at pH 6.5 (after Dasklakis and Helz, 1993).

$$ZnS_{(s)} + H_2S^O = Zn(HS)_2^O \qquad \log K_{eq} = -5.3 \qquad (12)$$

and

$$ZnS_{(s)} + H_2S^O = Zn^{2+} + 2HS^- \qquad \log K_{eq} = -18.47 \qquad (13)$$

(Dasklakis and Helz, 1993)

Figure 13 presents solubility of Zn^{2+} with respect to H_2S over the range of total zinc and H_2S observed in the Travona shaft. Although the proportional relationship holds within the observed range of observations, the values for H_2S and total zinc predicted by the above equations are much lower than those observed. In the observed range of H_2S concentrations (4.0E-6 to 3.0E-5 molal), the observed zinc concentrations are generally greater than 2.0E-9 molal.

A second model was constructed to address the relationship between H_2S and iron and zinc concentrations. The model used to simulate the early period of flooding was used to represent baseline conditions with another step added to introduce H_2S. Table 4 compares model results for the period of mid-1987 during which concentrations showed the greatest change; the input file is described in detail in Appendix II. Figure 14 presents a graphical comparison between the model results and sample data for mid-1987. The model gives better results than the calculations based on individual reactions for iron. The change in H_2S concentration required to change the iron concentration was not enough to change the zinc concentration; this disagrees with the results predicted by Dasklakis and Helz (1993) presented in figures 12 and 13, but generally agrees with observed results.

Table 4. Comparison of model results to a sample collected in mid-1987 from the Travona shaft.

	Model		Travona		Difference		RPD*
Analyte	molality	mg/L	molality	mg/L	molality	mg/L	
Al	8.30e-07	0.02	<IDL**	0.00	-8.30e-07	-0.02	
As	2.86e-06	0.21	2.34e-06	0.18	-5.22e-07	-0.04	20
C	7.25e-03		7.52e-03		2.74e-04	3.29	4
HCO3-	4.08e-03		4.84e-03		7.59e-04	0.00	17
CO2	2.91e-03		2.93e-03		2.70e-05	0.00	1
Ca	5.15e-03	206.21	4.62e-03	185.21	-5.24e-04	-21.00	11
Cl	1.19e-03	42.15	9.80e-04	34.73	-2.09e-04	-7.42	19
Cu	8.43e-26	0.00	<IDL**		-8.43e-26	-0.00	
F	3.48e-05	0.66	2.11e-05	0.40	-1.37e-05	-0.26	49
Fe	1.13e-04	6.29	1.58e-04	8.83	4.54e-05	2.54	34
K	1.43e-04	5.61	1.28e-04	5.00	-1.54e-05	-0.60	11
Mg	2.42e-03	58.85	2.32e-03	56.45	-9.90e-05	-2.41	4
Mn	3.93e-04	21.57	5.25e-04	28.83	1.32e-04	7.26	29
Na	1.37e-03	31.53	2.87e-03	65.84	1.49e-03	34.31	70
S(6)	5.47e-03	175.34	4.08e-03	130.64	-1.39e-03	-44.69	29
Zn	1.55e-06	0.10	1.69e-06	0.11	1.38e-07	0.01	9
S(-2)	2.21e-06	0.08	no data	-	-	-	-

*relative percent difference

** less than instrument detection limit; RPD is not calculated

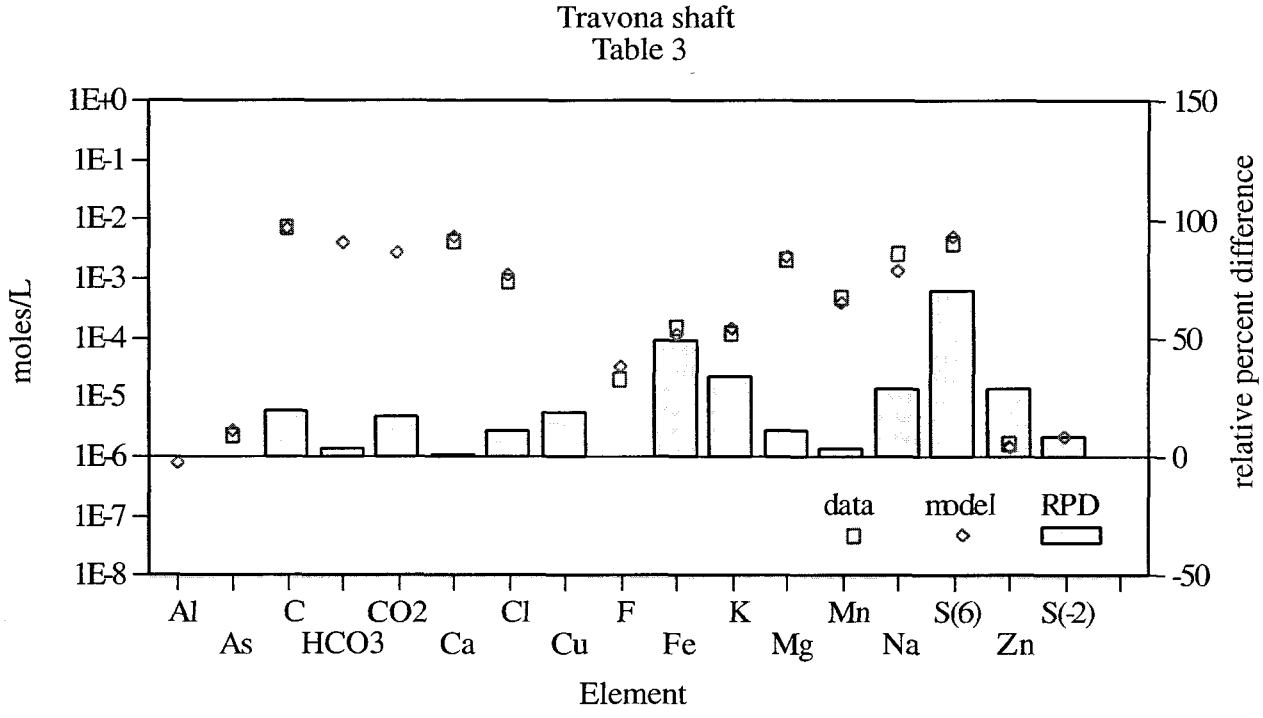

Figure 14. A comparison of concentration data generated by the model to sample results from the Travona shaft collected in 1987. The relative percent difference (RPD) was not calculated for sample data below the detection limit.

Period of 2nd Transition (1987 to present)

The concentration of nearly all of the dissolved constituents decreased steadily after the flooding of the uppermost workings of the Travona (figure 8). Concentrations of As III and As V indicate a slight decrease in redox conditions; H_2S measurements by Gammons and others (2003) indicate a slight increase in concentration compared to early flooding and a slight decrease compared to data collected during the pumping test of 1989. Pumping from the mine shaft was initiated in 1989 to control water levels. For the first several years, the shaft was pumped at 400 to 500 gallons per minute for several months and then allowed to rise. In 1995, pumping was made continuous and the pumping rate was reduced; in 1996, the pumping station (and sampling point) was moved from the shaft to a well completed in the upper workings. Modeling to reproduce the gradual decrease in concentrations during the latter period of flooding consisted of increasing the concentration of H_2S. The values of H_2S were increased from values used for the 1986-1987 period, but were less than those used to simulate the early period of flooding (1984-1986).

Summary of Travona Mine

With respect to several major cations and anions (e.g. Ca, Mg, K, Si, N, and Al), ground water flowing into the Travona mine shows variation greater than that of the water within the shaft. Conversely, other constituents such as arsenic, iron and zinc are controlled by processes within the workings of the mine.

Controls on the water chemistry of the Travona mine have varied with progress of flooding; there is evidence of at least minor acid generation in the earliest flooding of the mine in the 1950's. The Travona, and the West Camp in general, are upgradient of and isolated from the other mines in the district. As a result, the water chemistry is influence only by ground water flowing into the mine and local mineralogy rather than by waters flowing in from another mine. As the mine flooded, the interaction of mineral and oxygen was reduced and redox conditions favored the production of H_2S until this, more than any other influence, controlled the chemistry of iron, zinc and manganese.

Anselmo Mine

Water levels in the Anslemo shaft are the highest in the East Camp (figure 5). The shaft is down-gradient of the Travona (West Camp) and the Orphan Boy - Orphan Girl mines (Outer Camp). The Anslemo shaft gives an opportunity to evaluate the potential influence of up-gradient mines and provides the basis for evaluating the "source water" for down-gradient mines (Steward and Kelley).

Background

The Anselmo mine was originally developed as the Trifle mine for silver production in about 1900; by 1905, a shaft and workings to a depth of 150 feet (46 meters) were completed. At this depth silver values were marginal and interest in the mine waned. Sphalerite, however, was abundant, but there was little market for zinc, nor were there mills in the area capable of processing the ore until about 1910. By 1924, the Butte district was one of the world's largest producers of zinc (Daly and others, 1925) and the Anslemo was the largest producer of sphalerite in the district. The Anselmo mine was connected by workings to the Orphan Girl mine on the western edge of the district (Outer Camp) and to the Steward mine in the central portion of the district by 1925; at that time, the shaft was 1,900 feet (580 meters) deep. Ore production continued through the 1950's until all mining in the district was suspended by a worker's strike in 1959. Although many mines re-opened after the strike, operations were suspended at the Anslemo. At the time of closure the shaft was 4,300 feet (1,310 meters) deep and there were 27 levels of mine workings connected to 4 surface shafts and numerous raises. The mine was connected on several levels to the Steward mine east, to the Orphan Girl - Orphan Boy mines in the Outer Camp west, and to the Missoula mine through shallow workings northwest (figure 15). Although exploration drill holes extended that direction, there were no connections by workings to the Travona - Emma mines of the West Camp.

Pumping and draining of water from the Anslemo continued after the mine was closed in 1959 through 1982 when all pumping was stopped. Bulkheads and obstructions in the shafts prevented water-level monitoring and sampling until 1986 when water levels

rose to within 1,000 feet (300 meters) of the surface. Figure 16 presents the hydrograph and monthly water-level change for the Anslemo shaft. Two of the main levels, the 800 and 600 levels, have been flooded within the period of record. These levels coincide with major connections to the Steward and other mines of the East Camp as reflected in the change in slope of the hydrograph. The most notable changes in the rate of water-level rise occurred in 1988, 1995, and 2000; the first two rate changes coincide with the flooding of the 800 and 600 level. Smaller variations in monthly water-level change probably coincide with subordinate workings (raises and stopes) within the Anselmo that are not connected to the shaft. The water-level rate change diminished as water levels rose and fewer workings were available for flooding.

Mineralogy

As noted, the primary ore mineralization in the Anselmo is sphalerite; chalcopyrite, bornite, and chalcocite are present in only small amounts above the 2800 level (about 2,400 feet [730 meters] below the surface). Pyrite is never mentioned in any documentation on the mine and very little was observed in related specimens in the Anaconda Collection. At the depth of about 2,400 feet (730 meters), the Anselmo workings transcend the Central Zone - Intermediate Zone boundary characterized by the outer limit of copper minerals and the inner limit of zinc minerals (sphalerite). This transition from the intermediate zone to the peripheral zone was first described by Sales (1914) and later mapped by Meyers and others (1968). Specimens from this area of the mine showed a marked increase in pyrite, chalcopyrite, and bornite.

Wall-rock alteration minerals in the Anselmo grade from argillic, montmorillonitic of a greenish cast to more intense kaolinitic alteration next to the vein. The main shaft and many of the mine workings near the shaft expose a large, east-west striking, rhyolite dike that extends below the deepest workings. Alteration near this dike is reportedly intensely kaolinitic.

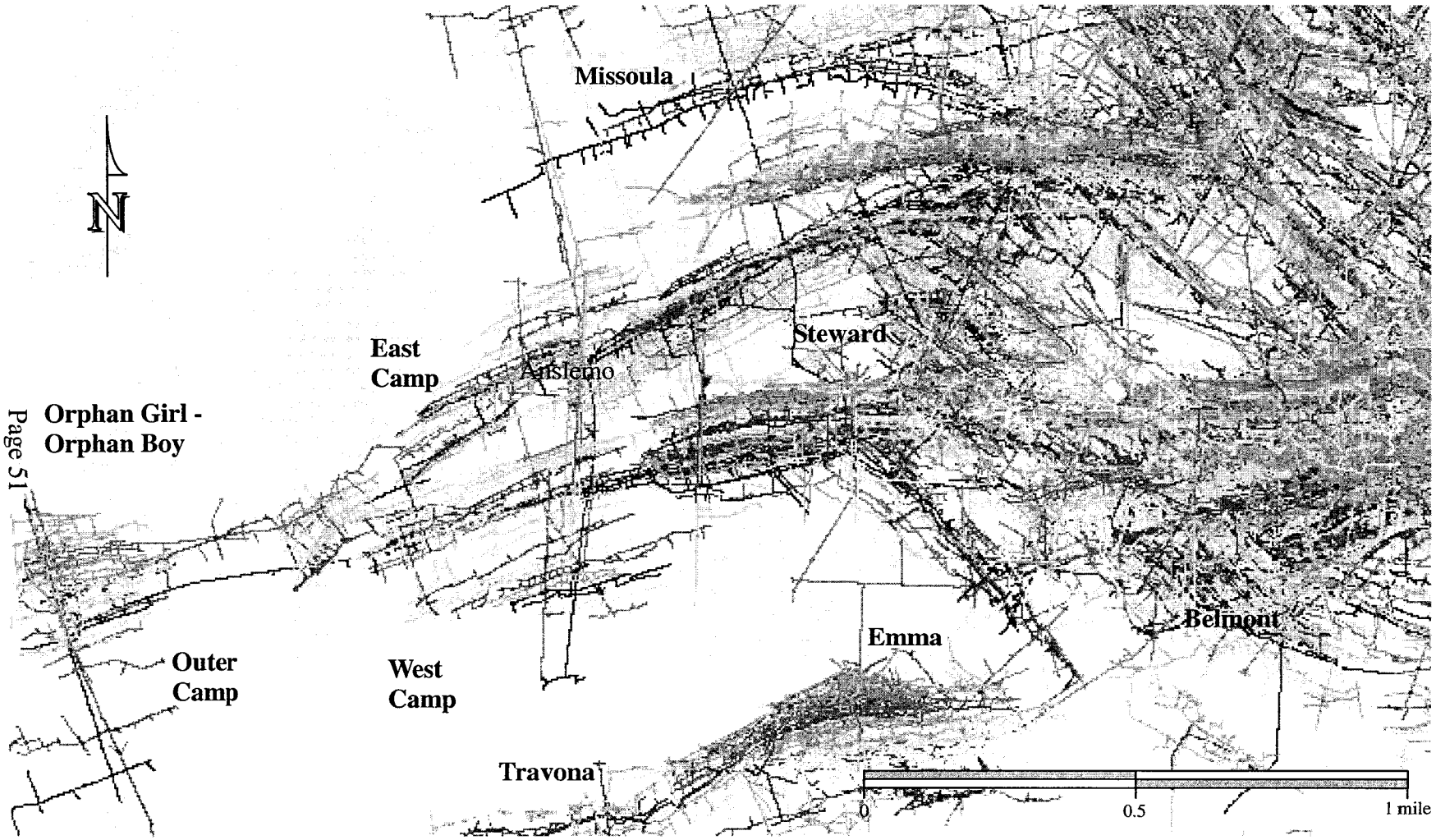

Figure 15. Composite map of mine workings in the East Camp (Anslemo, Missoula, Steward, and Belmont mines), in the West Camp (Travona, Emma, and Ophir mines) and the Outer Camp (Orphan Girl - Orphan Boy mine).

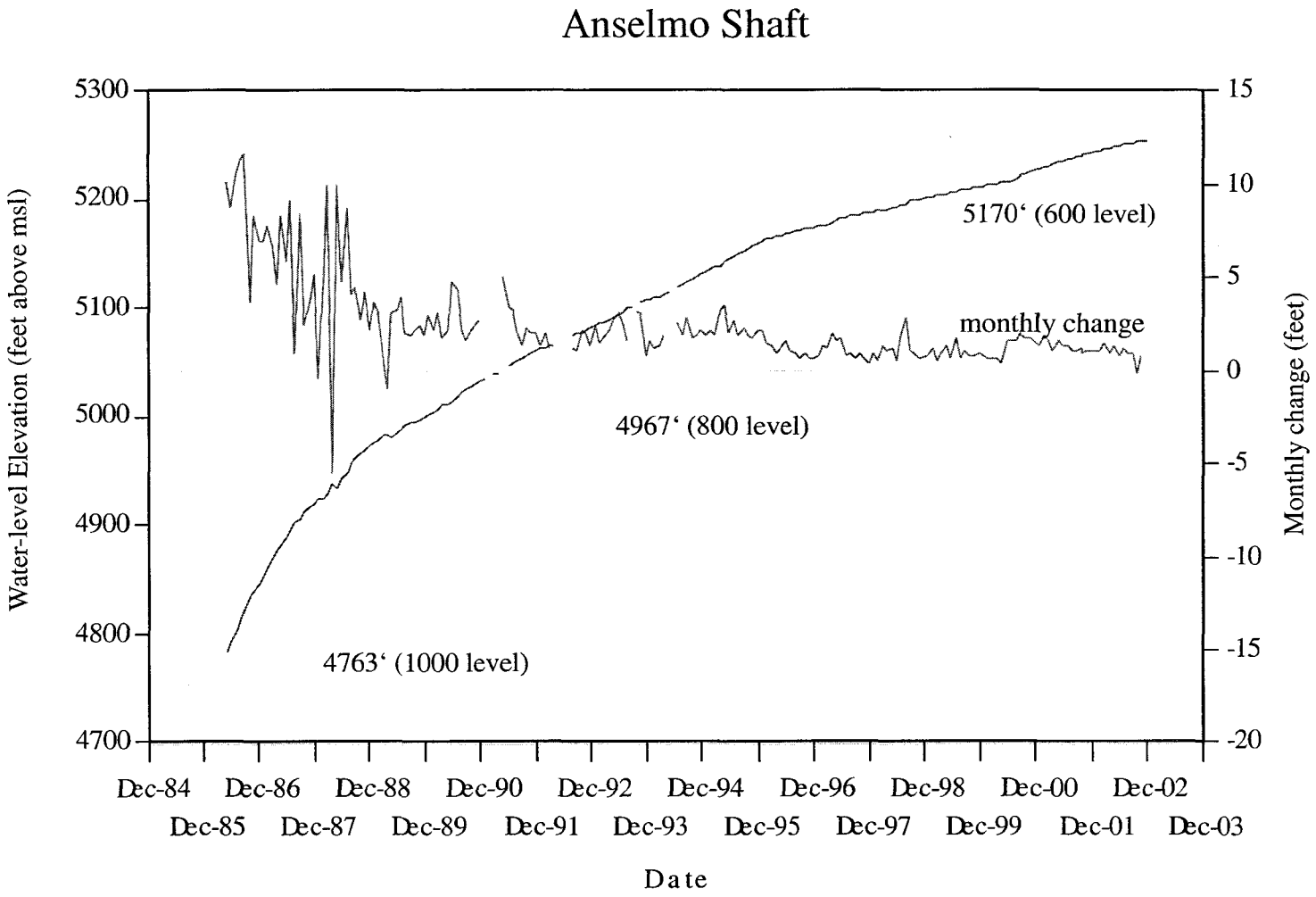

Figure 16. Water levels compared to mine-workings elevations in the Anselmo mine. Two levels of mine workings have been flooded within the period of record. The monthly water-level change decreased as flooding continues.

Water Quality

Concentrations of dissolved constituents in the Anselmo shaft are generally low compared to other mines of the East Camp. Arsenic concentrations are usually less than 12 μg/L and are much lower than those of the Travona and Emma mines (> 100 μg/L) of the West Camp. Similarly, iron concentrations in the Anslemo shaft are less than 1 mg/L compared to 7 mg/L in the Travona shaft. Manganese concentrations have varied between 8 and 24 mg/L in the Anselmo (figure 17)and are about 18 mg/L in the Travona. Sulfate concentrations in the Anselmo are about 1000 mg/L and have varied through the period of record. Most notable is the high concentration of zinc (compared to less 50 μg/L in the Orphan Boy and less than 20 μg/L in the Travona) and its variation from 6,000 to almost 60,000 ug/L over the period of record (figure 17). Zinc concentrations also show a slight downward trend and sulfate shows a slight upward trend over the period of record.

Nearly all of the dissolved constituents exhibit a cyclical variation in concentration over the 19-year sampling period. The largest variations appear to coincide with the changes in the water-level rate change. Zinc, for example, increased from 10,000 to nearly 60,000 and back to 10,000 μg/L in 1989 (figure 17); this coincides with the flooding of the 800 level of the mine. The 600 level was flooded in about 1996; the concentration of zinc and several other constituents increased in the following year. Also notable is the observation of mild degassing of some samples from the shaft. Although no direct sampling of the gas was conducted, there was no evidence of H_2S and, more likely, the gas is comprised of at least some CO_2.

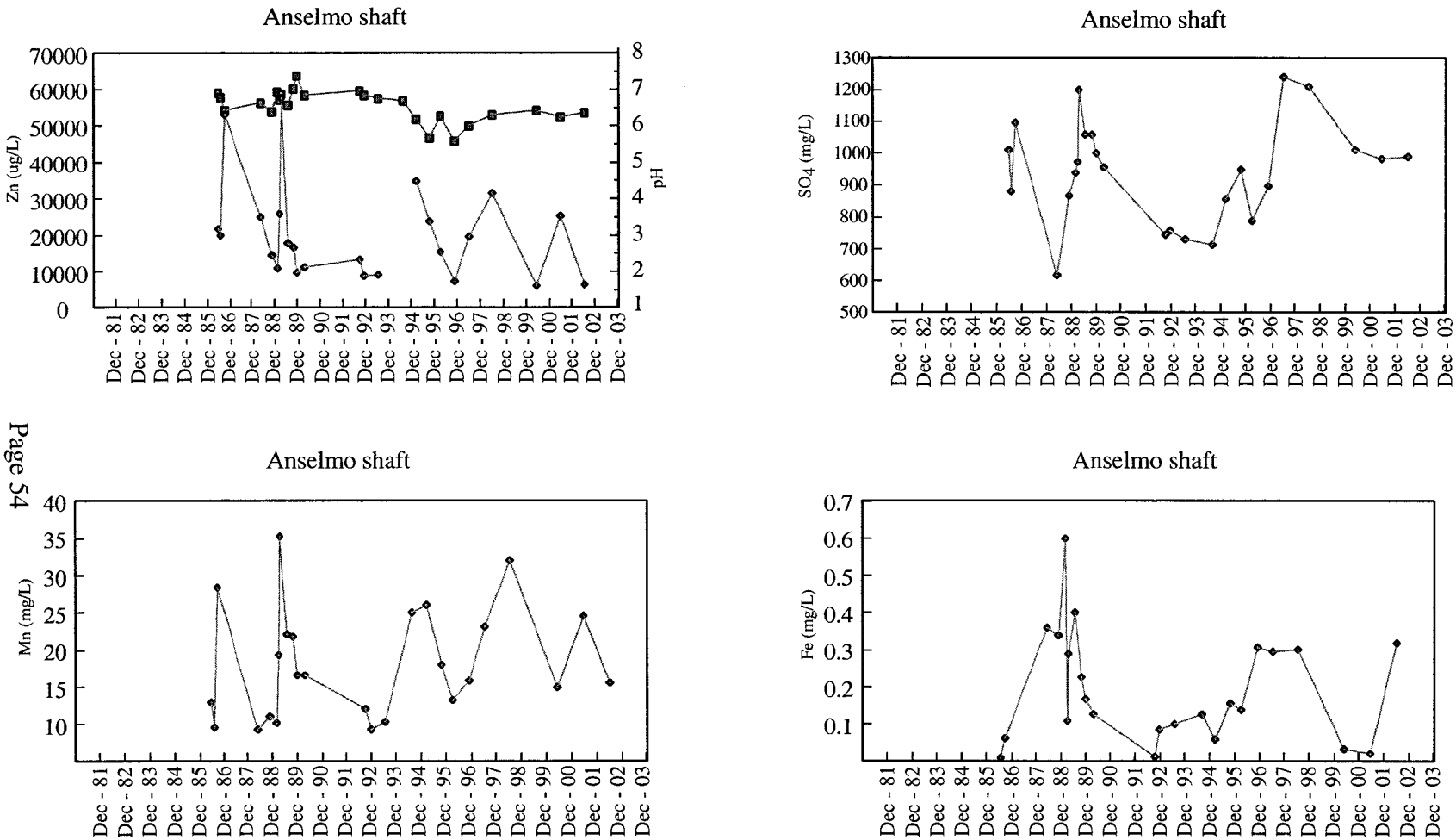

Figure 17. The concentration trends in the Anselmo shaft. The trends generally reflect flooding of the workings; Large changes in chemistry in 1988, 1994, and 1996 coincide with the flooding of mine levels with extensive workings.

Equilibrium Modeling - Anselmo shaft

The equilibrium model, PHREEQECI (Charlton and others, 1997) was used to evaluate the controls on the shaft water-chemistry, particularly zinc and manganese concentrations during the flooding of the Anslemo mine. Minerals indigenous to the mine (table 5) were equilibrated with water whose chemistry represented ground waters entering the mines. Oxidation-reduction potential and the concentration of dissolved CO_2 and O_2 was varied until calibration with measured concentrations was achieved. No direct measurements of dissolved CO_2 or O_2 have been conducted on samples from the Anselmo. Thus, the lower limit of the partial pressure of CO_2 was assumed to be at atmospheric conditions ($P_{CO2} = 10^{-3.5}$ atmospheres [atm]). The upper limit of the partial pressure of CO_2 was assumed to be 1 atmosphere based on the observation of effervescence during some sampling; the partial pressure must exceed ambient pressure to cause the degassing. The lower limit for the partial pressure of O_2 was assumed to be 0 and the upper limit was assumed to be that of surface water under atmospheric conditions (0.2 atm). As with other simulations, concentration data from shallow monitoring wells were used with the assumption that the water quality of the ground water recharging the mine is constant. All of the mineral phases listed were used throughout the simulation.

Table 5. Mineral phases used in the Anselmo simulation.

Mineral Phase	comments
Sphalerite	ore mineral in shallow workings
Kaolinite	alteration mineral
Quartz	country rock
Rhodochrosite	reported as "occurrences"
Chalcopyrite	ore mineral in deep workings
Arsenolite	based on tennantite (rare)

Table 6 presents a comparison between the model based on minerals in table 5 and those of a sample collected early in the period of record. The model results generally agree well with those of the sample, except for copper and sulfate. Figure 18 compares model results to sample data obtained during the early period of flooding.

Table 6. Comparison of model results with sample collected in the early period of flooding (1984) of the Anselmo shaft.

Analyte	Model molality	mg/L	Anselmo molality	mg/L	Difference molality	mg/L	RPD*
Al	2.330E-006	0.06	1.077E-006	0.03	-1.25E-006	-0.03	74
As	7.213E-008	0.01	6.418E-008	0.005	-7.95E-009	-0.00	12
CO_2	1.363e-002		1.731e-002		-3.68E-003		24
HCO3-	4.377e-003		4.426e-003		-4.90E-005		1
Ca	5.146E-003	206.25	7.548E-003	302.52	2.40E-003	96.27	38
Cl	1.189E-003	42.15	9.042E-004	32.05	-2.85E-004	-10.10	27
Cu	3.278E-010	0.00	3.153E-007	0.02	3.15E-007	0.02	200
F	3.478E-005	0.66	4.218E-005	0.80	7.40E-006	0.14	19
Fe	1.854E-007	0.01	1.794E-007	0.01	-6.00E-009	-0.00	3
K	1.434E-004	5.61	1.947E-004	7.61	5.13E-005	2.01	30
Mg	2.421E-003	58.85	4.001E-003	97.26	1.58E-003	38.41	49
Mn	2.023E-004	11.11	2.352E-004	12.92	3.29E-005	1.81	15
Na	1.372E-003	31.53	2.092E-003	48.07	7.20E-004	16.55	42
S(6)	5.675E-003	181.94	1.053E-002	337.59	4.86E-003	155.65	60
Zn	3.270E-004	21.38	3.326E-004	21.75	5.60E-006	0.37	2

* relative percent difference

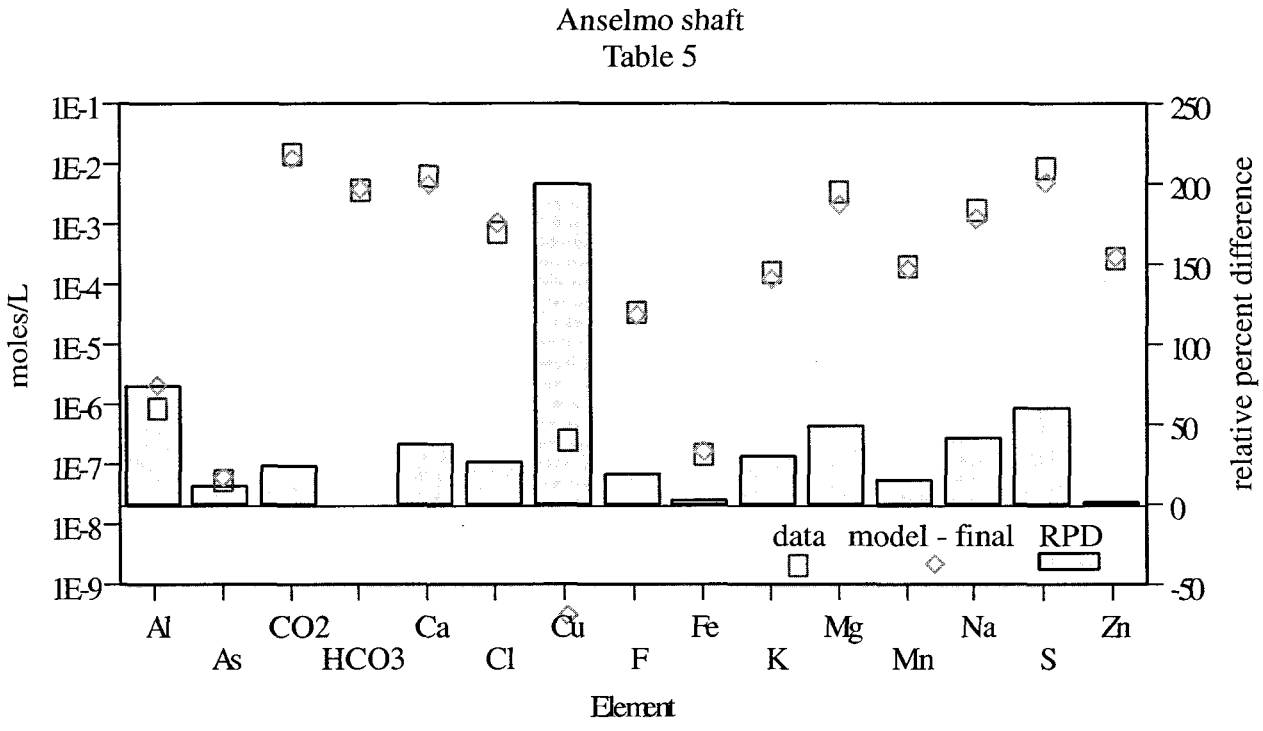

Figure 18. Concentration data generated by the model are compared to sample data from the Anselmo shaft. The model results generally agree with data collected from the shaft except for copper. In this simulation background water was equilibrated with Anselmo minerals including sphalerite and chalcopyrite.

Other constituents of interest may or may not show sensitivity to O_2 or CO_2 concentrations. Most concentrations, however, fall within the range of calibration without large adjustments to either gas. Figures 19 and 20 compare the effects of increasing dissolved O_2 at a fixed high partial pressure of CO_2 (0.1 atm) and at the fixed atmospheric partial pressure of CO_2 ($10^{-3.5}$ atm), respectively. Copper and zinc show the greatest sensitivity with a 2 to 3 order of magnitude range at a high partial pressure of CO_2 (figure 19) and show a 1 order of magnitude sensitivity at atmospheric partial pressure of CO_2 (figure 20). Both copper- and zinc-carbonates form in the presence of high CO_2 and, particularly for copper, limit the solubility: chalcopyrite and sphalerite are oxidized, but combine with the abundant CO_2 to from carbonates. In both cases, the range of zinc concentration is within the range of observed measurements even with the formation of zinc-carbonate. Conversely, copper only approaches the observed values at low partial pressure of CO_2 and high partial pressure of O_2 (figure 20); chalcopyrite is oxidized, but copper-carbonate does not form. At these partial pressures, however, aluminum concentrations are far below the observed range. The input file for simulating the effects of CO_2 and O_2 is described in more detail in Appendix III.

Oxidation of chalcopyrite and sphalerite

In the preceding simulations increasing the P_{CO2} from atmospheric conditions ($10^{-3.5}$ atm) to as much as 0.1 atm, increases the dissolution of sphalerite (pH is reduced and pe is increased), but does little to produce sufficient Cu concentrations. In fact, chalcopyrite did not dissolve under any conditions in the presence of sphalerite). Conversely, the presence of chalcopyrite or its dissolution products exerts little control on the oxidation of sphalerite.

Oxidation by dissolved O_2 increases the amount of dissolution for both minerals, of course, but the dissolution ratio of sphalerite to chalcopyrite remains the same. Simulating conditions for the Anslemo shaft where the background inflow water is equilibrated with chalcopyrite and sphalerite with concentrations of CO_2 and O_2 varied within the expected conditions, little or no chalcopyrite is dissolved and, in most cases, total copper concentrations decrease because of the formation of copper-carbonate

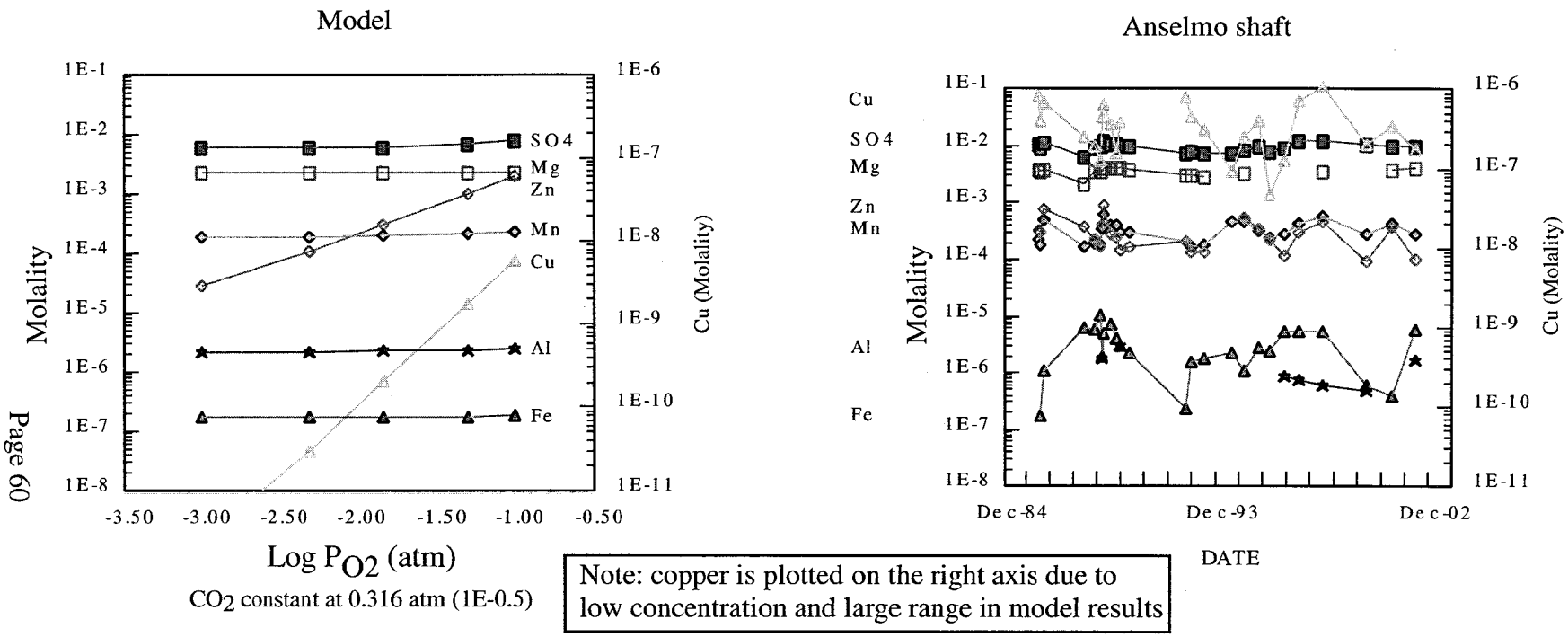

Figure 19. The results of modeling high partial pressure of CO_2 and changing O_2 is compared to the range of sample data from the Anselmo shaft. Simulating conditions with a relatively high partial pressure of CO_2 produces results that tend to agree with observed concentrations except for copper.

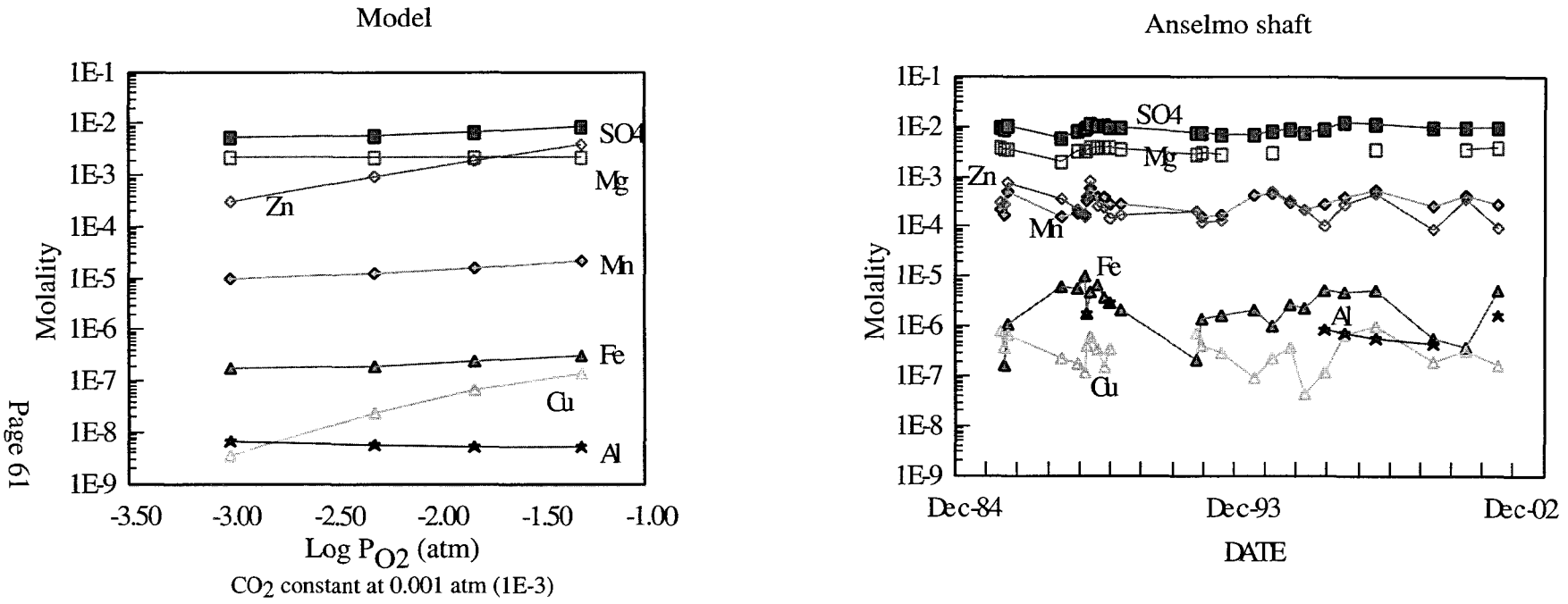

Figure 20. The results of modeling low partial pressure of CO_2 and changing O_2 is compared to the range of sample data from the Anselmo shaft. Simulating conditions with a relatively low partial pressure of CO_2 produces results that tend to underestimate observed concentrations except for copper.

or -sulfate complexes (table 7). The input file and description of the model is provided in the Appendix III.

Table 7. Oxidation of chalcopyrite and sphalerite at various concentrations of CO_2 and O_2; other minerals present in the Anselmo mine were excluded from these simulations.

P_{CO2}(atm)	P_{O2} (atm)	Zn (mol/L)	Cu (mol/L)	SO_4 (mol/L)	pe (mv)	pH
-3.5	-4.0	1.1E-005	7.5E-012	5.4E-003	-2.4	7.31
-3.5	-0.7	4.2E-003	1.5E-007	9.6E-003	-1.8	6.90
-2.0	-4.0	1.1E-005	4.6E-012	5.4E-003	-2.1	7.04
-2.0	-0.7	4.2E-003	1.2E-007	9.6E-003	-1.6	6.80
-1.0	-0.7	4.2E-003	4.2E-008	9.6E-003	-0.1	6.20
Observed		1 to 8E-004	1.3 to 8E-007	1.0E-002	6.0 to 7.4	
Inflow		8.3E-006	1.3E-007			

The apparent "competition" between chalcopyrite and sphalerite exists whether the oxidation reactions are driven by O_2 or Fe^{3+}. Indeed, the higher solubility of sphalerite manifests itself in the processing of the ores. Flotation of ore minerals relies on the adherence of finely crushed sulfide particles to air bubbles rising through the solution. The bubbles and sulfides are then adsorbed on a froth of carbon-based collectors. Each sulfide ore exhibits different responses to flotation and collection; strict control of the process enables selectivity in the recovery of each metal. Sphalerite presents a unique problem in flotation due to its high solubility and its neutral surface charge.

Flotation of sphalerite requires "activation" of the mineral surface by inducing the precipitation of another sulfide. Arsenic is often used in low pH (4-5) solutions; copper is often used in neutral-pH solutions. Early studies using copper sulfate (for example, Ravitz and Wall, 1934) as the activator described an ionic exchange between zinc and copper on the surface of the mineral:

$$ZnS + Cu^{2+} = CuS + Zn^{2+}$$

More recent studies suggest other sulfides such as covellite or a bi-metallic compound ($Zn_{1-x}Cu_xS$) is precipitated (Kartio and others, 1998). Bacterial leaching of sulfide-ores also demonstrates the control of sphalerite on metals recovery. Zinc from sphalerite is far more readily solubilized than iron or copper from pyrite or chalcopyrite (Harahuc, 2000). The rate of sphalerite oxidation by ferric iron is enhanced by the same *Thiobaccillus ferrooxidans* bacteria involved in the indirect oxidation of pyrite (Fowler and Crundwell, 1998).

Sphalerite and chalcopyrite oxidation by Fe^{3+} are similar, but the oxidation of chalcopyrite produces more acid and requires more Fe^{3+}:

$$ZnS + \mathbf{8Fe^{3+}} + 4H_2O > Zn^{2+} + SO_4^{2-} + 8Fe^{2+} + 8H^+ \qquad LogK = -47.23$$

$$CuFeS_2 + 8H_2O + \mathbf{16Fe^{3+}} > Cu^{2+} + 17Fe^{2+} + 2SO_4^{2-} + 16H+ \qquad LogK = -102.67$$

It would require a concentration of 6.4E-06 mol/L of Fe^{3+} to produce the concentration of copper (4.0E-07) observed in the Anslemo shaft; however, an additional 1.2E-03 mole/L Fe^{3+} is required to produce the 3.0E-04 mol/L concentration of zinc also observed in the shaft. This far exceeds even the highest total iron concentration observed (6.4E-06 mol/L).

The alternative means of sphalerite and chalcopyrite oxidation are by dissolved oxygen:

$$ZnS + 2O_{2(aq)} > Zn^{2+} + SO_4^{2-} \qquad LogK = -45.32$$

$$CuFeS_2 + 4O_{2(aq)} > Cu^{2+} + Fe^{2+} + 2SO_4^{2-} \qquad LogK = -102.67$$

Assuming a partial pressure of 3.16E-03 atm for CO_2 (atmospheric conditions), 2.0E-02 atmospheres of O_2 will produce 4.1E-4 mol/L zinc and an equal amount of sulfate from sphalerite. Again, assuming an atmospheric partial pressure of CO_2, 4.0E-05 atmospheres

of O_2 will produce about 4.0E-07 mol/L copper, an equal amount of iron and twice that amount of sulfate from chalcopyrite. The concentrations of these products are well within the range observed in the Anslemo shaft.

As with oxidation by Fe^{3+}, oxidation of chalcopyrite in the presence of sphalerite requires considerably higher partial pressure of O_2. A partial pressure of 0.2 atmospheres of O_2 is required to produce 1.7E-07 mol/L copper. At this partial pressure, however, sphalerite oxidation produces 4.1E-03 mol/L of zinc which is about one order of magnitude greater than that observed in the shaft samples.

The chalcopyrite - sphalerite oxidation issue leads to two possible models for the Anslemo shaft. Down-hole camera data indicates a slight but consistent upward flow of water in the upper 1,000 feet (300 meters) of the shaft. Whether driven by pressure differences within the flooding workings or by a geothermal gradient with warmer waters rising from the depths, some type of mixing must occur. In either case, there must be some upward flow of water in the working to produce the dissolved copper observed.

In the first model, chalcopyrite is oxidized and equilibrated with inflow water in the deeper workings and sphalerite is oxidized and equilibrated with inflow water in the shallow workings. The two waters then mix as the deeper water circulates upward.

The second model is similar to the first in that chalcopyrite is oxidized in the deeper workings and sphalerite is oxidized in the upper workings. Rather than mixing, however, sphalerite and other minerals are equilibrated with the water from the deeper workings rather than with "fresh" inflow water. Table 8 presents the results of the first model where mixing occurs; a graphical comparison is presented in figure 21. The mixture of the two waters that produced the best comparison to observed data used 10% of the deeper waters. An annotated input file and flow diagram used for the model is provided in Appendix III. The results generally show good agreement except for aluminum and sulfate.

Table 8. Results of mixing deep and shallow waters compared to data from the Anselmo shaft (all values are mol/L).

	Deep	Shallow	best mix 10% deep	Anselmo	RPD
CO2 (atm)	3.16e-04	3.16e-01			
O2 (atm)	5.00e-05	1.00e-02			
Al	1.16e-07	1.15e-05	1.03e-05	1.08e-06	162
As	7.21e-08	7.21e-08	7.21e-08	6.42e-08	12
CO2	4.53e-04	4.47e-04	1.36e-02	1.73e-02	24
HCO3	4.05e-03	4.04e-03	4.42e-03	4.43e-03	0
Ca	5.15e-03	5.15e-03	5.15e-03	7.55e-03	38
Cl	1.19e-03	1.19e-03	1.19e-03	9.04e-04	27
Cu	7.39e-07	1.73e-07	2.30e-07	3.15e-07	31
F	3.48e-05	3.48e-05	3.48e-05	4.22e-05	19
Fe	9.25e-07	3.59e-07	4.15e-07	6.79e-07	48
K	1.43e-04	1.43e-04	1.43e-04	1.95e-04	30
Mg	2.42e-03	2.42e-03	2.42e-03	4.00e-03	49
Mn	8.24e-06	1.98e-04	1.79e-04	2.35e-04	27
Na	1.37e-03	1.37e-03	1.37e-03	2.09e-03	42
SO_4	5.36e-03	5.57e-03	5.55e-03	1.05e-02	62
Zn	8.35e-06	2.21e-04	1.99e-04	3.33e-04	50

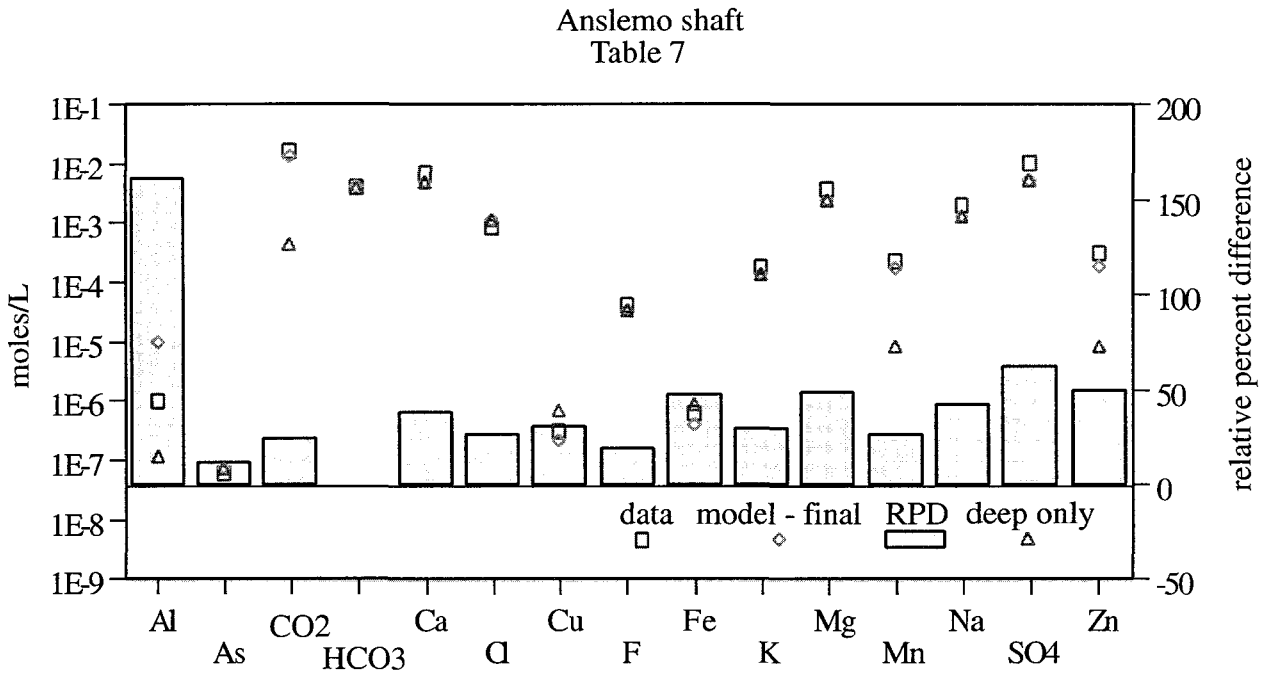

Figure 21. Sample chemistry from the Anselmo shaft are compared to model results where shallow and deep waters are mixed. The results of the deep equilibration model before mixing are also shown.

Table 9 presents a comparison of the simulation where deep waters are equilibrated with minerals in the shallow workings; the input file is described in more detail in Appendix III. Figure 22 presents a graphical comparison between the model results and sample data. These results are similar to those of the mixing model, but there is better agreement with observed data for aluminum and sulfate.

Table 9. Results of deep waters equilibrated with shallow minerals in the Anselmo shaft compared to sample data (all values are mol/L).

	Modeled Deep	Modeled Shallow	Anselmo	RPD*
CO_2 (atm)	3.16e-04	3.16e-01		
O_2 (atm)	5.00e-05	1.00e-02		
Al	8.21e-09	2.31e-06	1.08e-06	73
As	7.21e-08	7.21e-08	6.42e-08	12
CO2	4.51e-04	1.36e-02	1.73e-02	24
HCO3	4.07e-03	4.43e-03	4.43e-03	0
Ca	5.15e-03	5.15e-03	7.55e-03	38
Cl	1.19e-03	1.19e-03	9.04e-04	27
Cu	7.40e-07	7.40e-07	3.15e-07	81
F	3.48e-05	3.48e-05	4.22e-05	19
Fe	9.26e-07	9.25e-07	6.79e-07	31
K	1.43e-04	1.43e-04	1.95e-04	30
Mg	2.42e-03	2.42e-03	4.00e-03	49
Mn	8.77e-06	2.12e-04	2.35e-04	10
Na	1.37e-03	1.37e-03	2.09e-03	42
SO_4	7.44e-03	7.66e-03	1.05e-02	32
Zn	8.35e-06	2.21e-04	3.33e-04	40

*relative percent difference between the Modeled Shallow results and the Anselmo.

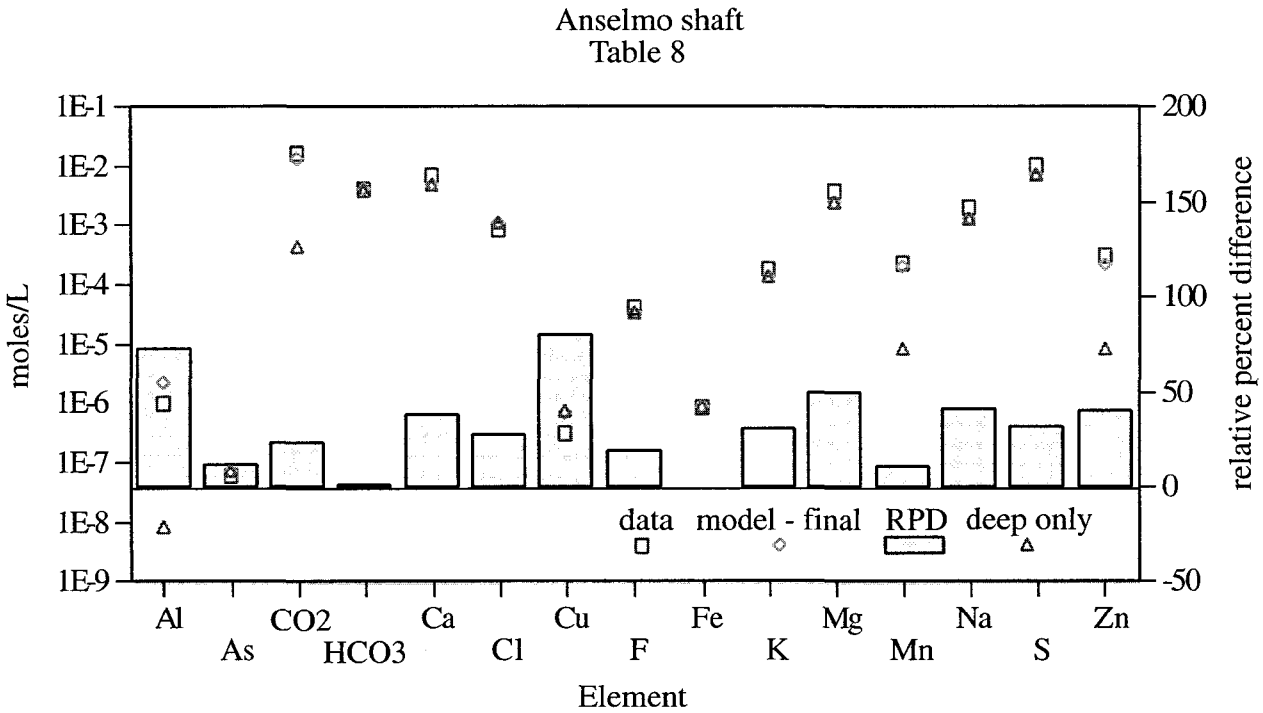

Figure 22. Model concentration results from equilibrating deep and shallow waters is compared to data collected from the Anselmo shaft. The results of the deep equilibration model before equilibration with shallow minerals are also shown.

Summary of Anslemo mine

The mineralogy of the Anselmo mine reflects the transition from "copper mineralization" of the intermediate zone to the "sphalerite mineralization" of the peripheral zone described by Myer and others (1968). The transition coincides with the workings of the 2800-level, about 2,400 feet (730 meters) below the surface. Water samples from the shaft were restricted to a depth of 1,000 feet (300 meters) or less due to a bulkhead. Down-hole video shows a notable upward flow of water at depths below about 100 feet (30 meters) as indicated by the movement of particulate matter. The water then likely flows eastward through workings connected with the Steward mine (next section).

Water-quality in the Anselmo shaft shows some degree of correlation between the flooding of mine levels and the difference in the concentration of several constituents. As waters flood new workings, oxidized minerals (particularly chalcopyrite and sphalerite) are dissolved in the flooding waters and their influence is greatest. As flooding continues between the levels with workings, oxidation and dissolution of these minerals is less important. Equilibrium modeling demonstrates the influence of mineral solubility under the conditions found in the shaft. When compared to the products of solubility such as iron and sulfate, sphalerite oxidation exerts greater control than chalcopyrite on the final chemistry of water in the shaft. Chalcopyrite in the deeper or eastern workings of the mine is oxidized at moderately low partial pressures of O_2. The water then flows upward through the shaft and through the shallower mine workings. Sphalerite is oxidized under similar conditions to produce dissolved zinc and sulfate. Minor fluctuation of CO_2 levels, likely caused by microbial decay of wood, and the fluctuation of O_2 levels, caused by the variation between flooding workings, are sufficient to cause the variation in the concentrations of several constituents. As the upper workings become flooded and the available space for O_2 diminishes, sphalerite oxidation will decline and zinc concentrations will decrease.

Steward and Kelley mines

Background

The Steward and Kelley mines were the last fully active underground mines in the Butte district just prior to flooding. Access to these shafts and nearly 4,000 feet (1,232 meters) of clear access down the shafts for sampling enabled detailed monitoring throughout the flooding of the mines, especially during the first few years of flooding when water-levels and water-chemistry changed on a daily basis. Although these two mines differ with respect to ore production, mineralogy, and mine construction, they are treated here as a single topic because they were intricately related in the first years of flooding. Also included in this discussion is the Belmont mine which was mined via the Steward workings and was included in the early monitoring efforts.

There are two distinct time periods during the flooding of these mines: the period of early flooding before water levels rose to the bottom of the Berkeley Pit, and the later period after the pit began to fill.

The Steward mine is one of the oldest mines in the Butte area (figure 23). The mining claim was patented by the famous W.A. Clark in 1877 and the mine started soon after. In the period from 1877 to 1895, the primary production from the mine was silver ore. In 1895, the mine production had shifted from silver to copper and prompted the construction of several large mills and smelters along Silver Bow Creek. The main shaft reached a depth of about 4,156 feet (1266 meters) (1,756 feet [535 meters] amsl) with 31 levels of workings. Information on the early history and ore production at the Belmont mine is scarce. In the 20 years prior to shut-down copper ore was mined and transported from the Belmont via underground to the Steward mine. The shaft reached a depth of nearly 3,800 feet (1,160 meters) with 27 levels of workings that extended northeast along the Rarus Vein (Berkeley Pit) or northwest to the Steward mine.

The Kelley mine, started in 1947, was a relatively new mine in the Butte district, but was one of the largest and most productive (figure 23). Unlike other mines however, the workings of the Kelley were not constructed to retrieve ore in the vicinity of the shaft,

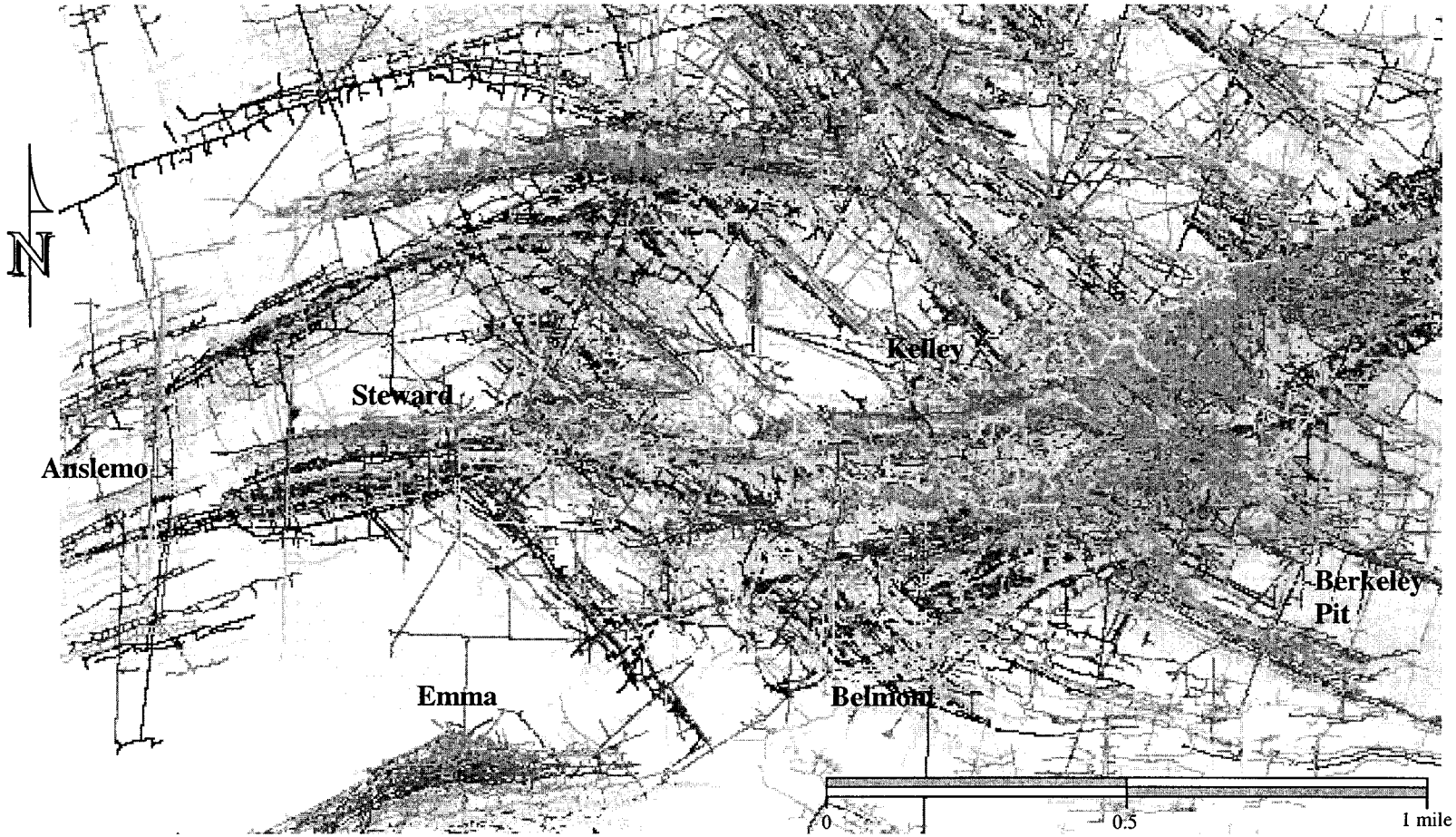

Figure 23. Composite map of mine workings in the East Camp near the Berkeley Pit. The West Camp mines (Emma) are connected to the East Camp (Belmont), but the workings were reportedly bulkheaded in the 1950's.

but rather to transport ore from other mines in the area of the Berkeley Pit and serve a centralized ore transport and water management system for the entire district. The Kelley was also used to experiment with a new mining method by "cave-blocking" and hoisting large volumes of low- grade ore to the surface for leaching. A reported 15,000 tons of ore per day were produced during the 1950's - the most production of any mine in the area. The mine was served by 3 shafts operating on 41 working levels and six haulage levels from nearby mines including the Anslemo, Steward, and Belmont mines. The main shaft was about 4,810 feet (1,466 meters) deep with a bottom elevation of 1,159 feet (353 meters) amsl.

All three of these mines were operated in some capacity until 1975, when all underground mining in the Butte district was suspended. Pumping from the mines was reduced slightly in 1978 when the lowest levels were flooded to the 4000 level of the Kelley mine.

Mineralogy

The workings of the Steward mine exploit minerals of the Intermediate Zone between the Anselmo in the Peripheral Zone and the Kelley mine which lies on the western (outer) edge of the Central Zone. The Intermediate Zone is characterized as the transition from sphalerite-dominated mineralization to chalcopyrite - bornite dominated mineralization. Meyer and others (1968) mapped the "inner edge" of the sphalerite zone as mid-way between the Steward and the Kelley mine to the east and the "outer edge" of the copper zone mid-way between the Steward and the Anselmo mine to the west (figure 24). Sales (1913) described the Intermediate Zone as predominantly copper (chalcopyrite), but "seldom free of sphalerite". Meyer and others (1968) place the Belmont mine in the Peripheral Zone with the Steward mine; however, workings extend well into the Central Zone. Thompson (1973) reported a production rate of 800 to 900 tons per day from both mines for that year and an average ore assemblage of 40% bornite, 30% chalcopyrite, 15% tennantite, 10% enargite, and 5% chalcocite. In the years just prior to suspension, most production was from the deeper workings that exploited the

pyrite - chalcopyrite zone (figure 24). Rock alteration is generally described as slightly more intense than that of the Anselmo: primarily argillic (montmorilillonite or kaolinite) to mildly sericitic near the veins.

The mineralogy of the Kelley is rarely discussed in the literature, but rather as the western (outer) margin of the Central Zone most often characterized as abundant in copper ore and free of sphalerite. Like the Steward and Belmont mines, the Kelley workings also expose the transition from deep, large pyrite-chalcopyrite veins to enargite-chalcocite-bornite veins (figure 24). As noted, the mine served a unique purpose of transport for other, traditional mines in the district.

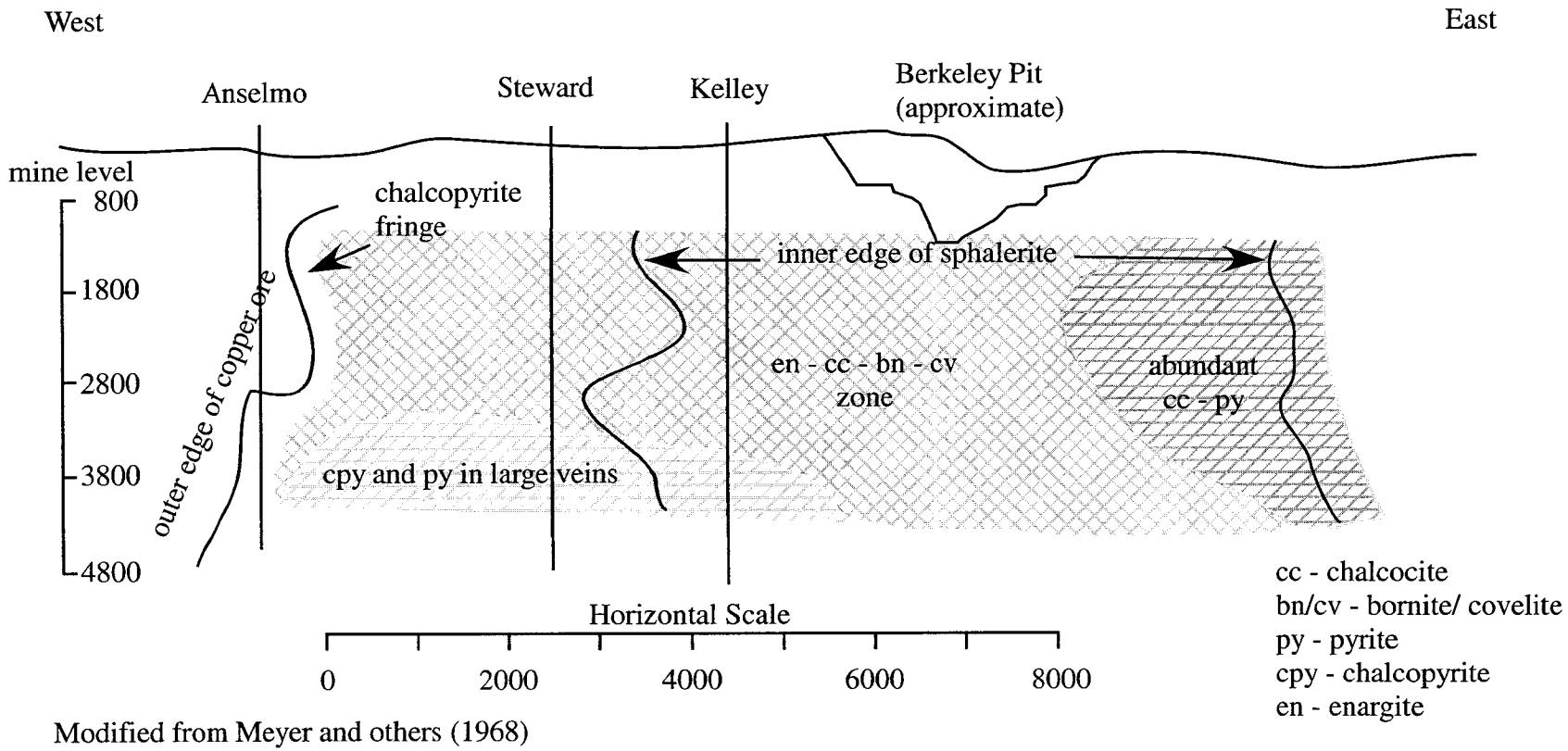

Modified from Meyer and others (1968)

Figure 24. Cross-section of the mineralogic zones in the Butte area. The Anselmo, Steward, and Kelly mines represent the mineralogic transition from the Peripheral Zone to the Intermediate Zone to the Central Zone. The Belmont mine (not shown) lies within the Intermediate. At depth, the mine workings expose deep chalcopyrite zone described by Meyers and others (1968).

Mine-flooding Water-balance

The movement of water throughout the underground mines was part of a large circuit designed to keep the mine workings dry, keep the Berkeley Pit dry, augment the milling process, transport tailings as a slurry, recover copper from low-grade waste-rock, and recover dissolved copper from solution. Spindler (1977) reported a total process-water use of over 10.5 million cubic feet (Mcf) (0.37 million m^3) per day for the underground mines, surface mines, leach pads, mill, and tailings pond circuits during the 1970's. On April 22, 1982 the pumps for the underground mines were shut off allowing the flooding of the workings to begin and all operations in Berkeley Pit were shut down by July of the same year. Mining continued at the Southeast Berkeley (now known as the Continental Pit) and the leaching operation continued for about another year; all operations were suspended by July of 1983. It is important to note that no water from any part of the circuit was allowed to flow out of the mine area after the suspension of operations. The timing of these shut-downs, the water chemistry of each component of the circuit, and volume of the water related to each component of the circuit play an important role in the final chemistry of the receiving waters.

The Kelley mine and the nearby High Ore mine (figure 25) served as the main pumping station for all mine waters in Butte district for over 20 years prior to the shut down in 1982. Water was drained or pumped from all of the East Camp mines including the Anslemo, Steward, Granite Mountain, and Belmont mines to the 3800-level of the Kelley. The water was then pumped to the surface, discharged through the copper-precipitation plant near the northeast rim of the Berkeley Pit (figure 25), and discharged to Silver Bow Creek after additional treatment with lime. The pumps had a capacity of 1.5 Mcf (42000 m^3) per day (Piper, 1960), but the long-term average discharge was about 0.96 Mcf (27000 m^3) per day.

In addition to waters from the mines, the copper-precipitation plant processed waters circulated through leach pads constructed of low-grade waste rock mined from the underground workings, the Berkeley Pit, and other surface mines (figure 25). The leach pad - precipitation plant circuit, which included the 0.87 Mcf (25000 m^3) per day discharge from the underground mines, return flow from the leach pads, and a large

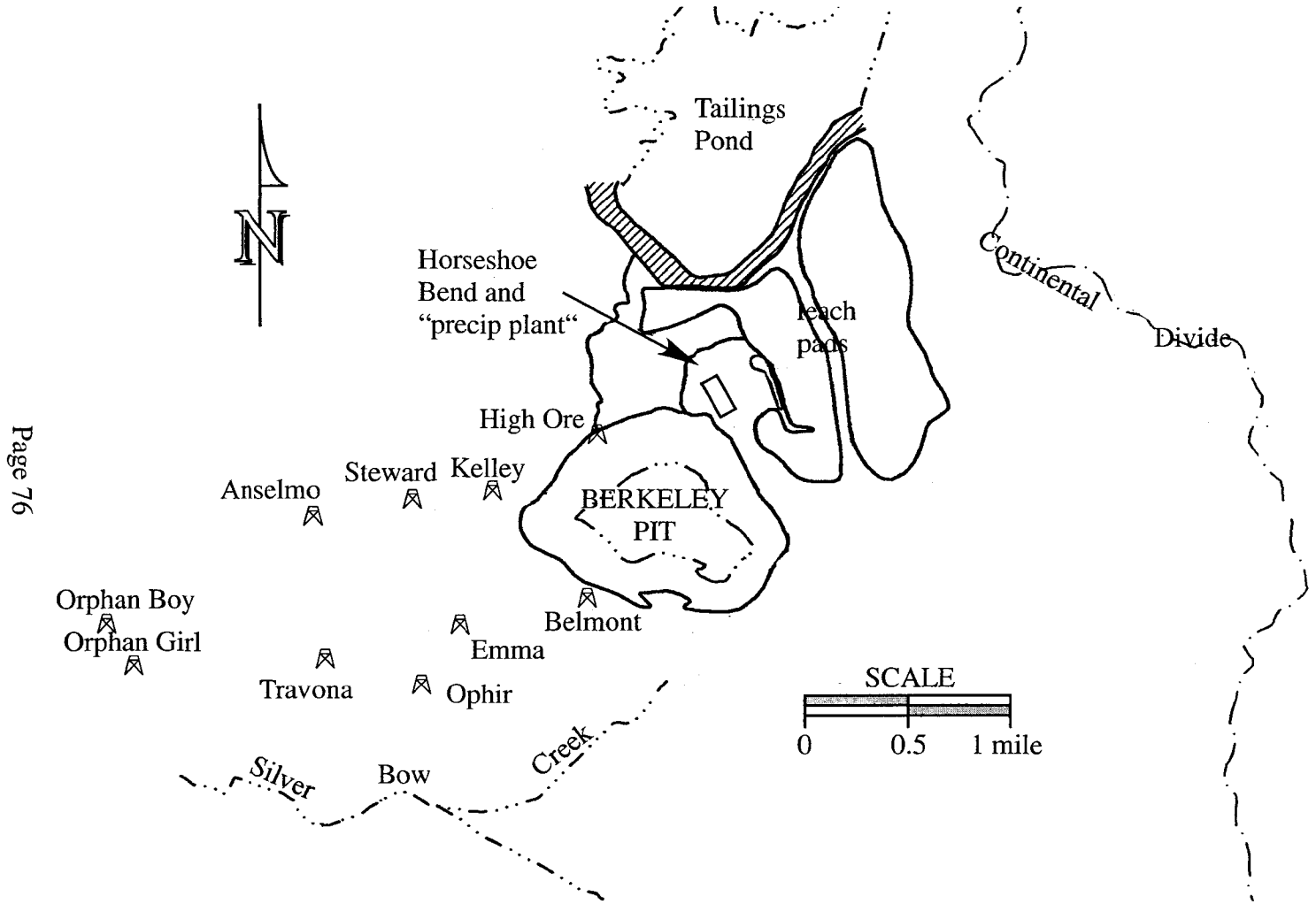

Figure 25. Surface features of the Butte area mines. The flooding of the mines began with the shut down of pumping at the Kelley and High Ore shafts in April of 1982. Surface water, include discharge from Horseshoe Bend and the leach pads, was routed into the Berkeley Pit to prevent discharge to Silver Bow Creek.

spring known as Horseshoe Bend, totaled about 5.8 Mcf (164,000 m^3) per day (Spindler, 1977). When mining was suspended in 1982, Horseshoe Bend and other surface waters not within the leach pad - precipitation plant circuit were diverted to the Berkeley Pit to prevent discharge to Silver Bow Creek. Thus, the water balance throughout the mining complex was redefined and controlled by gravity and elevation rather than pumps.

Upon shut down, the mining company was required by the Montana Department of State Lands (MDSL) to initiate monitoring of water levels and some water chemistry. All of the data for the first two years of flooding was done by the mining company and reported to MDSL and is public record. Monitoring of water levels and water quality in the Kelley shaft was initiated within a few hours of the start of flooding. Monitoring of the Steward and Belmont shafts was started about five months later and monitoring of the other shafts were added over the next several years as flooding continued. Although observations were made, detailed water-level monitoring in the Berkeley Pit did not begin until December of 1983 when water levels were first observed to rise; measurements were made by using elevation survey points established when the pit was active. The first water-quality samples were collected from the pit in November of 1984 by means of a helicopter; regular sampling of the pit began in 1991 when access was more reliable. Measurement of surface-water inflow to the Berkeley was initiated by the MBMG in April of 1984; no earlier data are available.

In the 21 months between April of 1982 and December of 1983, water levels in the Kelley shaft rose nearly 2,200 feet (670 meters); although water was ponded at the bottom of the Berkeley Pit, no significant rise was observed until water levels in the mines reached the elevation of the pit bottom. The slope of the hydrograph for the Kelley shaft shows the effect of this change in storage capacity from underground workings to a large open pit. Similarly, the rate of water-level rise dropped from feet per day to feet per month (figure 26).

As of about 1992, the mining company has been monitoring pit water-volumes, which are measured several times per year, and are compared to the cumulative volume of surface water flowing into the pit during the same time period. Although several

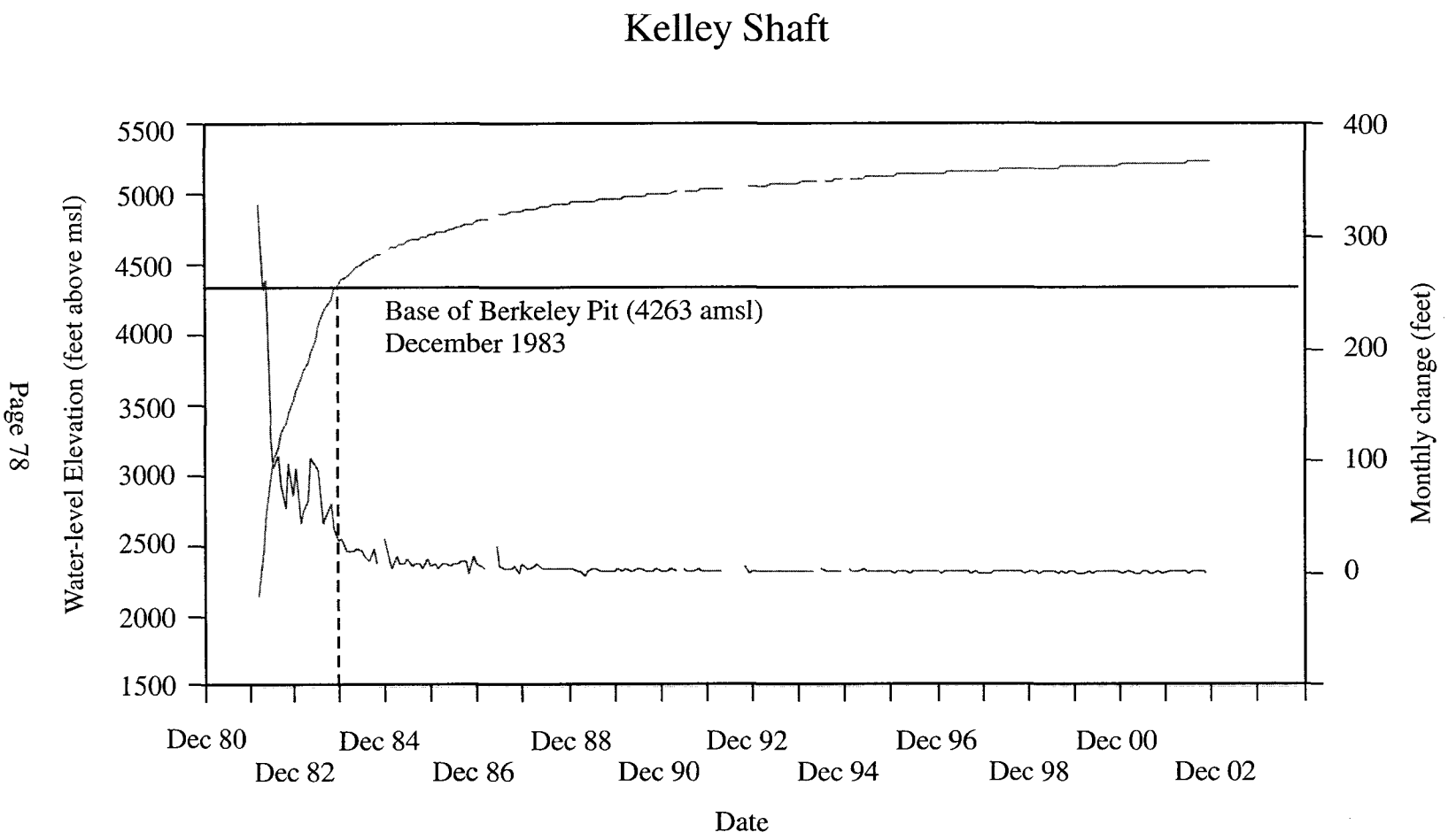

Figure 26. Water levels and monthly changes in water levels in the Kelley mine. Water levels reached the bottom of the Berkeley Pit in December of 1983. The rate of rise decreased dramatically after that time.

methods have been used, the most common method is to use pit wall contours generated from aerial photography or contour maps (Canonie, 1992) and estimate the volume of water based on the elevation of the water surface. In a recent analysis, the MBMG identified a large deficit in the water volume compared to the cumulative surface-water inflow. This deficit, on the order of several hundred million cubic feet, indicates that more water has flowed into the pit than can be accounted for in the measured volumes. This prompted a more detailed analysis of the water balance for this investigation using mine volumes, water discharge rates, and flow gradients to better define conditions during the first months of flooding.

The MBMG has recently digitized maps of the mine workings throughout the Butte area. The scale of the original maps is such that workings are represented as lines rather than polygons; that is, no width or height of the workings was depicted. Assuming a 6-foot by 8-foot opening for each working represented by a line and the total length of the lines on each level, the total volume of workings below the base of the Berkeley Pit is approximately 980 Mcf. This value neglects vertical stopes, cave-blocks, and shafts which would add to the estimated volume. The estimated value also assumes all of the workings depicted on the map are open when, in fact, it was common to back fill stopes and workings with waste rock; the result would reduce the estimated volume.

As noted, Spindler (1977) reported a total discharge rate of about 0.87 Mcf (25,000 m^3) per day from the underground mines. Assuming that when the pumps were shut off, this water accumulated in the workings at the same rate, over a 21-month period the cumulative volume would have been about 527 Mcf (14 million m^3). This accounts for about 54% of the total 980 Mcf (27 million m^3) flooded during that period and leaves a deficit of 453 Mcf (13 million m^3).

Measurements of flow from the Horseshoe Bend spring in 1984 range from over 3,200 to 5,000 gpm (12,000 to 19,000 liters per minute). As noted, this water was diverted to the Berkeley Pit at the same time the underground pumps were shut down. At a rate of 4,000 gpm (15,000 liters per minute) or 0.76 Mcf (21,000 m^3) per day, the cumulative discharge to the Berkeley Pit would have been 465 Mcf over a 21-month

period. If most of this water infiltrated the bottom of the pit and flowed into the workings, the volume would represent 47% of the total volume flooded (figure 27). This agrees well with the missing 46% not accounted for by ground water and suggests that about half of the water flooding the mines during the first 21 months was ground water originating in the workings and half was leakage from the Berkeley Pit.

As flooding of the mines progressed, flow gradients reversed and induced flow from the underground workings to the Berkeley Pit. By the end of 1984, all of the shafts in which water levels were measured, showed higher water levels than those of the Berkeley Pit. The water balance then shifted and the underground mines were no longer the hydraulic sink for the district.

As noted, monitoring of the Berkeley Pit began in 1984 when water levels were observed to rise. Table 10 presents the annual change in water volume in the Berkeley Pit, the total annual flow of surface water to the pit, and the annual difference. From 1984, when water levels began to rise in the pit, to December of 2000, the volume of water in the Berkeley Pit increased by nearly 4 billion cubic feet (112 million m^3). The cumulative discharge of surface water into the pit during that same time period was nearly 2 billion cubic feet (56 million m^3).

Table 10. Annual cumulative volumes for the Berkeley Pit and annual discharge from the Horseshoe Bend spring (after Duaime, 2002).

Year	Berkeley Pit (cubic feet)	HSB (cubic feet)	Difference (cubic feet)
1984	186,617,358	279,152,567	(92,535,209)*
1985	238,510,203	175,788,770	62,721,433
1986	302,427,000	158,209,893	144,217,107
1987	307,981,925	140,631,016	167,350,909
1988	286,957,588	140,631,016	146,326,572
1989	204,758,759	140,631,016	64,127,743
1990	250,323,209	116,934,690	133,388,519
1991	252,995,198	108,989,037	144,006,160
1992	217,415,551	108,989,037	108,426,513
1993	237,877,364	108,989,037	128,888,326
1994	266,214,513	160,600,620	105,613,893
1995	293,637,561	171,569,840	122,067,722
1996	199,485,096	42,892,460	156,592,636
1997	150,475,187	0**	150,475,187
1998	203,071,187	0**	203,071,187
1999	140,279,439	0**	140,279,439
2000	222,618,898	80,511,257	142,107,642
Total	3,961,646,037	1,854,009,000	2,027,125,781

* indicates volume loss

** surface water diverted away from the pit

The difference of 2 billion cubic feet (56 million m^3) can be attributed to ground-water recharge, but does not include the change in the storage of water in the mine workings and therefore underestimates the contribution by ground water.

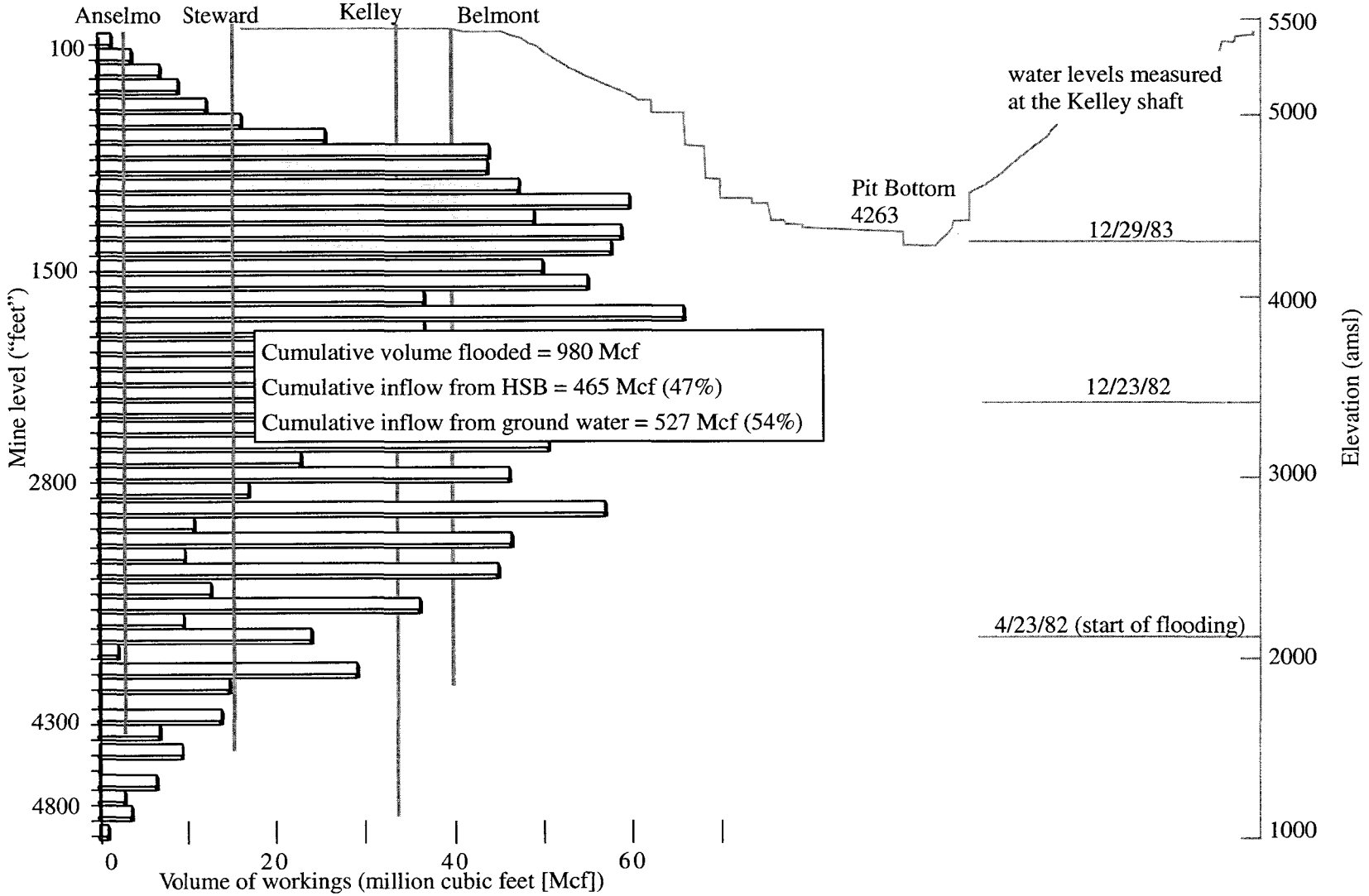

Figure 27. Volume of mine workings below the Berkeley Pit. In the 21 months after flooding began, water levels in the Kelley rose nearly 2,200 feet to the bottom of the Berkeley Pit. About half of this water originated as surface water from the Berkeley Pit.

The water elevation in the Kelley shaft at the end of 2000 corresponded with the 700 level of the mine. Using the same set of data and assumptions as for mine volumes below the base of the pit, about 411 Mcf of workings were flooded from 1984 to 2000; thus, a total of 1,390 Mcf of workings were flooded from 1982 to 2000. Table 11 presents the distribution of cumulative volumes for flooding of the mines and Berkeley Pit.

Table 11. Water balance for the period from 1984 to 2000.

Pit volume change (ΔS_{pit})	3,961 Mcf (table 10: Berkeley Pit) 112 million m^3
Volume of workings (ΔS_{mine1})	410 Mcf (base of pit to Kelley 700 level) 12 million m^3
Volume of workings (ΔS_{mine2})	980 Mcf (to base of pit) 27 million m^3
Volume of all workings ($\Delta S_{allmines}$)	1,390 Mcf (to Kelley 700 level) 39 million m^3
Surface water inflow ($V_{surface}$)	1,854 Mcf (table 10: HSB flow) 52 million m^3
Ground-water recharge to pit and workings 1984 through 2000 ($\Delta S_{pit} + \Delta S_{mine1} - V_{surface} = V_{ground\ water}$)	2,517 Mcf 71 million m^3

The 2,500 Mcf that originated as ground water within the workings is equivalent to about 6 mine volumes above the base of the pit. In other words, the water in the workings above the base of the pit have been exchanged about 6 times between 1984 and 2000; this assumes that there was no exchange with water in the workings below the pit. Under the better assumption that there was circulation of water throughout the workings, from 1982 to 2000 the total volume of ground-water flow through the workings is equivalent to about 1.8 total mine volumes. At a total of 1,400 Mcf (39 million m^3) of water stored in the underground workings in 2000, 465 Mcf (13 million m^3) or 33% originated as surface

water (figure 27) and 938 Mcf (26 million m^3) or 67% originated as ground water. Of course, after 1984, all of the water entering the workings was ground water. Thus, between 1984 and 1988, the same amount of water that had flowed from the pit to the workings had flowed from the workings to the pit. Between 1984 and 1991, there had been one mine volume (1,400 Mcf [40 million m^3]) of water originating as ground water within the workings that flowed from the workings to the pit.

These relationships between surface water and ground water assume that all of the ground water around the pit flows through the workings. While not entirely true, given that the pit is surrounded by and intersects workings along its entire perimeter, certainly the great majority of ground water flowing into the pit originates in the workings.

The general concept expressed by earlier investigations was that the Kelley mine was the hydraulic sink until the workings filled with water to the base of the Berkeley Pit. At that point, the Berkeley Pit became the sink. If, as indicated by the water balance calculations, surface water was draining from the Berkeley Pit into the underground workings at a rate nearly equal to that of the mine discharge, the rate of filling would far exceed that expected under "natural" conditions. Simply put, the mine produced about 1 Mcf per day for several decades before the pumps were shut off; then filled at a rate of about 2 Mcf per day for almost two years. Under these conditions, it is likely that the Kelly mine, as the initial hydraulic sink, would be overwhelmed by such inflow and water would flow outward to other mines.

A detailed evaluation of mine water-level elevations, collar elevations, and their relationship to the Kelley mine was used to determine flow gradients throughout the period of record. Figure 28 presents a comparison of water levels in several shafts to those of the Kelley shaft. The Steward and Belmont mines show a large negative departure from the Kelley until late 1983 and early 1984, after which time the water elevations in the Steward and Belmont exceeded that of the Kelley. The Steward maintained a gradient toward the Kelley throughout the period of record; however, water-elevations in the Belmont again became lower than the Kelley from 1988 through 1993 as

a result of experimental pumping during this period (the collar of the Belmont collapsed in the spring of 1987, so no measurements have been made since) . The difference between the Kelley and the Berkeley Pit always indicates a hydraulic gradient toward the Berkeley Pit after 1983, but the gradient decreases as flooding progresses. Water-level measurements at the Granite Mountain mine north of the Kelley and Berkeley Pit began in January of 1987; the water-elevation was lower than the Kelley until late-1994.

The water-elevation differences indicate a strong hydraulic gradient from the Kelley to the Steward and Belmont mines in the first 21 months after flooding began. This could only be induced by an inflow of water in excess of the 1 Mcf per day required to de-water the mines and supports the evidence that the excess water was the result of leakage from the Berkeley Pit. The presence of a gradient, however, does not always result in water movement along the gradient.

Figure 29 presents a summary of the connections between the Anselmo, Steward, Kelley, and Belmont mines as depicted on maps of each level. When flooding began in 1982, water levels were at about the 4000 level; the 3900 level, common to all of the mines, was the pumping station for the Kelley - all of the mines were well connected by workings. The Kelley is isolated from the other mines between the 3900 and 3000 level whereas the Anslemo, Steward, and Belmont are connected on several levels. The 3000 level, a major haulage way for the mines, was flooded in October of 1982. As indicated, water levels in the Kelly reached these workings about two weeks before the Steward. The Kelley mine is again isolated from the other mines between the 3000 level and the 1500 level which coincides with the base of the Berkeley Pit. The Kelley and Belmont mines are, however, connected to the mines beneath the Berkeley Pit. To summarize, the Kelley is connected to the Berkeley Pit area via workings, but is generally isolated from the other mines. The Belmont is also connected to the Berkeley Pit and is connected to the other mines on the deeper levels, but is several thousand feet southeast.

Summary of water balance

Analysis of the volumetric balance, the flow balance, and flow gradients suggest a much different chain of events in the early period of flooding than suggested by earlier reports. The rate of rise and the sustained elevation difference indicates the Kelley mine, with several connections to the Berkeley Pit, received much more surface water than the other mines in the area. The Belmont mine, also with connections to the Berkeley Pit received surface water as well, but better connections to the other mines, particularly the Steward, affected a reduced gradient. The inclusion of surface water entering the mines via the Berkeley Pit is prerequisite to further analysis of the chemistry changes in the underground workings.

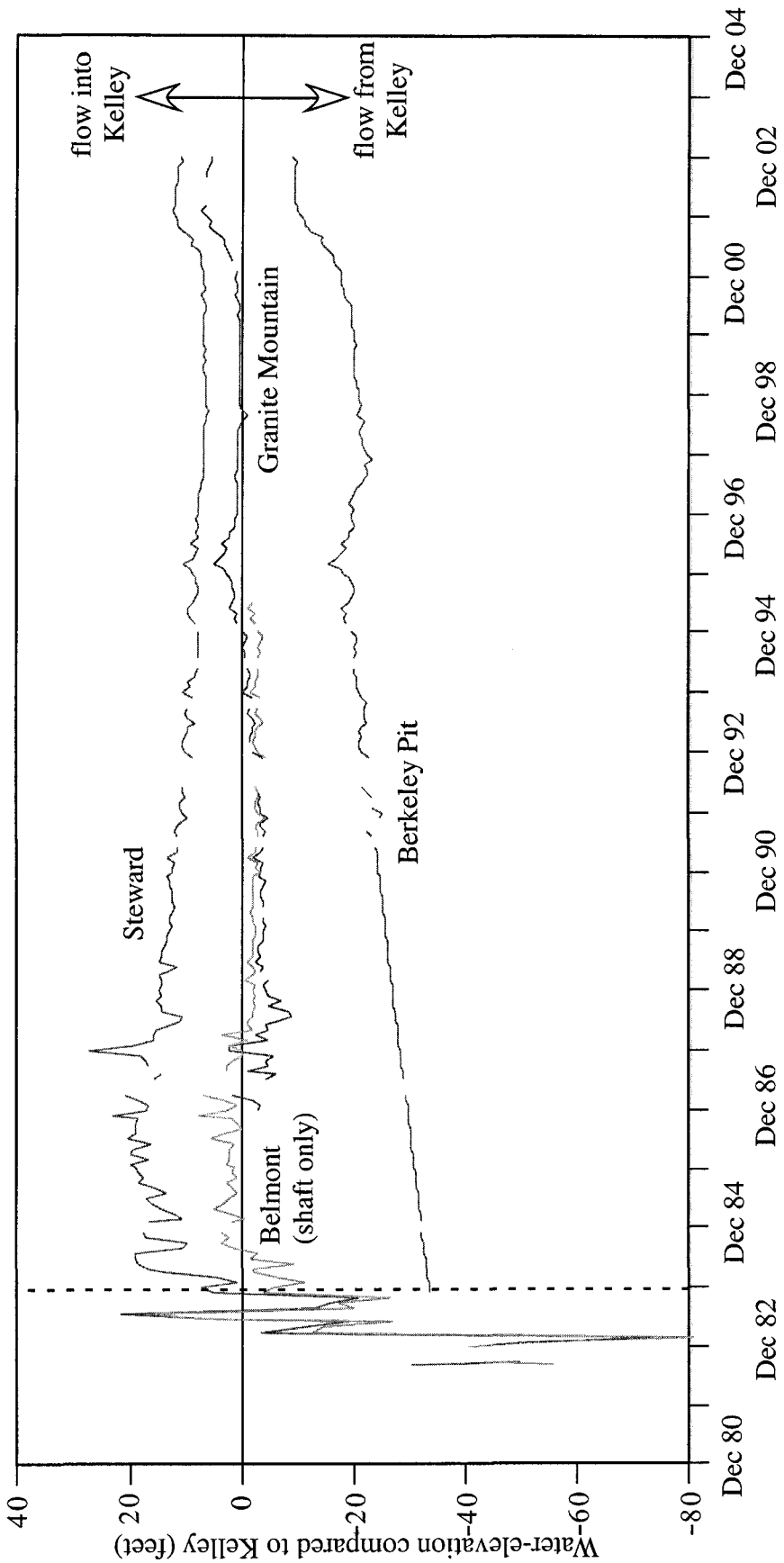

Figure 28. Comparison of water elevations in the East Camp mines. Water elevations in the Steward and Belmont mines were lower than that of the Kelley mine during the early period of flooding. The flow gradients shifted toward the Kelley and Berkeley Pit in 1983 and 1984. Although variable, water flowed from the Kelley to the Granite Mountain mine until 1994.

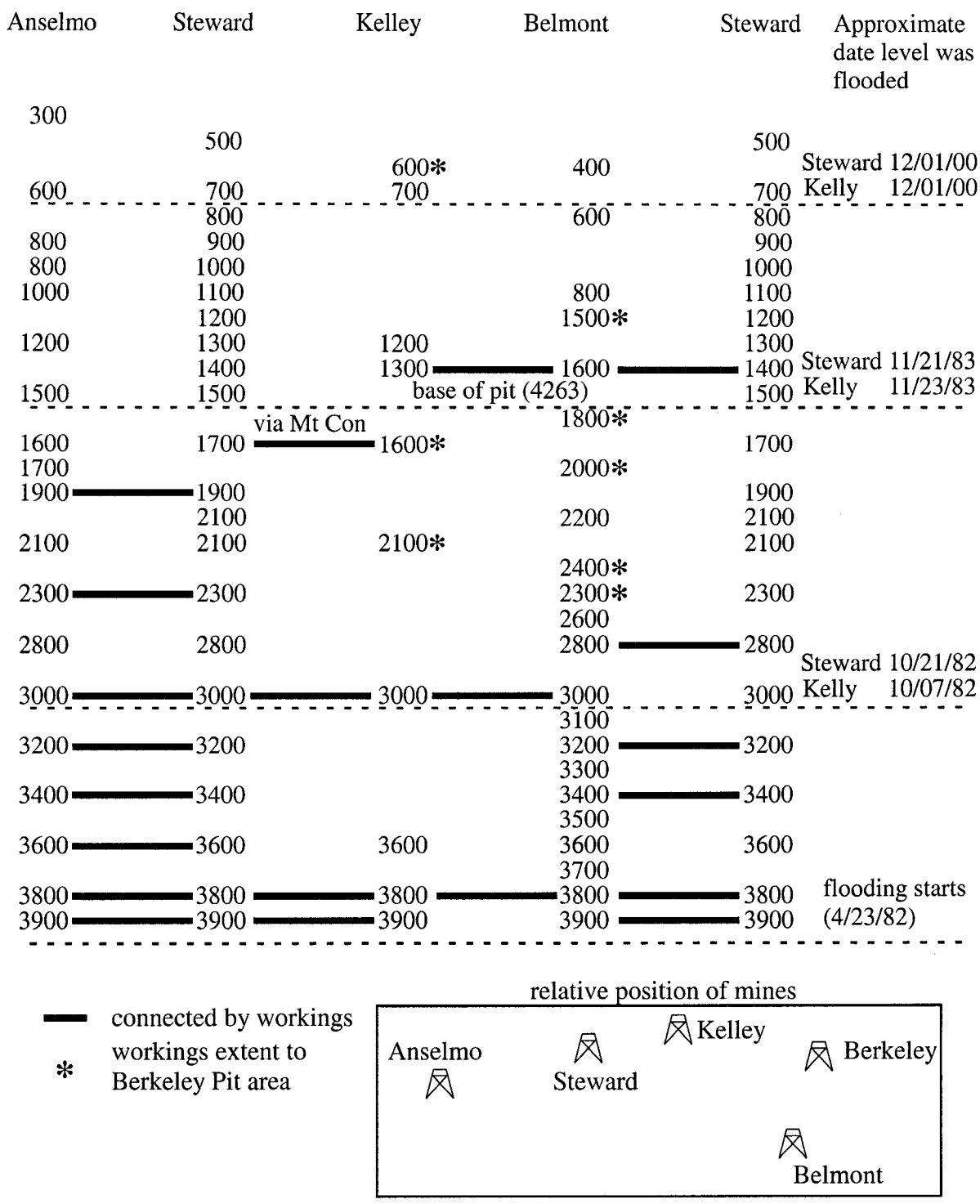

Figure 29. Connections between the East Camp mines. Although workings are extensive, the East Camp mines are connected only on specific levels. The dashed lines indicate the approximate date water levels reached and flooded that level.

Water Quality

The chemistry of the mine waters prior to flooding is generally unknown, although some analyses for specific elements are available. As noted, mine waters were directed into the Kelley and High Ore mines and then pumped to the surface for copper recovery. Goddard (1960) reported copper values and discharge rates for several of the mines to determine the distribution of "copper credits" for each mine. The Steward mine produced 846 gallons per minute with an average copper concentration of 114 mg/L, the Kelley reportedly produced neither water nor copper, and the Anselmo produced 200 gpm with "no significant copper"(it was noted that although the Anselmo waters contained little copper, there was likely to be copper-rich waters in the deeper undrained workings). The Steward produced almost one-half of the soluble copper produced (360 mg/L) by the mines that year (1960) at 20% of the total discharge (4,957 gpm [19,000 liters per minute]). Spindler (1977) gives a more complete analysis and reports an average copper concentration value of 186 mg/L and an average iron concentration of 706 mg/L from all the mines.

Copper, iron, and zinc concentration data for the Kelley shaft were collected by the mining company on a bi-weekly basis beginning within 12 hours of the onset of flooding. Data collection from the Steward and Belmont shafts were initiated about 5 months later. All of these data are total recoverable concentrations; samples were acidified without filtering. Figure 30 presents total recoverable iron concentrations and the ratio of ferrous iron to ferric iron for the Kelly shaft. The iron concentration spikes to well over 2,000 mg/L on two occasions: mid-1982, a few weeks after flooding began, and in the last half of 1983. The high concentration of iron is observed at only one source throughout the Butte district: the leach pad - precipitation plant circuit. Spindler (1977) reports the iron concentration of the plant effluent at 3,450 mg/L. Canonie (1993) reported a value of 1,763 mg/L for the pregnant solution from the leach pads. The first spike corresponds to the diversion of Horseshoe Bend into the Berkeley Pit in 1982. Although not reported, it is likely that some of the precipitation plant discharge was

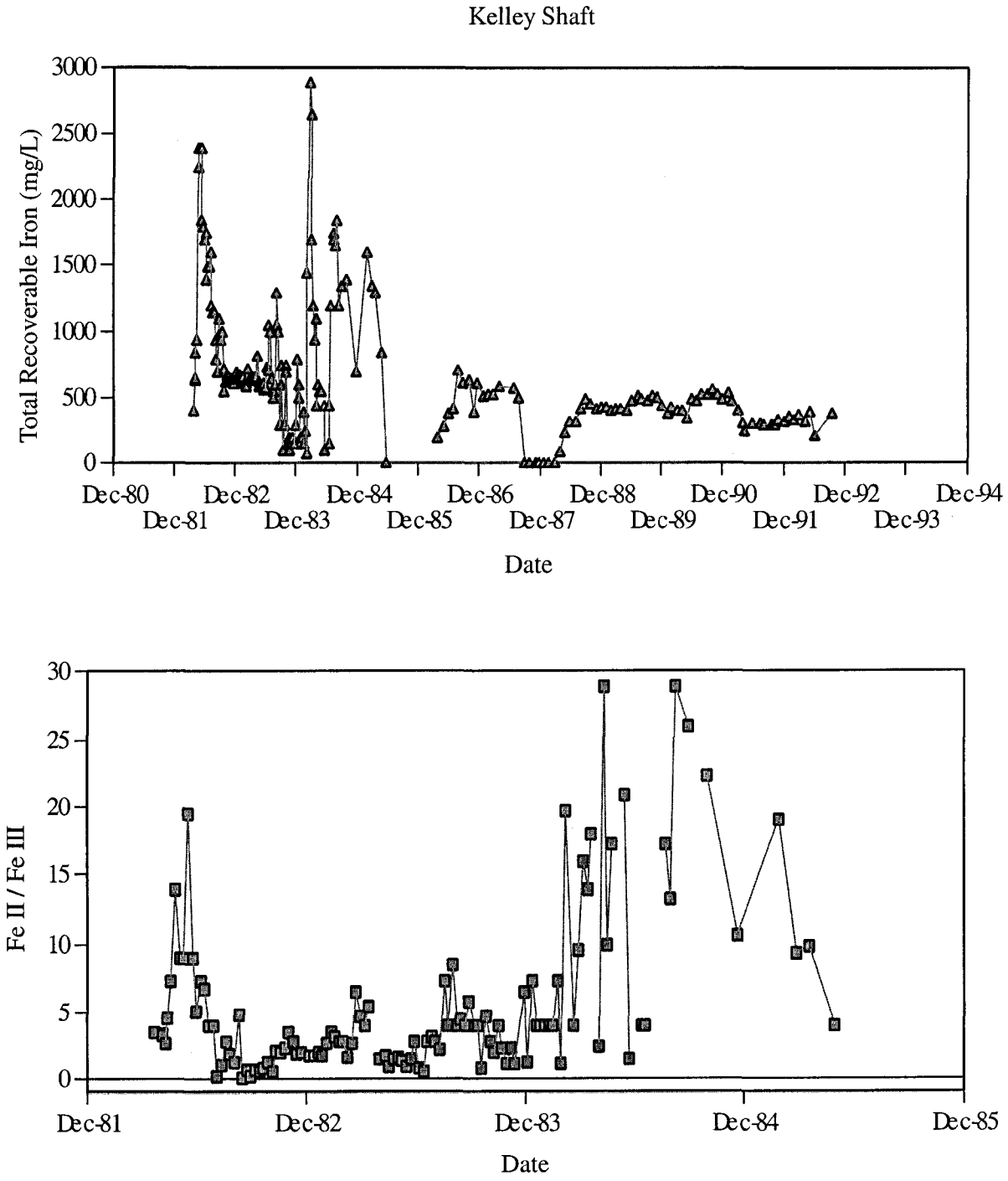

Figure 30. Concentrations of total iron and iron speciation in the Kelley shaft. The data reflect two influxes of water with very high iron that coincide with the diversion of Horseshoe Bend water into the Berkeley pit in the Spring of 1982 and the draining of the precipitation plant in the Spring of 1983. The effect on iron speciation in the shaft is equally evident.

included in this water. The second corresponds to the draining of the leach pads and precipitation plant in 1983. The iron in both the Horseshoe Bend water and the precipitation plant discharge is predominantly reduced iron. However, recent data indicates nearly all of the iron in solution is oxidized by the time it flows into the pit. It follows then that the water flowing out of the bottom of the pit contained predominantly ferric iron. This effect is demonstrated by the spikes of ferric iron in figure 30 which, again, coincides with the diversion of surface water to the pit.

Similar to iron, the concentration of copper in the Kelley shaft spiked well above the initial concentrations of about 50 mg/L to 600 mg/L in 1982 and to 400 mg/L in 1983 (figure 31). The leach pad - precipitation plant circuit exhibited copper concentration of over 350 mg/L in 1992 (Canonie, 1993) and was likely higher 10 years earlier when fresh waste-rock was deposited on the leach pads. The Belmont shaft shows similar spikes in copper concentrations (figure 31). The spikes in the Belmont generally occur several weeks after those in the Kelley shaft, but the maximum concentration is greater. Zinc concentrations in the Kelley shaft increased from about 300 mg/L to about 1,700 mg/L and from less than 5 mg/L to over 1,100 mg/L in the Belmont shaft during these events (figure 32). Again, the response in the Belmont generally follows that of the Kelley after 2 to 3 weeks, but the maximum concentration is greater in the Belmont shaft.

The pH of the waters sampled from the shafts reflect the influence of inflowing waters. Values fluctuate from less than 3 to about 5.5 during the initial flooding; unfortunately, no pH measurements were collected from any shaft at the start of flooding. The pH values in both shafts increase and concentrations decrease to those observed in the initial samples; no further trend is apparent after 1984.

Although the hydraulic gradient between the Kelley and Steward is as strong as that of the gradient between the Kelley and Belmont, water quality in the Steward did not show as much response to the influx of water from the Berkeley Pit. Data were not collected during the initial influx, but concentrations of iron and zinc (figure 33), as well as copper show a significant decrease as flooding progressed. There appears to be a slight response (increase) in 1983 that coincides with the increase in the other shafts. As noted

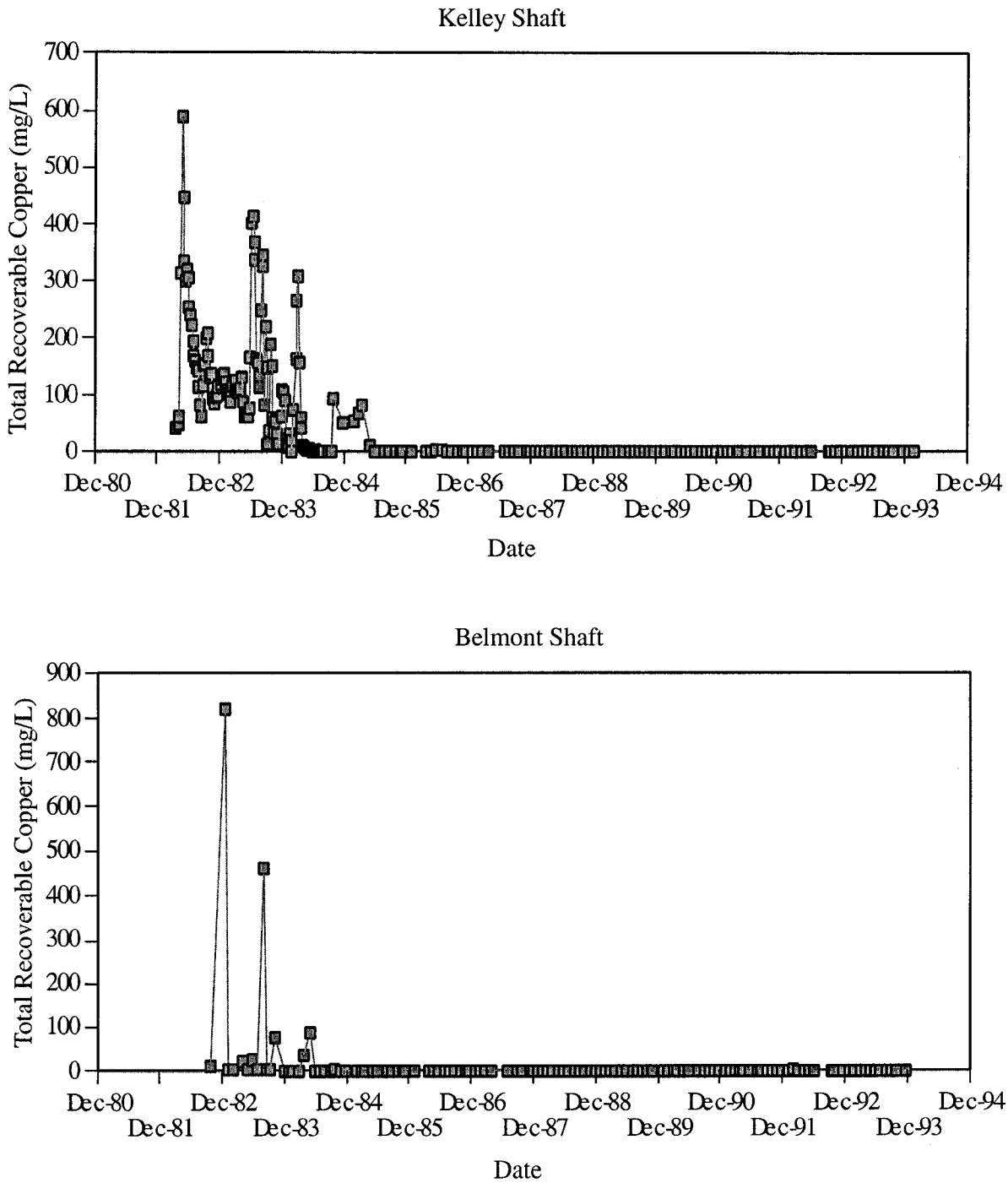

Figure 31. Copper concentrations in the Kelley and Belmont shafts. Concentrations show sharp fluctuations in both shafts during the initial period of flooding.

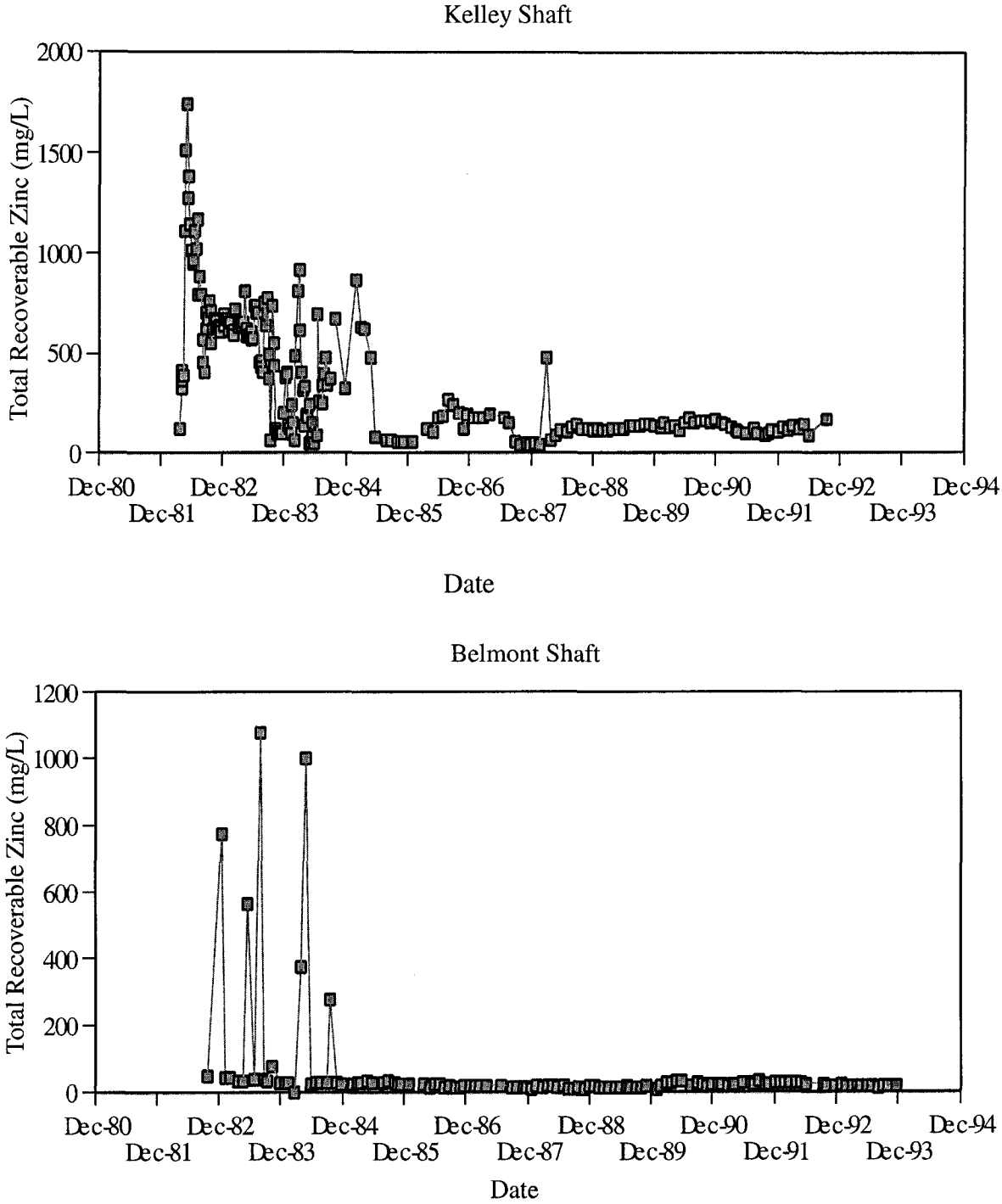

Figure 32. Zinc concentrations in the Kelley and Belmont shafts. The concentrations show similar fluctuations during the initial period of flooding. The concentration values return to initial values after 1984.

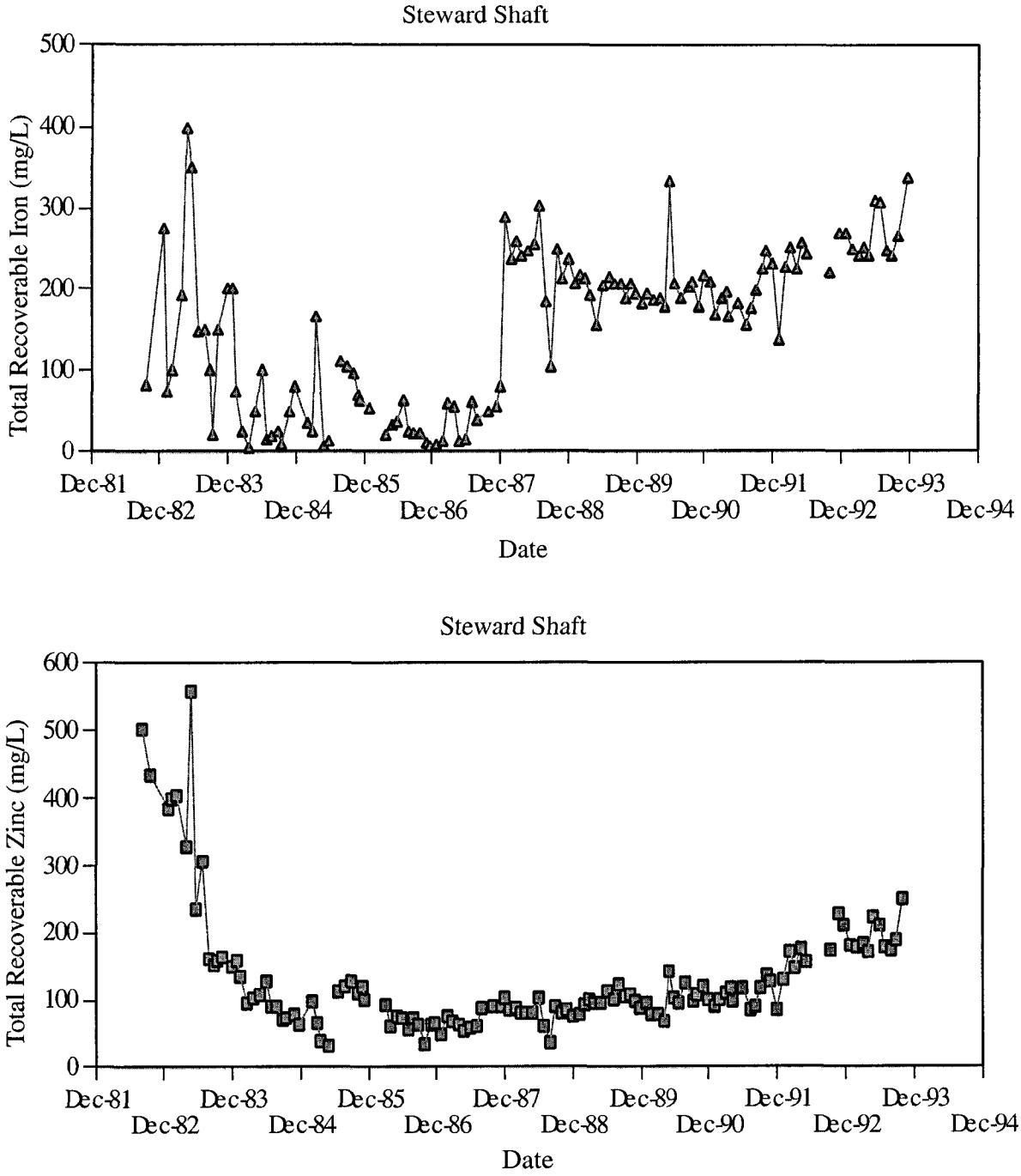

Figure 33. Concentrations of iron and zinc for the Steward shaft. Data were not collected during the first 5 months of flooding at the Steward shaft, but some response in concentrations of iron and zinc are evident.

in the discussion of the water balance, the Kelley and Steward mines are connected only on a few levels; the Belmont and Steward are connected on several levels, but the distance between the mines is much greater. The longer, indirect flow path from the pit to the Belmont and to the Steward may account for a subdued response in the chemistry. Also in contrast to the Kelley and Belmont shafts, concentrations of all three constituents in the Steward shaft show a steady increase after 1987. Again, this may show the lesser influence of the Kelley and Belmont waters affected by distance and workings.

As with the volumetric calculations, chemistry data for the Kelley shaft reflects the impact of the inflow of surface water via the Berkeley Pit on the chemistry of the flooding waters. When the pumps were shut off in the underground mines in April of 1982, the workings began to fill with ground water originating within the workings. Within weeks, surface water originating at the Horseshoe Bend spring and precipitation plant was diverted to the Berkeley Pit; although some retention of water occurred, most of the water reaching the bottom of the pit infiltrated through old workings and entered the underground mines. The Kelley mine, with apparently the best connection to the pit received most of the water. Initially, water levels were lowest in the Kelley, but with a filling rate twice that of the pumping rate, water flowed out of the Kelley and into the surrounding mines. The Belmont mine, also with connections to the pit, probably received some surface water from the pit, but received most from the Kelley workings. About one year later in the Spring of 1983, the leach pad - precipitation plant circuit was shut down and there was a period of increased flow of water that entered the pit and the underground workings. In late 1983 and early 1984, water levels in the underground workings reached the elevation of the bottom of the Berkeley Pit. As the gradient reversed, water began flowing from most of the workings into the pit and marked the beginning of another change in water chemistry within the underground workings. The Steward shaft with no direct connection to the pit showed less of a response to the influx of pit water. As gradients toward the pit developed, water quality in this shaft exhibited a trend toward what may be background concentrations for that mine.

Although exceptional in the frequency of collection, the water quality data collected by the mining company lacks the completeness necessary to develop a detailed analysis of conditions during flooding. The MBMG began monitoring the water quality of several shafts in July of 1983 and continues at present. In contrast to the data collected by the mining company, these samples were analyzed for complete chemistry and all values are total dissolved concentrations (acidified after filtering with a 0.45 micron filter). Although the sample frequency is much less, the MBMG data (figure 34) generally shows good agreement with respect to copper, iron, and zinc data collected by the mining company and give opportunity to evaluate the trends of other constituents.

Dissolved constituents showing decreases similar to copper, iron, and zinc include aluminum (figure 35), cadmium, and nickel. The concentration of aluminum also decreased about two orders of magnitude over the period of record (1983 to 2000). Other constituents, such as sulfate show little change over the same period of record (figure 35).

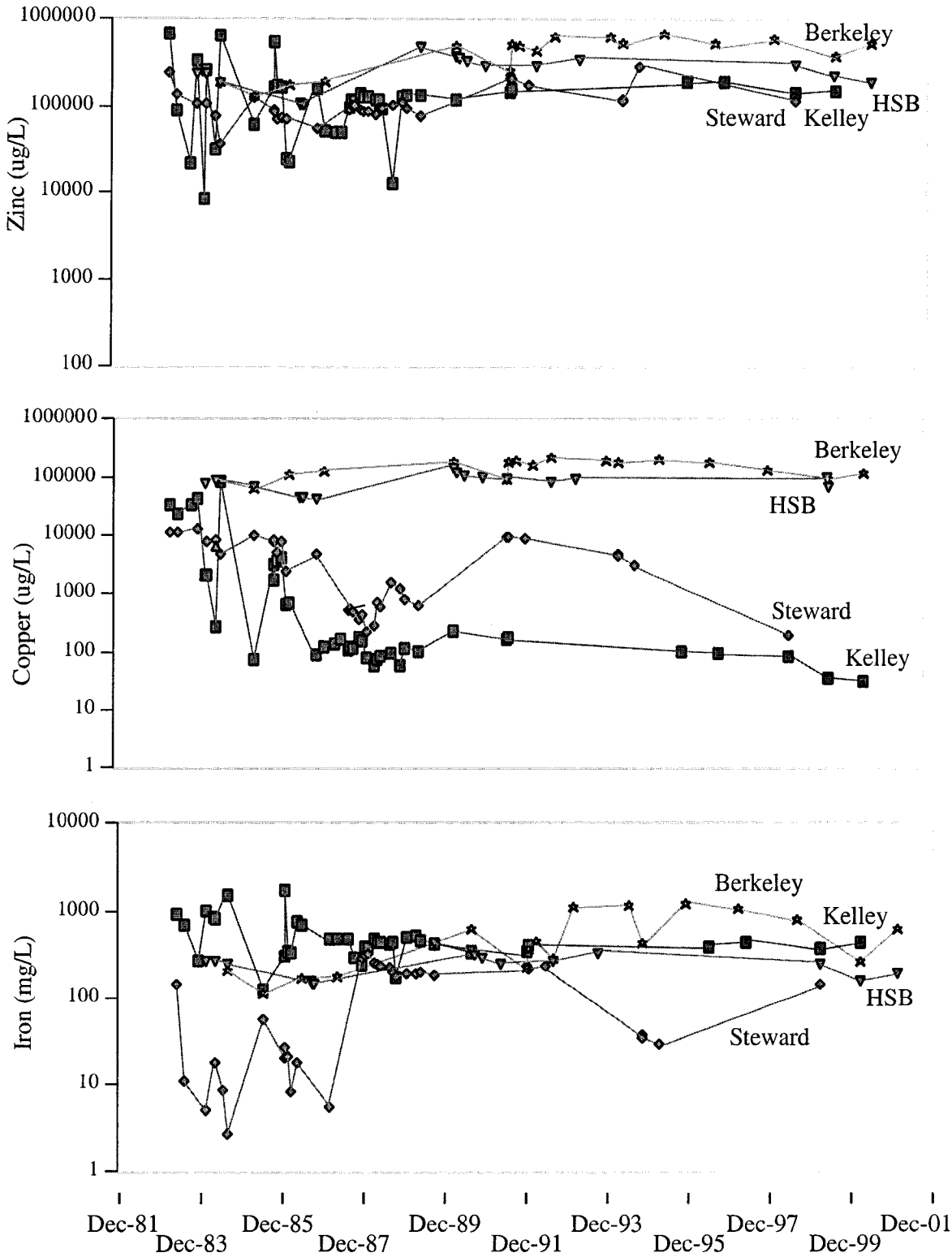

Figure 34. Water-quality data for the East Camp mines. Data collection by the MBMG did not start until after the initial flooding occurred. The period of record for which there is overlap shows similar trends with those data collected by the Anaconda Company.

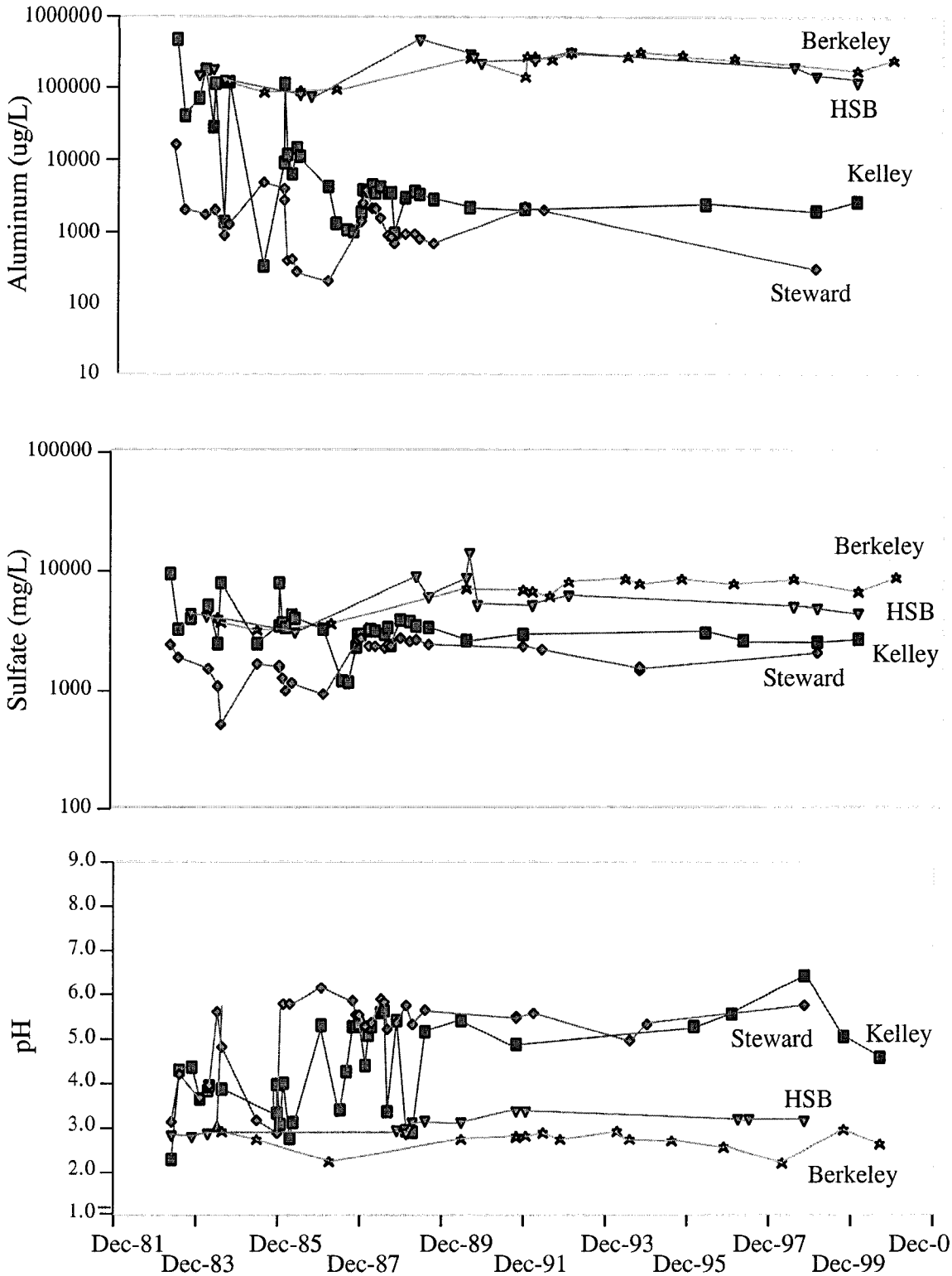

Figure 35. Water quality for the East Camp mines. Water quality in the Kelley and nearby mines was similar to that of the Horseshoe Bend and Berkeley Pit water during initial flooding. As water levels rose above the bottom of the pit, notable changes in concentrations occurred for some constituents.

Equilibrium Modeling - Kelley shaft

As noted, complete chemistry for pre-flooding mine waters is scarce and not representative of true conditions due to the addition of acid. Likewise, the surface waters entering the pit were not sampled until 1984 after water levels in the underground workings had reached the base of the pit. However, there is sufficient data to evaluate the mixing model suggested by the water balance. If indeed, half of the water entering the workings originated as pit water as of 1984 and less than one-third originated as pit water as of 2000, the water quality of the shaft in 2000 should be close in composition to pre-flooding mine water. This can be demonstrated by mixing surface waters entering the working via the pit with water similar to that in the later period of flooding. The resulting chemistry should be that of the early flooding waters.

Table 12 presents the results of mixing surface water and pre-flooding water at a 50:50 ratio; the annotated input file is provided in Appendix IV. Figure 36 presents a comparison of the mixing model results to Kelley shaft data collected in 1983. The surface water chemistry was assumed to be that of the leach pads and Horseshoe Bend spring as sampled in 1999 and the pre-flooding water chemistry was assumed to be that of the Kelley shaft sampled in 2000. No equilibration with minerals was allowed nor were O_2 or CO_2 gasses exchanged. The mixing ratio is based on the water balance estimated for the first 21 months of flooding where half of the water entering the workings originated as surface water from the leach pad area and the other half originated within the underground workings.

The results of the mixing model generally agree well with the sample results obtained from the Kelley shaft in the early period of flooding; the difference in concentrations between the mixing model and the results obtained from the Kelley shaft in 1983 generally lie within the range of concentrations for that time period. A notable exception is the ratio of ferrous iron to ferric iron. Although the total iron concentration is similar, the mixing model indicates a higher concentration of ferrous iron than that observed.

Table 12. A comparison of the mixing model with sample results from the Kelley shaft (all concentration values are moles/L).

	Surface flow	50:50 mix	Kelley 1983	RPD
Al	5.16e-02	2.59e-02	1.91e-02	30
Ca	9.70e-03	1.14e-02	1.06e-02	8
Cd	4.52e-05	2.26e-05	3.75e-05	50
Cu	5.56e-03	2.84e-03	5.44e-03	63
Fe(2+)	9.22e-04	3.12e-03	6.28e-04	133
Fe(3+)	1.73e-02	9.71e-03	1.69e-02	54
Fe (total)	1.82e-02	1.28e-02	1.75e-02	31
K	1.31e-03	1.01e-03	3.76e-04	91
Mg	6.81e-02	3.82e-02	2.33e-02	49
Mn	1.18e-02	6.60e-03	4.39e-03	40
Na	1.42e-04	8.24e-04	2.51e-03	52
SO4	2.31e-02	1.32e-01	1.01e-01	26
SiO2	7.19e-04	8.70e-04	5.70e-04	42
Zn	2.12e-02	9.66e-03	1.10e-02	13
pe (mv)	13.77	11.97	12.71	
pH (S.U.)	2.55	3.06	3.04	

The water balance calculations indicate by 1991 one mine volume had flowed through the underground workings and an exchange of about 2 mine volumes had occurred by 2000. Thus, as flooding progressed, the chemistry of the water within the workings progressively reflected conditions representative of the mine mineralogy rather than that of the surface water inflow from the Berkeley Pit. Indeed, the concentrations of most dissolved constituents show only moderate trends and fluctuations after about 1991 and the ratios of iron, copper, and zinc to sulfate tend to be nearly constant. Figure 37 shows the molal concentrations of these elements for the Anselmo, Steward and Kelley shafts. The concentration of zinc is always higher than iron or copper in the Anselmo shaft and Belmont shaft (not shown). The concentration of zinc and iron alternate with respect to the higher concentration in the Steward shaft; and iron concentrations are always higher in the Kelley shaft. Copper concentrations in all of the shafts have declined and are approaching the detection limit; the Belmont shaft showed similar values and trends when last sampled in 1995. The concentration of copper is always less than that of iron in each of the shafts. In the Anselmo, the difference is small and supports the

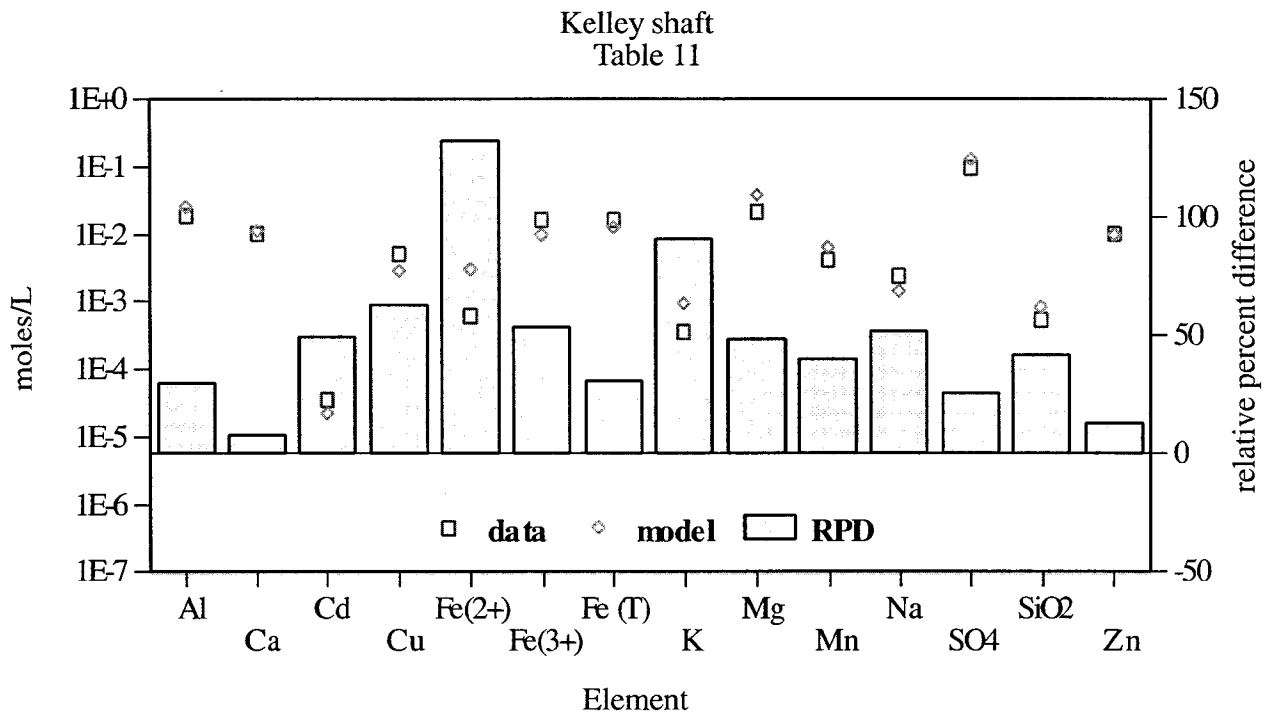

Figure 36. A comparison of modeled concentrations and sample data from the Kelley shaft. Results from mixing late flooding water (2000) with surface water from the pit compares well with data collected from the Kelley shaft in 1983.

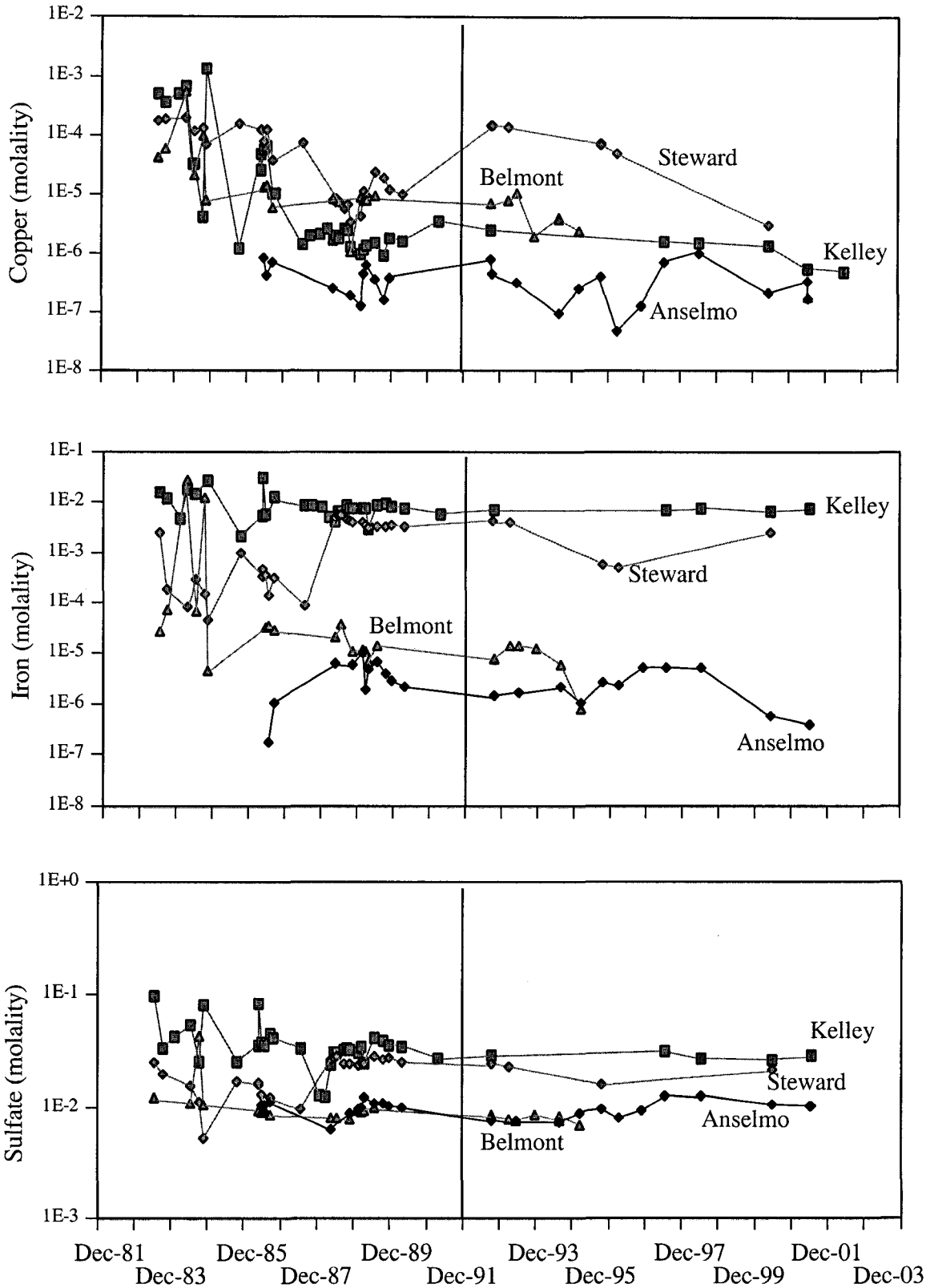

Figure 37. Concentration trends for copper, iron, and sulfate showed notable moderation after 1991.

concept that the dissolved iron and copper result from the dissolution of chalcopyrite. The Steward and Kelley, however, indicate a difference of several orders of magnitude.

Equilibrium Modeling of the Steward - Kelley system

As discussed with the Anselmo model, the relative solubility and "competition" for oxidation reactions helps define the development of the model. Both shafts exhibit iron concentrations far greater than that of copper; thus, the oxidation and dissolution of chalcopyrite is not the only source of iron. Unlike the Anselmo shaft, sulfate concentrations are also far greater than could be generated by the oxidation and dissolution of chalcopyrite and sphalerite. The local mineralogy must be considered; the Steward and Kelley workings expose pyrite and chalcopyrite in the deeper reaches and in the upper reaches, covelite, bornite, enargite, and chalcocite. The Steward shaft exhibits a strong upward flow of water within the shaft; the Kelley shaft shows little or no movement of water in the shaft.

The Steward shaft was modeled in a two step simulation: water from the Anselmo model was equilibrated with minerals associated with the deep and then shallow workings of the mine. Minerals of the deeper workings were assumed to dominated by pyrite and chalcopyrite and the minerals of the shallow workings were assumed to be dominated by sphalerite (table 13).

Table 13. Mineral phases used in the Steward simulation.

Mineral Phase	comments
Sphalerite	ore mineral in shallow workings
Kaolinite / Montmorillonite	alteration minerals
Quartz	country rock
Pyrite	gangue mineral in deep workings
Chalcopyrite / covelite	ore mineral
Arsenolite	weathering product of enargite

Table 14 presents the results of the Steward shaft simulation compared to a sample collected in 1997; the input file is described in more detail in Appendix IV. Figure 38 presents a graphical comparison of table 14. With the possible exception of calcium and potassium, the model results generally agree well with those of the shaft sample. The Steward shaft, being one of the last active mines in Butte, was supported by cement in the shaft and "shotcrete" in the many of workings and this may account for the increased calcium concentration. Sources for additional potassium include explosives (potassium nitrate) or muscovite, a common alteration mineral after biotite. Neither of these were included in the simulation because the overall effect of these differences on the pH or electrical balance was small.

Table 14. Comparison of Steward shaft sample data to model results (all concentration data are moles/L).

	Steward 1997	model	RPD
Al	1.90E-005	1.785E-005	6
As	3.42E-006	4.084E-006	-18
Ca	1.05E-002	5.147E-003	68
Cu	7.57E-005	8.950E-005	-17
Fe	6.84E-004	6.737E-004	2
K	4.08E-004	1.434E-004	96
Mg	3.56E-003	2.422E-003	38
Mn	3.22E-004	2.124E-004	41
Na	1.73E-003	1.372E-003	23
S	1.67E-002	1.104E-002	41
Zn	1.79E-003	1.651E-003	8
pe (mv)		-0.475	
pH (S.U.)	5.39	5.66	

The simulation of conditions in the Kelley shaft in the later period of flooding were more problematic. All of the shafts in the Butte area show some evidence of a chemocline; at a depth of 50 to 100 feet (15 to 30 meters) below the water surface there is a marked change in temperature as well as the concentration of dissolved constituents. In most cases, the difference is small and can be attributed to water cascading down the shaft. The Kelley shaft, however, shows a greater difference between the shallow and

deep waters. Although only a few samples from depths greater than 1,000 feet (300 meters) have been collected, samples indicate little change since 1983 with the exception of copper (figure 39) which has decreased.

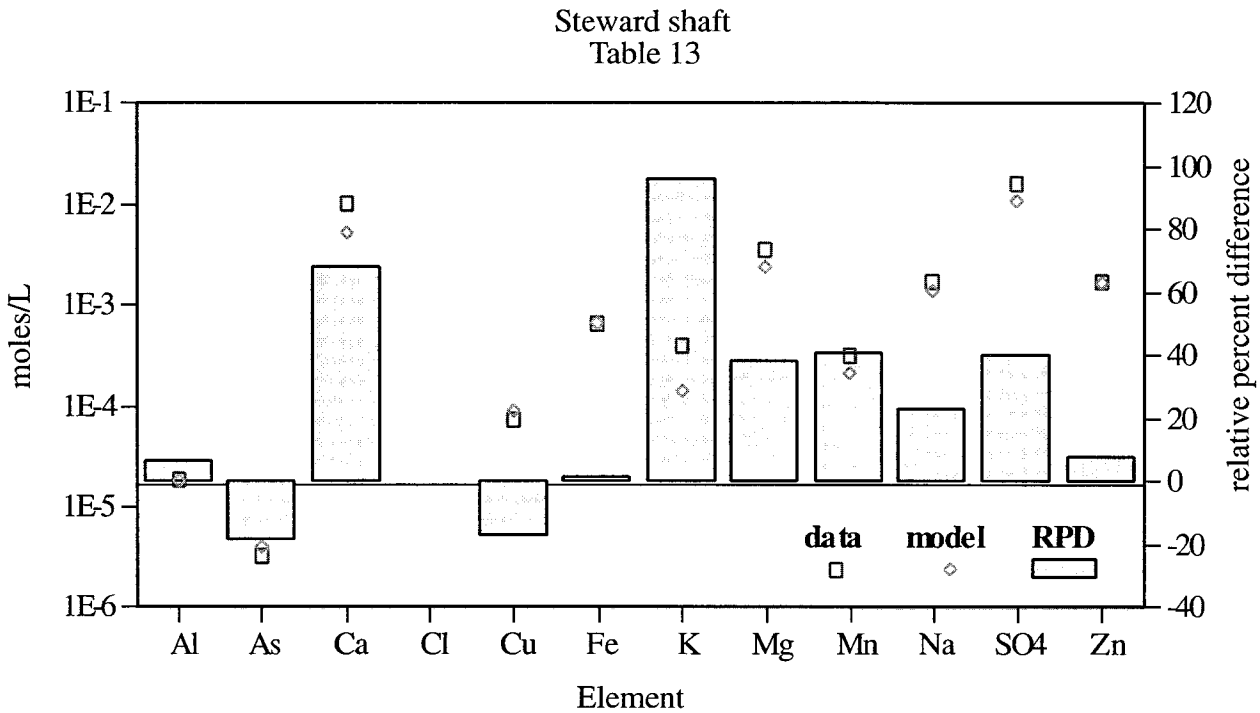

Figure 38. Comparison of modeled concentration and sample results from the Steward shaft. Results from a 2 step model of deep and shallow minerals in the Steward workings is compared to sample data from the shaft.

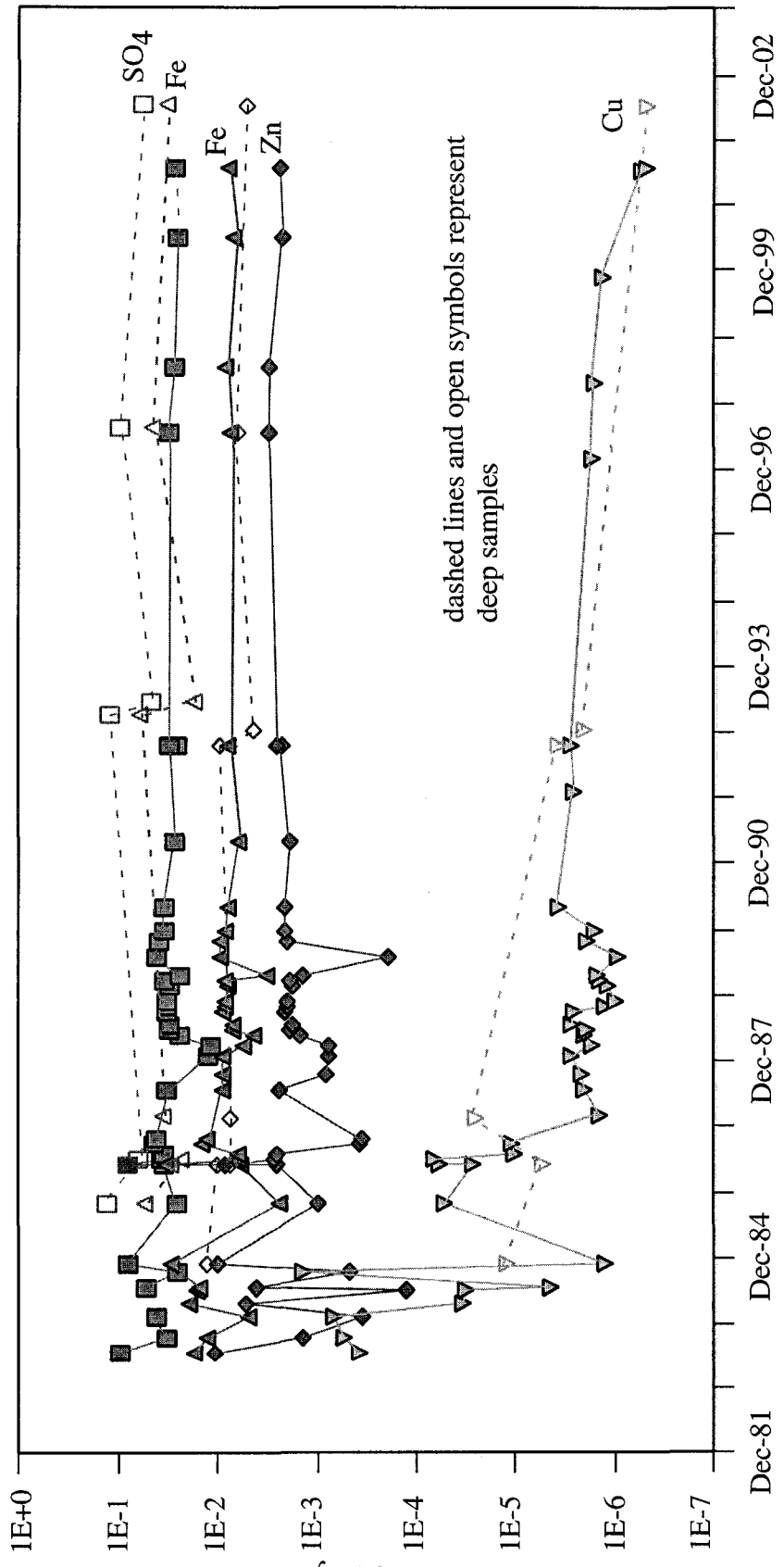

Figure 39. Concentration trends for the deep and shallow waters of the Kelley shaft. Although the trends are similar, the concentrations of dissolved constituents are markedly higher in the deeper waters of the Kelley shaft.

Potential flow directions and sources of water for the Kelley shaft were also considered in the modeling. Flow gradients in the later period of flooding indicated water flows from the Anselmo to the Steward, then to the Kelley, and then to the Berkeley pit. The limited connections between the Steward and Kelley, however, probably restricts the direct flow of water to a few levels. As shown in figure 29, the Steward and Kelley are connected by workings on the deepest level (3800 level) and the 3000 level. Two alternatives were considered: 1) flow from the deep Steward workings into the deep Kelley workings and 2) flow from the shallow Steward workings into the Kelley on both the deep and intermediate levels.

Simulation of the first condition produced reasonable results for copper and other constituents, but significantly underestimated the concentration of iron, zinc, and sulfate. In addition, the pH and pe estimated by the model were higher than observed values. Simulation of the second alternative produced the best results (table 15 and figure 40). In both simulations, the model underestimated the concentration of calcium; as with the Steward, the Kelley shaft is lined with concrete and shotcrete was used in the larger workings. A small addition of lime (cement) to the list of minerals produced good results without causing a large change in pH.

Table 15. Comparison of Kelley shaft sample data to model results (all concentration data are moles/L).

	Kelley 1997	model	RPD
Al	9.15E-005	5.700E-005	47
As	4.34E-005	3.213E-005	30
Ca	1.05E-002	1.316E-002	-22
Cu	1.69E-006	1.117E-009	200
Fe	7.52E-003	8.220E-003	-9
K	8.62E-004	1.435E-004	143
Mg	6.55E-003	2.439E-003	92
Mn	1.10E-003	9.408E-004	16
Na	2.08E-003	1.373E-003	41
S	3.25E-002	2.547E-002	24
Zn	3.04E-003	1.652E-003	59
pH (S.U.)	5.29	5.33	
pe (mv)		-0.52	

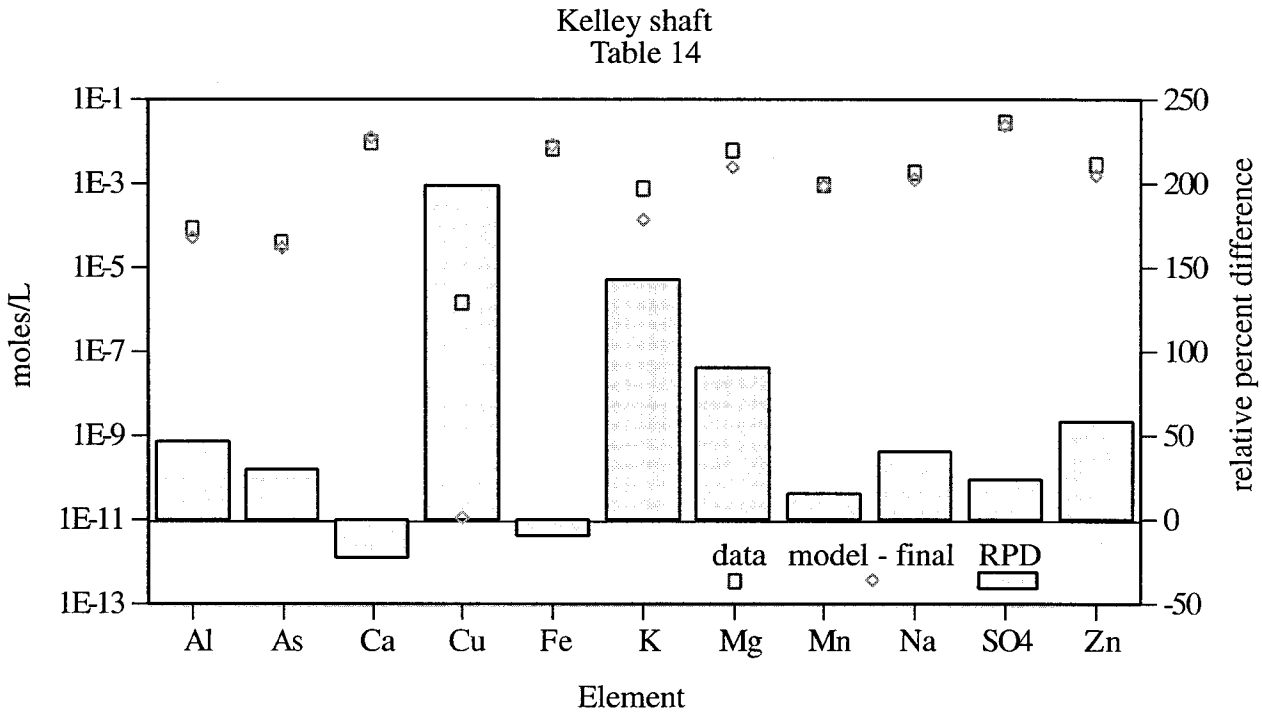

Figure 40. Comparison of modeled concentrations to sample data from the Kelley shaft. Results from the model that starts with the Anselmo (shallow and deep), the Steward (shallow and deep) and ends with the Kelley is compared to data collected from the Kelley shaft in 1997.

Summary of the Steward - Kelley mines

At midnight on April 22, 1982, the pumps draining the underground workings of the Butte districts were shut down and immediately the workings began to flood with ground water originating within the workings. At the same time, many of the activities related to the surface mine were also stopped; within a few days surface water originating the area of the copper precipitation plant was diverted to the Berkeley Pit. The diverted waters probably included at least a portion of the pregnant solution from the leach pad or effluent water from the precipitation plant. Several connections via underground workings between the Kelley and Belmont mines provided conduits for water to flow out the base of the pit and into the underground workings at a rate nearly equal to that of the ground-water influx. Contrary to the concepts proposed in previous studies, the mines nearest the pit filled much more rapidly than those at a distance and flow gradients were outward from the pit and the Kelley mine. The chemistry of the surface water flowing into the workings was markedly different; iron, zinc, and copper concentrations were several time greater than those of the water in the workings. Most notable is the mixing of predominantly ferrous-iron waters from the workings with predominantly ferric-iron waters from the surface. The chaotic mixing of surface and ground waters produces large fluctuations in water quality and pH.

In the Spring of 1983, all remaining mining activities were ceased; any water related to the leach pads, precipitation plant and other surface waters were diverted to the Berkeley Pit. The very high concentrations of zinc, copper, and iron of the leach pad waters produced another cycle of response in the water quality and the rate of water-level rise in the mines nearest the pit.

Water levels in the underground workings reached the bottom of the Berkeley Pit in late 1983 and early 1984. By this time, about half of the waters in the mine workings had originated as ground water and half had originated as surface water from the pit. This 6 to 8 month period was a transition of hydraulic gradients and water chemistry. Gradients reversed and water no longer flowed from the pit to the workings. After the transition, ground water continued to flow into the workings. As water levels in the

workings rose above that of the pit a new hydraulic gradient toward the pit was established and remains at present. About one-third of the water in the underground workings had originated as surface water and the balance originated as ground water within the workings as of 2000.

Summary and Conclusions

The Summit Valley mining district in Butte, Montana is a large porphyry copper deposit that has been extensively mined over a 100-year period. Although the level of mining activities were cyclical, mining by underground and/or surface mining was continuous until 1982 when all mining was shut down. From the earliest efforts to extract ore, in was necessary to pump ground water from the workings. As mines became deeper and more extensive, pumping requirements increased. Just prior to the shut-down in 1982, most of the underground mines were connected by workings and water was drained to a central location at the Kelley and High Ore mines and pumped to the surface at a rate of about 5,000 gallons per minute. This was only part of a large circuit of water used in the mining and milling process in Butte. In 1977, a reported 54,000 gallons per minute (204,000 Liters per minute) were circulated through the mines, the open pits, the leaching operation, and the milling operation.

On April 22, 1982, all of the pumping from the underground mines was stopped; within a year, all other pumping within the vast circuit was also stopped. All of this water was diverted by one means or another to the Berkeley Pit to prevent discharge to the Clark Fork River basin. Geochemical, hydrological, and historical data presented herein have demonstrated that much of that water initially received by the Berkeley Pit continued to the underground workings. The filling rate of the underground mines far exceeded what had been the pumping rate required to keep the mines dry. In the first 21 months of flooding, gradients in the workings were reversed and water flowed from Kelley outward to the surrounding mines (figure 41). Water levels in the Kelley were as much as 80 feet (24 meters) above those in the Belmont mine south and the Steward mine west of the Kelley.

The chemistry of the infiltrating water had a profound effect on the chemistry of the rising waters. High concentrations of strongly oxidized iron and high concentrations of copper and zinc originating from the leaching operation on the surface flowed through the pit and mixed with a roughly equal amount of water originating as ground water within the workings. Two events where water generated by the copper precipitation plant

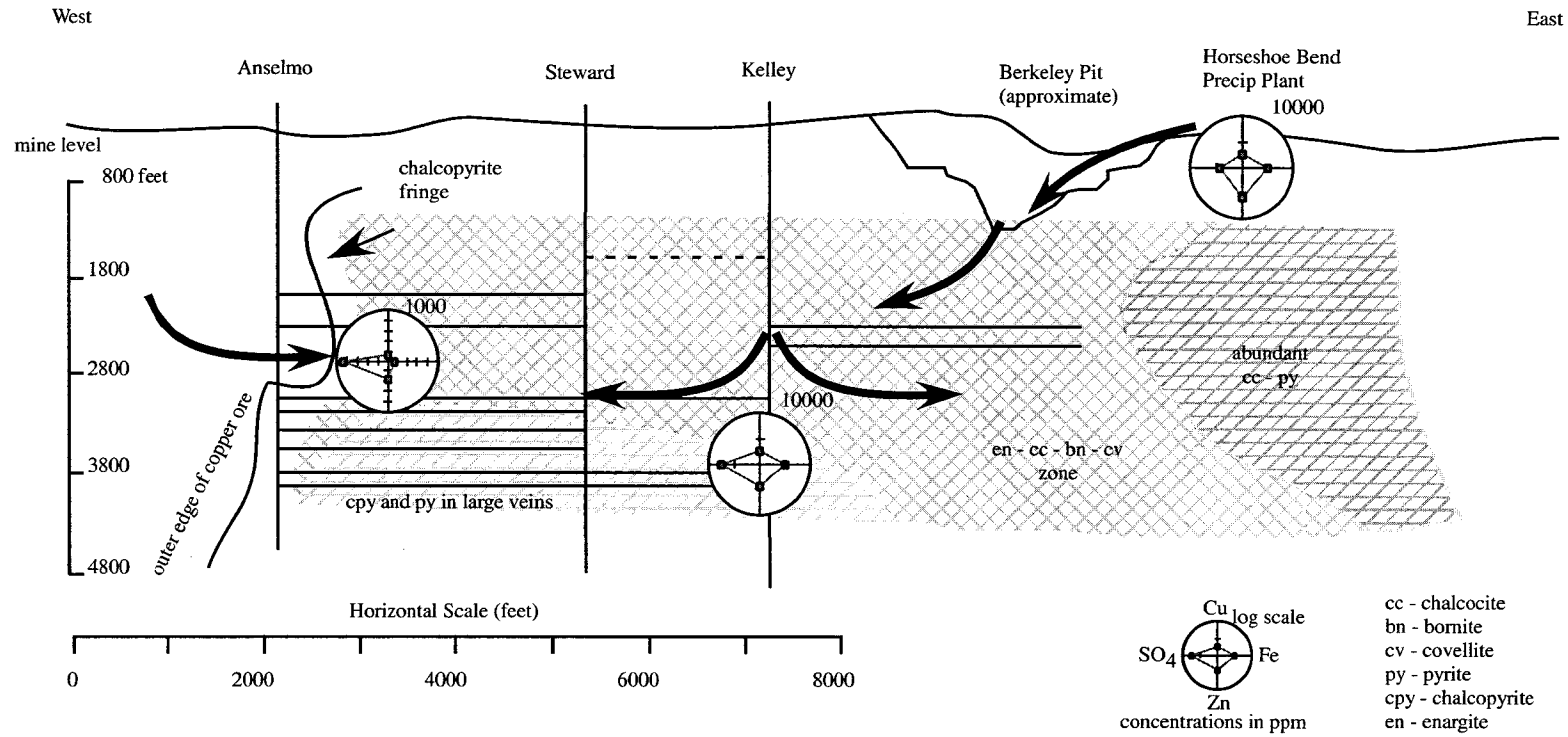

Modified from Meyer and others (1968)

Figure 41. Conceptual model of the early period of flooding. Flow arrows indicate the source and direction of waters filling the underground workings in the early period of flooding (1982 to 1984). Waters entered the workings as ground water from the edge of the district and as surface water from the Berkeley Pit. The mine connections are based on figure 21; additional connections between the Belmont and the pit area are not shown.

entered the pit and workings were reflected in the data collected in the Kelley. The latter event, which coincides with the shut-down of all leaching operations in 1983 are reflected in the chemistry of the waters collected from Kelley and Belmont mines.

In late-1983 and early-1984, water levels in the working reached the elevation of the bottom of the Berkeley Pit. Flow gradients reversed and water began flowing from the workings to the pit (figure 42). Over the next several years, water quality underwent a transition from the mixing of ground water and surface water to one where ground water dominates. By about 1991, concentrations and trends reflected what would probably have occurred without the influence of water from the Berkeley Pit. Rather than a system dominated by the oxidation of pyrite, the introduction of artificial leaching products and the dominant minerals in that portion of the ore body (sphalerite and chalcopyrite) controlled water quality.

As noted in the introductory discussion of ground-water flow in the Butte mines, water levels in the West Camp mines have been higher than those of the East Camp mines throughout the history of flooding. The West Camp and East Camp had been connected by workings, but were separated by water tight bulkheads prior to flooding. There remained, however, the potential for ground-water flow through the bedrock as flooding progressed. Concentrations of dissolved constituents within the mines most likely to receive those waters do not appear to show impact by the West Camp waters, trends and concentrations within the East Camp are better explained by processes and local mineralogy within each mine. On this basis, there is no evidence to suggest a significant amount of ground-water flows from the West Camp mines (Travona and Emma) to the East Camp mines (Belmont and Kelley).

The combination of several techniques, including geochemical modeling and water balance calculations, were valuable in redefining previous concepts of how the Butte mines flooded. Geochemical modeling was used successfully to evaluate the relative contribution (volume and quality) of several sources of waters flooding the mines and was best constrained by the water-balance calculations and local mineralogy. This

work demonstrates that the prediction of water quality in flooding mines requires collection of data commensurate with the physical scale and complexity of the mine and the ore body.

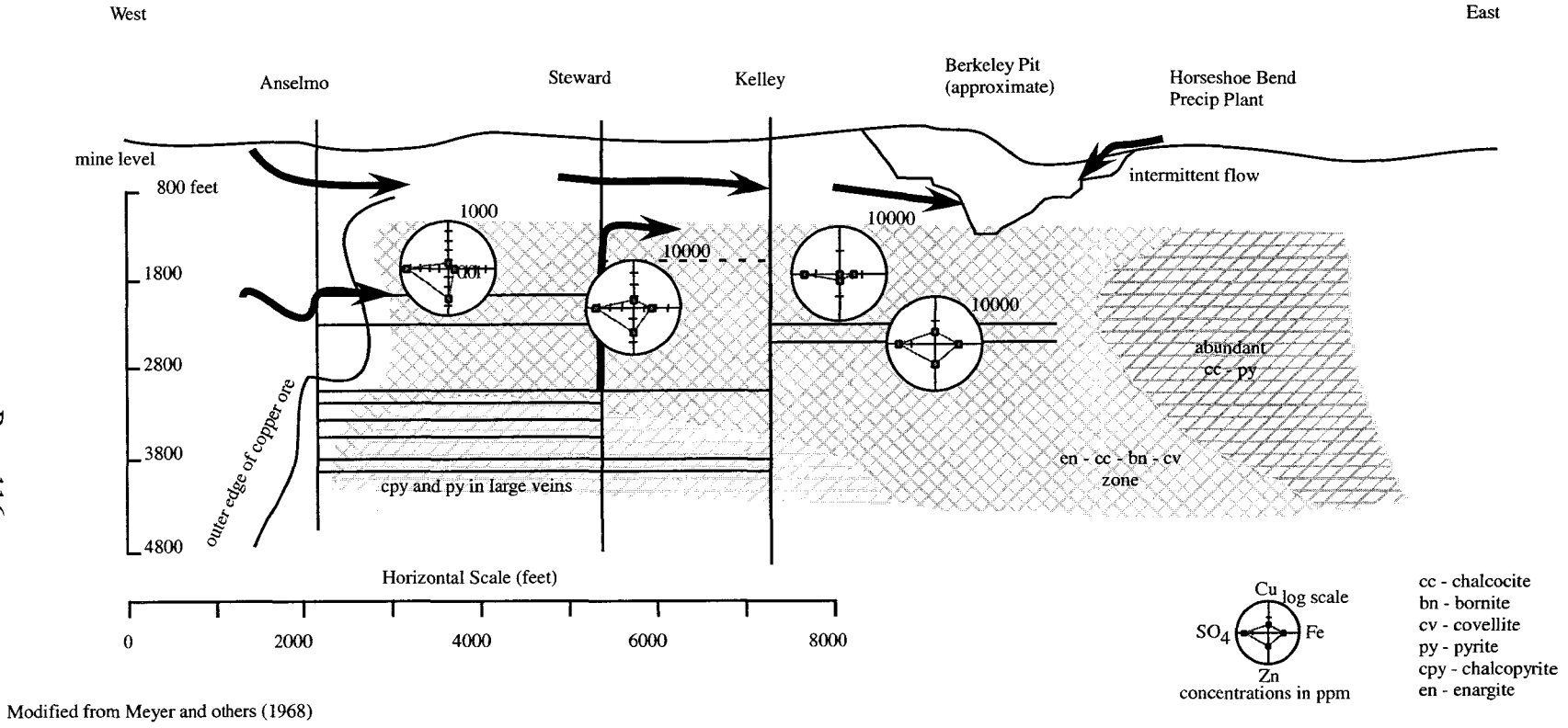

Modified from Meyer and others (1968)

Figure 42. Conceptual model of the late period of flooding. Flow arrows indicate the source and direction of waters filling the underground workings in the later period of flooding (1984 to 2000). Waters continue to enter the workings as ground water from the edge of the district, but gradients prevent the flow surface water from the Berkeley Pit. Upward flow in the Anselmo and Steward shafts mix with shallow waters and flow to the Kelley and Berkeley Pit.

References

Alpers, C.N., Blowes, D.W., Nordstrom, D.K., and Jambor, J.L., 1994, Secondary minerals and acid mine-water chemistry: *in* Environmental Geochemistry of Sulfide Mine-wastes, short course handbook, Jambor, J.L., and Blowes, D.W. eds., Mineralogical Association of Canada, p. 247-270.

Bassett, R. L. and Melchior, D.C., 1990, Chemical modeling of aqueous systems - an overview in: Chemical modeling of aqueous systems, Volume II, American Chemical Society Symposium Series, number 416, p. 1-14.

Balistreiri, L., Box, S., and Tonkin , J.W., 2003, Modeling precipitation and sorption of elements during mixing of river water and porewater in the Coeur d'Alene River Basin: Environmental Science and Technology, volume 37, p. 4694-4701.

Ball, J.W., Runkel, R.L., and Nordstrom, D.K., 1999, Transport modeling of reactive constituents from Summitville, CO; Preliminary results from the application of OTIS/OTEQ to the Wightman Fork/Alamosa River system, in Morganwalp, D.W. and Buxton, H.T., eds., U.S. Geological Survey Toxic Substances Hydrology Program-Proceedings of the Technical Meeting, Charleston, South Carolina, March 8-12, 1999: U.S. Geological Survey Water-Resources Investigations Report 99-4018, p. 305-311.

Benner, S.G., Blowes, D.W., Gould, W.D., Herbert, R.B., and Ptacek, C.J., 1999, Geochemistry of a permeable reactive barrier for metals and acid mine drainage: volume 33, number 16: Environmental Science and Technology, p. 2793-2799.

Brown, J.G., Bassett, R.L., and Glynn, P.D., 2000, Reactive transport of metal contaminants in alluvium--model comparison and column simulation: Applied Geochemistry, volume 15, number 1, p. 35-50.

Canonie Environmental Services, 1993, Butte mine flooding operable unit remedial investigation / feasibility report, prepared for ARCO, compiled by Canonie Environmental Services, 94 Inverness Terrace East, Suite 100, Englewood, CO, 80112, September, 1993, 3 volumes.

Cantrell, K.J., Yabusaki, S.B., Engelhard, M.H., Mitroshkov, A.V., and Thornton, E.C., 2003, Oxidation of H2S by iron oxides in unsaturated conditions: Environmental Science and Technology, volume2 37, p. 2192-2199.

Capo, R.C., Winters, W.R., Weaver, T.J., Stafford, S.L., Hedin, R.S., and Stewart, B.W., 2001, Hydrogeologic and geochemical evolution of deep mine waters, Irwin Syncline, Pennsylvania: in Proceedings of the West Virginia Surface Mine Drainage Task Force Symposium in Proceedings 22nd Annual West Virginia Surface Mine Drainage Task Force Symposium, April 3-4, 2001, Morgantown, West Virginia.

Charlton, S.R., Macklin, C.L. and Parkhurst, D.L., 1997, PHREEQCI--a graphical user interface for the geochemical computer program PHREEQC: U.S. Geological Survey Water- Resources Investigations Report 97-4222, 9 p.

Choi, J., Harvey, J.W., and Conklin, M.H., 2000, Characterizing multiple time scales of stream and storage zone interaction that affect solute fate and transport in streams: Water Resources Research, volume 36, number 6, p. 1511-1518.

Clark, D. W., 1995, Geochemical processes in ground water resulting from surface mining of coal at the Big Sky and West Decker Mine areas, southeastern Montana: U. S. Geological Survey WRI 95-4097, 80 p.

Clark, I.D., and Fritz, P., 1997, Environmental isotopes in hydrogeology: I.D. Clark, ed., Lewis Publishers, Boca Raton, FL, 328 p.

Daly, W.B., Gillie, J., Bruce, J.L., Berrien, C.L., and Braly, N.B., 1925, Mining Methods in the Butte District: Transactions of the American Institute of Mining and Metallurgical Engineers, Volume LXXII, presented at the New York meeting, February, 1923, Published by AIMME, New York, 1925, p. 234-287.

Dasklakis and Helz, 1993, The Solubility of sphalerite (Zns) in sulfidic solutions at 25°C and 1 atm pressure: Geochimica et Cosmochimica Acta, volume 57, p. 4923-4931.

dos Santos Afonso, M., and Stumm, W., 1992, Reductive dissolution of iron(III) (Hydr)oxides by hydrogen sulfide: Langmuir, volume 8, p. 1671-1675.

Davis, Robert E., 1984, Geochemistry and geohydrology of the West Decker and Big Sky coal-mining areas, southeastern Montana: U.S. Geological Survey Water-Resources Investigations Report No. 83-4225, 109 p.

Downey, J.S., 1984, Geohydrology of the Madison and associated aquifers in parts of Montana, North Dakota, South Dakota, and Wyoming: U.S. Geological Survey Professional Paper 1273-G, 47 p.

Drever, J.I., 1997, The Geochemistry of Natural Waters: Surface and Ground water, 3rd edition, Prentice - Hall, 436 pp.

Duaime, T.E., Metesh, J.J., Kerschen, M.K., and Dunstan, C.B., 1998, The flooding of Butte's underground mines and Berkeley Pit: 15 years of water-level monitoring (1982-1998): Montana Bureau of Mines and Geology Open-file report 376, 143p.

Duaime, T.E., 2002. Underground Mine Water Handling and Water-quality changes in the Butte Mines since 1982: Proceedings of the Mineral Symposium, Butte, Montana, April 6, 2002.

Dunne, T. And Leopold, L.B., 1978, Water in Environmental Planning, W.H. Freeman and Company, New York, N.Y., 818 p.

Eberts, S.M., and George, L.L., 2000, Regional ground-water flow and geochemistry in the midwestern basins and arches aquifer system in parts of Indiana, Ohio, Michigan,and Illinois: U.S. Geological Survey Professional Paper 1423–C, 102 p.

Fowler, T.A. and Crundwell, F.K., 1998, Leaching of zinc sulfide by thiobaccillus ferrooxidans: experiments with a controlled redox potential indicate no direct bacterial mechanism: Applied and Environmental Microbiology, volume 64, number 10, p. 3570-3575.

Fowler, T. A. and Crundwell, F.K., 1999, Leaching of zinc sulfide by Thiobacillus Ferrooxidans: bacterial oxidation of the sulfur product layer increases the rate of zinc sulfide dissolution at high concentrations of ferrous ions: Applied and Environmental Microbiology, volume 65, number 12, p. 5285–5292.

Fowler, T. A. , Holmes, P. R, and Crundwell, F. K., 1999, Mechanism of pyrite dissolution in the presence of Thiobacillus Ferrooxidans: Applied and Environmental Microbiology, volume 65, number 7, p. 2987–2993.

Friedly, J.C., and Rubin, J., 1992, Solute transport with multiple, equilibrium-controlled or kinetically controlled chemical reactions: Water Resources Research, volume 28, number 6, p. 1935-1953.

Fritz, P., and Fontes, J.C., (Eds), 1986, Handbook of Environmental Isotope Geochemistry, 2b, The Terrestrial Environment, Elsevier Science, Amsterdam, pp. 361-425.

Gammons, C.H, Simon R. Poulson, S.R., Metesh, J.J., Duaime, T.E, and Henne, A.R., 2003, Geochemistry and isotopic composition of H_2S-rich flooded mine waters, Butte, Montana: Mine Water and The Environment, accepted for publication.

Garrels, R.M., and Thompson, M.E., 1962, A chemical model for sea water at 25C and one atmosphere total pressure: American Journal of Science, number 260 , p.57-66 *in:* Garrels, R.M. and Christ, C.L., 1965, Solutions, minerals, and equilibria, Freeman, Cooper, and Company, 450 p.

Gi-Tak, C., Seong-Taek, Y., Sang-Ryul, K., and Chan H., 2001, Hydrogeochemistry of seepage water collected within the Youngcheon diversion tunnel, Korea: source and evolution of SO_4 rich groundwater in sedimentary terrain: Hydrological Processes, volume, number 9, June 2001, p. 1565-1583.

Goddard, C.C., 1960, Copper Water in the Butte Mines and suggestions as to distributions of copper derived therefrom to the various mine units, unpublished report, November 23, 1960, by Charles C. Goddard, Jr.

Goode, D. J., and Konikow, L. F., 1991, Testing a method-of-characteristics model of three-dimensional solute transport in ground water: p. 21-27 in: Symposium on Ground Water, Proceedings of the International Symposium, Nashville, Tenn., July 29 to August 2, 1991, American Society of Civil Engineers, New York.

Gosselin, D.C., Harvey, F.E., and Frost, C.D., 2001, Geochemical evolution of ground water in the Great Plains (Dakota) Aquifer of Nebraska: Implications for the management of a regional aquifer system: Ground Water, volume 39, number1, p.98-101.

Harahuc, L., Lizama, H.M., and Suzuki, I., 2000a, Selective inhibition of the oxidation of ferrous iron or sulfur in Thiobaccillus ferrooxidans: Applied and Environmental Microbiology, volume 66, number 3, p. 1031-1037.

Harahuc, L., Lizama, H.M., and Suzuki, I., 2000, Effect of anions on selective solubilization of zinc and copper in bacterial leaching of sulfide ores: Biotechnology and Engineering, volume 69, number 2, p. 196-203.

Hartog, N., Griffioen, J., and Van der Wijden, C.H., 2002, Distribution and reactivity of O_2-reducing components in sediments from a layered aquifer: Environmental Science Technology, volume 36, p. 2338-2344.

Hem, J.D., 1992, Study and interpretation of the chemical characteristics of natural water: U.S. Geological Survey Water-Supply Paper 2254, 263 p.

Hemingway, B.S., Seal, S.S., and Chou, I.M., 2002, Thermodynamic data for modeling acid mine drainage problems - compilation and estimation of data for selected soluble iron-sulfate minerals: U.S. Geological Survey Open-file report 02-161, 13 p.

Kartio, I.J., Basilio, C.I., and Yoon, R.H., 1998, An XPS Study of Sphalerite Activation by Copper: Langmuir (American Chemical Society), volume 12, number 18, p. 5274-5278.

Kawano, M., and Tomita, K., 2001, Geochemical modeling of bacterially induced mineralization of schwertmannite and jarosite in sulfuric acid spring water: American Mineralogist, volume 86, p. 1156–1165.

Kelly, W.R., 1997, Heterogeneities in ground-water geochemistry in a sand aquifer beneath an irrigated field: Journal of Hydrology, volume 198, p. 154-176.

Kent, D.C., Al-Shaieb, Z., Vaden, D.W., and Bayley, P.W., 1987, Hydrogeological and geochemical aspects of ground and surface water pollution associated with lead and zinc mines in the tri-state mining district: Chemical Quality of Water and the Hydrologic Cycle, Averett R.C., and McKnight, D.M., eds., 1987 Lewis Publishers, Inc.

Konishi, Y., Asai, S., Tokushige, M., and Suzuki, T., 1999, Kinetics of the bioleaching of chalcopyrite concentrate by acidophilic thermophile Acidianus brierleyi: Biotechnology Progresses, volume 15, p. 681-688.

Langmiur, D, 1997, Aqueous Environmental Geochemistry, Prentice-Hall, Inc., Upper Saddle River, New Jersey.

Lowel J.D. and Guilbert, J.M., 1970, Lateral and vertical alteration-mineralization zoning in porphyry ore deposits: Economic Geology, volume 65, number 4, June-July 1970, p. 373-408.

Macfarlane, P.A, Whittemore, D.O. Townsend, M.A., Doveton, J.H, Hamilton, V.J., Coyle III, W.G., Wade, A., Macpherson, G.L. Black, R.D., 1990, The Dakota Aquifer Program Annual Report, FY89: Kansas Geological Survey Open-file Report 90-27, 301 p.

Malmstron, M.E., Destouni, G.A., Banawart, S.A., and Stronmberg, B.H.E., 2000, Resolving the scale-dependence of mineral weathering rates: Environmental Science and Technology, volume 34, number 7, p. 1375-1378.

Meyer, C., Shea, E.P., and Goddard, C.C., 1968, Ore Deposits at Butte, Montana, in: Ore Deposits of the United States, 1933-1967, the Graton-Sales volume, John D. Ridge, editor, American Institute of Mining, Metallurgy and Petroleum Engineering, Inc., New York, New York, Volume II, p. 1373-1416.

Miller, R.N., 1973, Guidebook for the Butte Field Meeting of Society of Economic Geologists, Butte, Montana, August 18-21, 1973, R.N. Miller, editor, 236 p.

Mountain, B. W., and Seward, T.M.,1999, The hydrosulphide/sulphide complexes of copper(I): Experimental determination of stoichiometry and stability at 22°C and reassessment of high temperature data, Geochimica et Cosmochimica Acta, volume 63, p. 11-29.

Naik, M.S., Momin, G.A., Rao, P.S.P., Safai, P.D., and Ali, K., 2002, Chemical composition of rainwater around an industrial region in Mumbai, Current Science, volume 82, number 9, p. 1131-1137.

Nealson, K.H. and Stahl, D.A., 1991, Microorganisms and biochemical cycles, Applied and Environmental Microbiology, volume 57, p. 6-34.

Nordstrom, D.K., 1985, Aqueous pyrite oxidation and the consequent formation of secondary iron minerals, in: Acid Sulfate Weathering, Kittrick, J.A., Fanning, D.A., and Hossner, L.R., eds., Soil Science Society, p. 37-56.

Olsen, G.J., 1991, Rate of bioleaching by Thiobaccilus Ferrooxidans, results of an interlaboratory comparison: Applied and Environmental Microbiology, volume 57, p. 642-644.

Palmer, C.D., and Cherry, J.A., 1984, Geochemical evolution of groundwater in sequences of sedimentary rocks: Journal of Hydrology, volume 75, p. 27-65.

Parkhurst, D.L., Stollenwerk, K.G., and Colman, J.A., 2003, Reactive-transport simulation of phosphorus in the sewage plume at the Massachusetts Military Reservation, Cape Cod, Massachusetts: U.S. Geological Survey Water-Resources Investigations Report 03-4017, 32 p.

Paulson, A.J., and Balistrieri, L., 1999, Modeling removal of Cd, Cu, Pb, and Zn in acidic groundwater during neutralization by ambient surface waters and groundwaters: Environmental Science and Technology, volume 33, p. 3850-3856.

Piper, R.D., 1960, Investigation of Contamination of the Clark Fork River from Source in Silver Bow Creek, unpublished report by R.D. Piper, Mining Engineering Department, Anaconda Company, for E.I. Renouard, Vice-president, Anaconda Company, November, 1960, 15 p.

Podda, F., Zuddas, P., Minacci, A., Pepi, M., and Baldi, F., 2000, Heavy metal co-precipitation with hydrozincite from mine waters caused by photosynthetic micoorganisms: Applied and Environmental Microbiology, volume 66, number 11, p. 5092-5098.

Pohl, H.A., 1962, Solubility of iron sulfides: Journal of Chemical and Engineering Data, volume 7, number 2, p. 295-306.

Poreda, R.J., Cerling, T.E., and Solomon, D.K., 1988, Tritium and helium isotopes as hydrologic tracers in a shallow unconfined aquifer: Journal of Hydrology, volume 103, p. 1-9.

Postgate, J.R., 1984, The sulfate-reducing bacteria, second edition, Cambridge University Press, 198 p.

Ravitz, S.F and Wall, W.A., 1934, The Adsorption of copper sulfate by sphalerite and its relation to flotation: Journal of Physical Chemistry, volume 38, number 13, p. 13-18.

Ritchie, A.I.M, 1994, The waste-rock environment: *in* Environmental Geochemistry of Sulfide Mine-wastes, short course handbook, Jambor, J.L., and Blowes, D.W. eds., Mineralogical Association of Canada, p. 133-163.

Roberts, D.R., Schienost, A.C., and Sparks, D.L., 2002, Zinc speciation in a smelter-comtaminated soil profile using bulk and microspectroscopic techniques: Environmental Science and Technology, volume 36, p. 1742-1750.

Rubin, J., 1983, Transport of reacting solutes in porous media: relation between mathematical nature of problem and chemical nature of reactions, Water Resources Research, volume 19, number 5, p. 1231-1252.

Rubin, J., 1992, Solute transport with multi-segment, equilibrium-controlled, classical reactions--Problem solvability and feed forward method's applicability for complex segments of most binary participants: Water Resources Research, volume 28, number 6, p. 1681-1702.

Runkel, R.L., and Kimball, B.A., 2002, Evaluating remedial alternatives for an acid mine drainage stream: application of a reactive transport model: Environmental Science and Technology, volume 36, p. 1093-1101.

Sales, R.H., 1914, Ore Deposits and Butte, Montana: American Institute of Mining Engineering, volume 46, p. 3-109.

Shea, D., and Helz, G.R., 1989, The solubility of copper in sulfidic waters: Sulfide and polysulfide complexes in equilibrium with covellite: Geochimica et Cosmochimica Acta, volume 52, p. 1815-1825.

Silvester, E.J., Crieser, F., Meisel, D., Healy, T.W., and Sullivan, J.C., 1992, Oxidation kinetics of ultra-small colloidal chalcopyrite (CuFeS,) with one-electron oxidants: The Journal of Physical Chemistry, volume 96, number 11, p. 4382-4388.

Sokolov, I., Smith, D.S., Henderson, G.S., Gorby, Y.A., and Ferris, F.G., 2001, Cell surface electrochemical heterogeneity of the Fe(III)-reducing bacteria Shewanella putrefaciens: Environmental Science and Technology, volume 35, p. 341-347.

Spindler, J.C., 1977, The Clean-up of Silver Bow Creek: Mining Congress Journal, 1977, p. 58-63.

Third, K.A., Cord-Ruwisch, R., and Watling, H.R., 2002, Control of the redox potential by oxygen limitation improves bacterial leaching chalcopyrite: Biotechnology and Bioengineering, volume 78, number 4, p. 434-441.

Tonkin , J.W., Balistreiri, L., and Murray, J.W., 2002, Modeling metal removal onto natural particles formed during mixing of acid rock drainage with ambient surface water: Environmental Science and Technology, volume 36, p. 484-492.

Wang, F., and Tessier, A., 1999 Cadmium complexation with bisulfide: Environmental Science and Technology, volume 33, p. 4270-4277.

Welham, N.J., 2001, Ambient temperature oxidation of enargite (Cu_3AsS_4): Proceedings AusIMM, October 12-14, volume 306, number 1, 2001, p.79-81.

Widell, F. 1988, Microbiology and Ecology of Sulfate- and Sulfur-reducing bacteria, in: Biology of Anaerobic Microorganisms, A.J.B. Zehnder editor, Wiley Interscience, publisher, New York, p. 469-583.

Appendix I: Bioassay of Selected Mine shafts in the Butte area

Bio-assay of water in selected mine shafts

Several shafts throughout the district were sampled for bacteria and total organic carbon (TOC) to provide basic information on the role of microbial activities and water-quality. The assay was restricted to aerobic sampling and culturing, but both aerobic and anaerobic bacteria were considered for population estimates. Table 16 presents the sample depths, TOC and population counts for the 6 shafts sampled. The Marget Ann mine is in the outermost area of the district and is isolated from any other mines; the Emma mine is within the West Camp and is well connected by workings to the Travona mine; the Steward, Granite Mountain, Anselmo, and Pilot Butte mines are part of the East Camp. Live and dead bacteria were determined by staining with Molecular Probes brand live/dead bacLight bacterial viability kit; after preparation, counts were made using a Nikon Eclipse E800 microscope.

Table 16. Bacteria counts for mines shafts in the Butte area

Site	Depth* (feet[meters])	TOC (mg/L)	Live (/mL)	Dead (/mL)
Marget Ann	250 [76]	2	290,000	500,000
Emma	240 [73]	6	140,000	400,000
Steward	675 [206]	400	2,700,000	3,400,000
	800 [244]	9	300,000	300,000
Granite Mtn	850 [260]	7	300,000	200,000
	1200 [365]	6	40,000	140,000
Anselmo	550 [167]	4	40,000	70,000
	900 [274]	3	80,000	110,000
Pilot Butte	840 [256]	9	1,000,000	3,000,000

* Depth below land surface; the shallow samples (where indicated) were collected near the water surface

Total organic carbon is generally low in all of the samples with the exception of the shallow sample from the Steward shaft. Surface waters in natural systems generally have TOC concentrations above 20 mg/L (Langmuir, 1997, p. 421). Down-hole video of the Steward shaft indicated the presence of a floating iridescent sheen that suggests some type or oil or other petroleum product. The population counts are also low with the exception of the shallow Steward and the Pilot Butte samples; natural water systems generally exhibit total population counts well above 6 million.

Samples from all of the shafts were cultured under aerobic conditions with nutrient agar; in addition to plate counts, colonies were separated based on color and morphology, cultured again, and shipped for rRNA analyses. Nine species were isolated submitted for rRNA analysis and identification. Table 17 presents the 6 species identified (greater than 95% confidence) and the shaft(s) from which each species was collected.

Table 17. Identified species and locations

Species	**Site**
Variovorax paradoxus	Emma
Bacillus pumilus	Anselmo, Granite Mtn, Pilot B.
Microbacterium thalassium	Anselmo, Granite Mtn, Pilot B.
Arthrobacter oxydans	All sites
Chryseobacterium indologenes	Marget Ann, Steward
Flavobacterium hydatis	Emma

Thiobacillus ferrooxidans or related species were not identified in any of the samples collected. Although special nutrient agar is usually used to culture these types of bacteria, their presence, if in high numbers, is often detected in the rRNA analyses regardless of the type of agar used. These bacteria are acidophilic chemolithotrophs whose optimal growth occurs in waters of pH 1.5 to 3.5 and derive energy from the oxidation of ferrous

iron. At neutral pH these bacteria must compete with the abiotic oxidation of ferrous iron (Nealson and Stahl, 1991) . In the shafts sampled in this study, the pH of the waters ranged from about 5.5 to 6.5 and thus, the activity of Thiobacillus ferrooxidans is likely limited.

Appendix II: Annotated listing of model input files for Travona simulations

Travona shaft acid rock drainage simulation / oxidation of pyrite

This model was used to examine the oxidation of pyrite in the Travona workings using background ground-water inflow and the mineral assemblage indigenous to the West Camp. The partial pressure of CO_2 and H_2S were assumed to be insignificant during the oxidation period; pyrite, as well as most other minerals, was assumed to be an infinite solid. In other words, no controls were placed on the amount of solid to be dissolved in the model. PHREEQE allows the addition of oxygen to the solution by several means: O_2 gas can be introduced as an EQUILIBRIUM_PHASE as is normally done with mineral phases; the log partial pressure and the maximum amount to be dissolved is specified. In this method, only one value for the amount of O_2 can be used. Another method is to provide the partial pressure of the gas at a constant pressure or as a constant volume using the GAS_PHASE input module of PHREEQE. Again, the resulting simulation uses a constant value. The REACTION module, used in this simulation, allows the variation of the gas, input as moles, in steps. The step size and value is specified by the user.

```
EQUILIBRIUM_PHASES 1 Travona
minerals
  Arsenolite 0 3e-007
  Chalcopyrite 0 10
  CO2(g)  0 0
  H2S(g)  0 0
  Montmorillonite-Ca 0 10
  Pyrite  0 10
  Quartz  0 10
```

Mineral phases indigenous to the West Camp are used. CO_2 and H_2S are assumed to be zero.

```
  Rhodochrosite 0 10
SOLUTION 1 Geary well 88Q1549
  temp    11
  pH      7.32
  pe      0
  redox   pe
  units   mg/l
  density 1
  Alkalinity 211.36
  B       380 ug/l
  Ca      206
  Cl      42.1
  Cu      11 ug/l
  F       0.66
  Fe      0.2
  K       5.6
  Mg      58.8
  Mn      0.02
  N       4.12
  Na      31.5
  As      4.5 ug/l
  S(6)    514
  Si      23.3
  Zn      345 ug/l
  Al      30 ug/l
  -water  1 # kg
REACTION 1
  O2(g)   1
  0 0.001 0.0001 0.001 0 moles
SELECTED_OUTPUT
  -file           Travona_ard_gen
  -step           true
  -ph             true
  -pe             true
  -totals         Fe S(-2)
END
```

Ground-water quality from a well completed in the shallow bedrock near the mine was used as the initial solution. The alternative is to use pure water.

0.0, 0.001, 0.0001 moles of O_2 are added to the 1 Liter solution in the first 3 steps. The steps are then reversed: 0.001, 0.0 to simulate the flooding of workings and reduction of available O_2.

Selected output from the model is written to a separate file to facilitate graphics. The file named Travona_ard_gen is shown below.

sim	state	soln	dist_x	time	step	pH	pe	Fe	S(-2)
1	i_soln	1	-99	-99	-99	7.32	0	3.5852e-006	0.0000e+000
1	react	1	-99	0	1	7.33732	-3.24357	1.2013e-005	8.9393e-006
1	react	1	-99	0	2	6.93319	-2.67627	2.9262e-004	1.0081e-006
1	react	1	-99	0	3	7.28175	-3.14337	3.8320e-005	5.9090e-006
1	react	1	-99	0	4	6.93319	-2.67627	2.9262e-004	1.0081e-006
1	react	1	-99	0	5	7.33732	-3.24357	1.2013e-005	8.9393e-006

Oxidation of pyrite / early and late flooding of the Travona shaft

The following input file combines the three periods of changes in the Travona shaft: acid generation during oxidation of pyrite, the early period of flooding with the initial generation of H_2S, and the later period of flooding where H_2S changes due to the flooding of the uppermost workings. As with the initial model, background ground-water quality flowing into the mine was used in the initial solution. Pyrite is oxidized in one step using the optimum mole amount based on the general oxidation model. H_2S and CO_2 are introduced in the second part of the simulation based on the range of measured values and compared to water-quality analyses of that period. The last step of the model is to reduce the partial pressure of H_2S to those levels observed in the later period of flooding; no other conditions were changed.

```
EQUILIBRIUM_PHASES 1 Travona minerals
   Arsenolite 0 3e-007
   Chalcopyrite 0 10
   CO2(g)  -1.25 10
   Montmorillonite-Ca 0 10
   Pyrite  0 10
   Quartz  0 10
   Rhodochrosite 0 10
```

The mineral assemblage indigenous to the West Camp are used throughout the simulation

```
SOLUTION 1 well 88Q1569
   temp     11
   pH       7.32
   pe       0
   redox    pe
   units    mg/l
   density  1
   Alkalinity 211.36
   B        380 ug/l
   Ca       206
   Cl       42.1
```

Background water-quality from a well completed in the shallow bedrock aquifer near the mine.

```
  Cu      11 ug/l
  F       0.66
  Fe      0.2
  K       5.6
  Mg      58.8
  Mn      0.02
  N       4.12
  Na      31.5
  As      4.5 ug/l
  S(6)    514
  Si      23.3
  Zn      345 ug/l
  Al      30 ug/l
  -water  1 # kg
REACTION 1 oxidation of pyrite
  O2(g)   1
  0.00015 moles in 1 steps
SAVE solution 1
END
USE solution 1
EQUILIBRIUM_PHASES 2 reduction
and H2S generation for early flooding
  Arsenolite 0 3e-007
  Chalcopyrite 0 10
  CO2(g)  -1.25 10
  H2S(g)  0 7e-006
  Montmorillonite-Ca 0 10
  Pyrite  0 10
  Quartz  0 10
  Rhodochrosite 0 10
SAVE solution 2
END
USE solution 2
EQUILIBRIUM_PHASES 3 decrease
H2S in later flooding
  Arsenolite 0 3e-007
  Chalcopyrite 0 10
  CO2(g)  -1.25 10
  H2S(g)  0 8.245e-007
  Montmorillonite-Ca 0 10
  Pyrite  0 10
  Quartz  0 10
  Rhodochrosite 1 10
END
```

Oxidation of pyrite is simulated using the REACTION module. The optimum oxidation amount is used and the solution saved (solution 1) for subsequent equillibration.

The solution from the previous step is used to equilibration with the mineral assemblage and the introduction of gases.

The resulting solution is saved for the next step.

The later period of flooding uses the solution from the previous step and re-equilibrates the mineral assemblage with a lower partial pressure of H_2S.

Modeling Diagram
Travona shaft

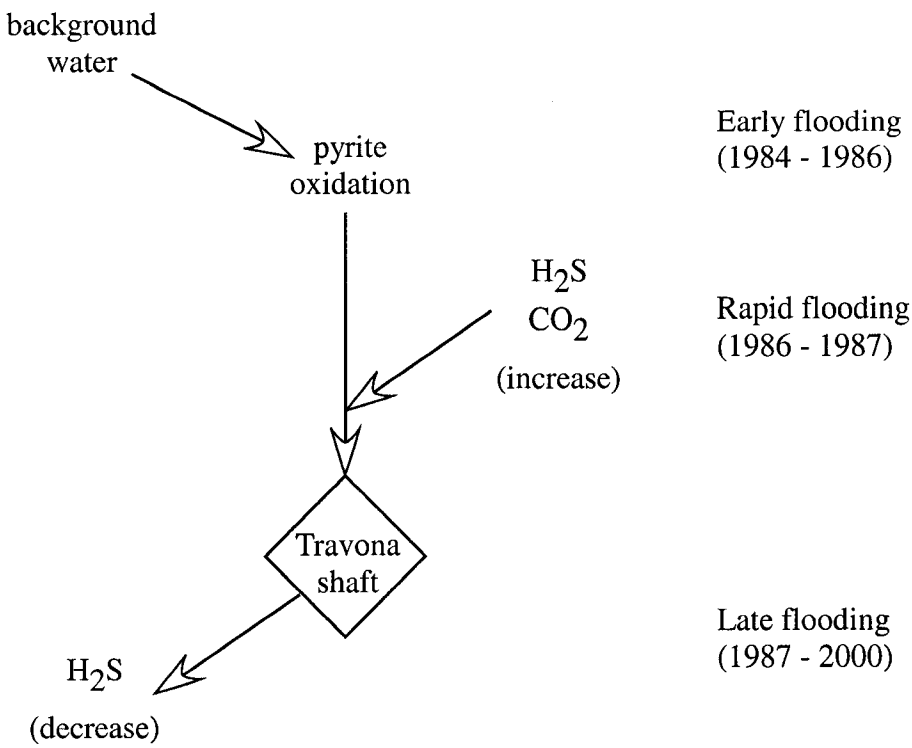

Appendix III: Annotated listing of model input files for Anselmo simulations

Oxidation of chalcopyrite and sphalerite in the Anselmo shaft

The model input presented here was used to evaluate oxidation of minerals found in the workings of the Anselmo, particularly chalcopyrite and sphalerite. Other minerals in the assemblage are based on alteration minerals and the country rock. The same input file was used to simulate the introduction of O_2 under high partial pressure CO_2 (1E-0.5 atm) and low partial pressure of CO_2 (1E-03 atm). As discussed in the Travona simulation, the gas was input to the model as an EQUILIBRIUM PHASE with the log partial pressure specified. Also, in a manner similar to previous simulations for oxidation in the Travona, the REACTION module was used to introduce increasing amounts of O_2 in mole amounts to 1 Liter of solution. Selected output from the model were saved to a file for graphing and comparison to water-quality data.

```
EQUILIBRIUM_PHASES 1 Anslemo minerals
   Arsenolite 0 3e-007
   Chalcopyrite 1 10
   CO2(g)  -0.5 10
   Montmorillonite-Ca 0 1
   Quartz  0 1
   Rhodochrosite 0 1
   Sphalerite 0 10
SOLUTION 1
   temp     14
   pH       7.32
   pe       -2
   redox    pe
   units    ppm
   density  1
   Alkalinity 211.36
   B        380 ppb
```

Mineral phases used in this simulation reflect both shallow and deep workings of the Anselmo mine.

The log partial pressure was set at -0.5 atm for this simulation and 1E-3 atm for the second simulation.

Background water quality is based on an analysis from a well completed in the shallow bedrock near the mines.

```
  Ca      206
  Cl      42.1
  Cu      11 ppb
  F       0.66
  Fe      0.02
  K       5.6
  Mg      58.8
  Mn      0.02
  N       4.12
  Na      31.5
  As      4.5 ppb
  S(6)    514
  Si      23.3
  Zn      545 ppb
  -water  1 # kg
REACTION 1
  O2(g)    1
  0.0004 0.0005 0.0006 0.0007 0.0008
0.0009 0.0008
  0.0007 0.0006 0.0005 0.0004 moles
SELECTED_OUTPUT
  -file            selected.out
  -step            true
  -totals          Alkalinity Cu Fe Mg
Mn Zn S(6)
  -gases           CO2(g) H2S(g)
END
```

O_2 is added for the reaction in 11 steps, first increasing then decreasing.

Selected output are saved to a file and used for graphics.

Oxidation of chalcopyrite and sphalerite in pure water with no other minerals

This model was used to evaluate the competitive nature of chalcopyrite and sphalerite oxidation and demonstrate the range of sulfate and iron concentrations necessary to produce similar results compared to sample data from the Anselmo shaft. The minerals to be equilibrated were restricted to chalcopyrite and sphalerite and pure water was used. The GAS_PHASE module was used to introduce CO_2 and O_2 at a fixed partial pressure specified. The model was re-run for each set of conditions and the results saved.

```
EQUILIBRIUM_PHASES 1
Chalcopyrite and sphalerite
   Chalcopyrite 0 10
   Sphalerite 0 10
GAS_PHASE 1
   -fixed_pressure
   -pressure 1
   -volume 1
   -temperature 25
   CO2(g)   0.000316
   O2(g)    0.2
SOLUTION 1 oxidation of Chalcopyrite
and Sphalerite  with O2
   temp     25
   pH       7
   pe       0
   redox    pe
   units    mol/kgw
   density  1
   -water   1 # kg
END
```

The saturation indices are set to 0 and maximum mole amount that can be dissolved is set to 10 moles.

Fixed partial pressure is used for both gases; these values are changed in each simulation.

Rather than use background water quality, pure water is used to simplify comparisons.

Mixing of deep and shallow water in the Anselmo shaft

Minerals indigenous to the deeper workings of the Anselmo, including chalcopyrite, were equilibrated to inflow ground water. In a separate step, minerals of the shallow workings, including sphalerite, were equilibrated with the same water. The resulting solution from the first two steps are mixed at a specified ratio in the third step. Partial pressures of both O_2 and CO_2 were assumed to be higher in the shallow workings.

```
EQUILIBRIUM_PHASES 1 Anslemo
minerals DEEP
   Arsenolite 0 3e-009
   Chalcopyrite 0 10
   Montmorillonite-Ca 0 10
   Quartz   0 1
   Rhodochrosite 0 1
SOLUTION 1 well 88Q1549 first
   temp     14
   pH       7.32
   pe       -2
   redox    pe
   units    ppm
   density  1
   Alkalinity 211.36
   B        380 ppb
   Ca       206
   Cl       42.1
   Cu       11 ppb
   F        0.66
   Fe       0.02
   K        5.6
   Mg       58.8
   Mn       0.02
   N        4.12
   Na       31.5
   As       4.5 ppb
   S(6)     514
   Si       23.3
   Zn       545 ppb
```

Mineral phases for the deep workings included chalcopyite.

Minerals were equilibrated with inflow ground water based on the water quality of a well completed in the shallow bedrock aquifer.

```
   -water    1 # kg
GAS_PHASE 1 oxidation of
chalcopyrite at atmospheric CO2
   -fixed_pressure
   -pressure 1
   -volume 1
   -temperature 14
   CO2(g)    0.000316
   O2(g)     5e-005
SAVE solution 2
SELECTED_OUTPUT
   -file              selected1.out
   -step              true
   -totals            Cu  Fe  Mg  Mn  Zn
S(6)  Al
   -gases             CO2(g)  O2(g)
END
SOLUTION 3 well 88Q1549 second
   temp      14
   pH        7.32
   pe        -2
   redox     pe
   units     ppm
   density   1
   Alkalinity 211.36
   B         380 ppb
   Ca        206
   Cl        42.1
   Cu        11 ppb
   F         0.66
   Fe        0.02
   K         5.6
   Mg        58.8
   Mn        0.02
   N         4.12
   Na        31.5
   As        4.5 ppb
   S(6)      514
   Si        23.3
   Zn        545 ppb
   -water    1 # kg
EQUILIBRIUM_PHASES 1 Anslemo
minerals SHALLOW
   Arsenolite 0 3e-009
```

Chalcopyrite, as well as the other minerals, was oxidized under atmospheric CO_2.

The solution for the deep mineral equilibration was saved for the mixing step.

The same ground-water inflow quality was used in the simulation of the shallow workings.

```
   Montmorillonite-Ca 0 10
   Quartz   0 1
   Rhodochrosite 0 1
   Sphalerite 0 1
GAS_PHASE 2 high CO2 oxidation of
sphalerite
   -fixed_pressure
   -pressure 1
   -volume 1
   -temperature 14
   CO2(g)   0.316
   O2(g)    0.01
SAVE solution 4
SELECTED_OUTPUT
   -file             selected2.out
   -step             true
   -totals           Cu  Fe  Mg  Mn  Zn
S(6)  Al
   -gases            CO2(g)  O2(g)
END
MIX 1
   2   10
   4   90
END
```

The same mineral phases were used as with the deep mineral except chalcopyrite was replaced with sphalerite.

In this simulation, 10% of solution 2 (deep) was mixed with 90% of solution 4 (shallow).

Equilibration of deep minerals then shallow minerals in the Anselmo shaft

As an alternative to the mixing model where deep and shallow water are equilibrated with local minerals separately and then mixed, this model equilibrates inflow ground water with deep minerals then with shallow minerals. Minerals in the deep workings, particularly chalcopyrite, are equilibrated and the solution saved. The saved solution is then the initial solution to equilibrate shallow minerals. The results of the second step were compared to water-quality data collected from the shaft. Partial pressures of CO_2 and O_2 were based on those used in previous simulations.

```
EQUILIBRIUM_PHASES 1 Anselmo
minerals DEEP                          Deep minerals of the Anselmo workings
   Arsenolite 0 3e-009                 include chalcopyrite.
   Chalcopyrite 0 10
   Kaolinite 0 1
   Quartz 0 1
   Rhodochrosite 0 1
SOLUTION 1 well 88Q1549                As with other models, water quality from
   temp    14                          a bedrock well was used as the initial
   pH      7.32                        solution.
   pe      -1
   redox   pe
   units   ppm
   density 1
   Alkalinity 211.36
   B       380 ppb
   Ca      206
   Cl      42.1
   Cu      11 ppb
   F       0.66
   Fe      0.02
   K       5.6
   Mg      58.8
   Mn      0.02
   N       4.12
   Na      31.5
```

```
    As      4.5 ppb
    S(6)    714
    Si      23.3
    Zn      545 ppb
    -water  1 # kg
GAS_PHASE 1
    -fixed_pressure
    -pressure 1
    -volume 1
    -temperature 14
    CO2(g)  0.000316
    O2(g)   5e-005
SAVE solution 2
SELECTED_OUTPUT
    -file           selected1.out
    -totals         Al As Cu Fe Mn S
Zn
END
EQUILIBRIUM_PHASES 1 Anslemo
minerals SHALLOW
    Arsenolite 0 3e-009
    Kaolinite 0 1
    Quartz  0 1
    Rhodochrosite 0 1
    Sphalerite 0 1
USE solution 2
GAS_PHASE 2
    -fixed_pressure
    -pressure 1
    -volume 1
    -temperature 14
    CO2(g)  0.316
    O2(g)   0.01
SELECTED_OUTPUT
    -file           selected2.out
    -totals         Al As Cu Fe Mn S
Zn
END
```

The solution from the first step is saved and used as the initial condition for the second step.

Chalcopyrite is replaced by sphalerite for minerals representative of the shallow workings of the Anselmo.

The partial pressures of CO_2 and O_2 are based on previous simulations.

Modeling Diagram
Anselmo shaft

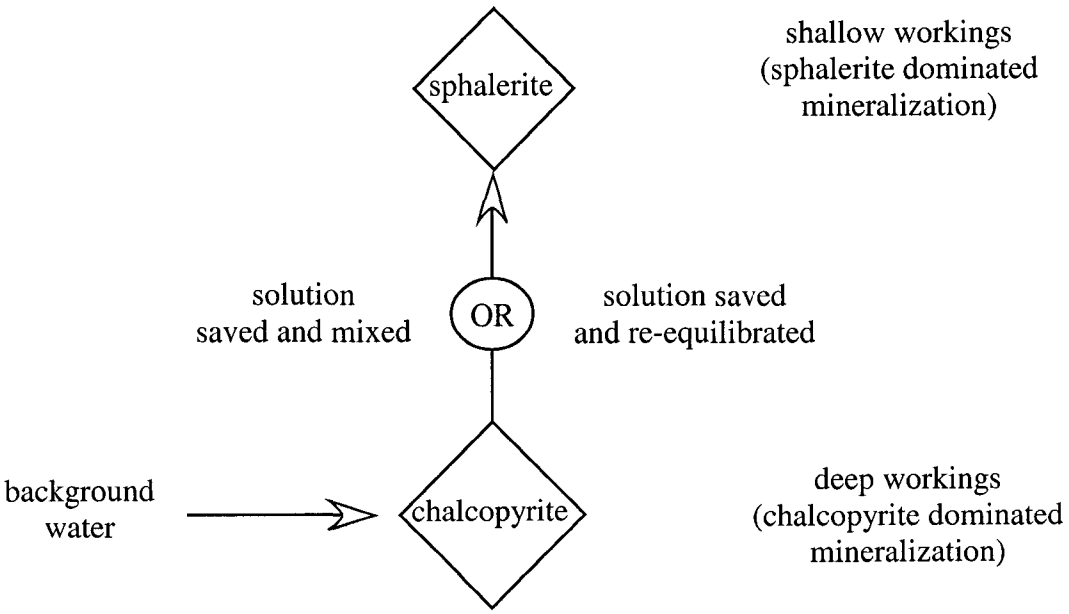

Appendix IV: Annotated listing of model input files for Kelley simulations

Mixing of precipitation plant (surface water) with late flooding water in the Kelley shaft

This model was constructed to further evaluate the influence of surface water flowing into the underground workings during the early period of flooding. Water discharging into the pit is mixed with water in the underground workings. Pre-flooding water quality is not know, but if the influence of surface water was significant, its influence would diminish with time. At some point, after water no longer flowed from the surface to the workings, the water quality of the Kelley would again reflect pre-flooding quality. To test this, waters sampled in the later period of flooding (2000) were used as an estimate of pre-flooding water quality. Complete chemistry for both waters were included in the input file and saved. Solution 1 (surface water) and shaft water (2000) were mixed at a 50:50 ratio as determined by the water balance for the first 21 months of flooding.

```
SOLUTION 1 precip plant outflow from RI
   temp      10
   pH        2.55
   pe        13.77
   redox     Fe(2)/Fe(3)
   units     mg/l
   density   1
   Al        1380
   As        136 ug/l
   Ca        385
   Cd        5.03
   Cu        350
```

Water quality for the surface water was obtained during the remidial investigation of mine flooding in 1990.

```
  Fe(2)   51
  Fe(3)   958
  K       49.6
  Mg      1640
  Mn      642
  Na      32.4
  Pb      38.6 ug/l
  Si      68.4
  S(6)    22000
  Zn      1072
  -water  1 # kg
SOLUTION 2 Kelley 2000
  temp    25
  pH      6.43
  pe      5.72
  redox   Fe(2)/Fe(3)
  units   ug/l
  density 1
  Al      2020
  As      4570
  Ca      525 mg/l
  Cd      5
  Cu      87
  Mn      64.3 mg/l
  S(6)    2600 mg/l
  Pb      2.6
  Zn      159000
  Na      34.4 mg/l
  K       27.4 mg/l
  Mg      170 mg/l
  Si      34 mg/l
  Fe(2)   294.75 mg/l
  Fe(3)   98.25 mg/l
  Alkalinity 116 mg/l
  -water  1 # kg
MIX 1
  1  0.5
  2  0.5
END
```

MBMG data for the Kelley shaft were used for the late flooding water quality.

The solutions were mixed without equilibration at a 50:50 ratio.

Equilibration model(s) for the Anselmo, Steward, and Kelley shafts

The model for the Kelley combines the components of the Anselmo and Steward mines discussed in previous sections. Each simulation represents a mineral assemblage for each mine and allows the combination or "use" of the saved solution in any of the succeeding simulations. In the example shown, simulation 6 was altered to use various prior solutions to model flow from the Steward to the Kelley. As shown, the shallow water from the Steward was used to equilibrate with Kelley minerals. In other variations, deep or intermediate Steward simulations (solutions 4 and 5, respectively) were used as the initial solution for simulation 6. The final simulation (7) was used to demonstrate the small amount of lime gained from the cement lined shaft.

SIMULATION 1

```
EQUILIBRIUM_PHASES 1 Anslemo
minerals DEEP
   Arsenolite 0 3e-009
   Chalcopyrite 0 10
   Kaolinite 0 1
   Quartz   0 1
   Rhodochrosite 0 1
SOLUTION 1 Geary well 88Q1549
   temp     14
   pH       7.32
   pe       -1
   redox    pe
   units    ppm
   density  1
   Alkalinity 211.36
   B        380 ppb
   Ca       206
```

The initial conditions are the as those used in the Anselmo model. Both shallow and deep components are simulated.

```
   Cl      42.1
   Cu      11 ppb
   F       0.66
   Fe      0.02
   K       5.6
   Mg      58.8
   Mn      0.02
   N       4.12
   Na      31.5
   As      4.5 ppb
   S(6)    714
   Si      23.3
   Zn      545 ppb
   -water  1 # kg
GAS_PHASE 1
   -fixed_pressure
   -pressure 1
   -volume 1
   -temperature 14
   CO2(g)  0.000316
   O2(g)   5e-005
SAVE solution 2
SELECTED_OUTPUT
   -file            selected1.out
   -totals          Al As Cu Fe Mn S
Zn
END
SIMULATION 2
EQUILIBRIUM_PHASES 1 Anslemo
minerals SHALLOW
   Arsenolite 0 3e-009
   Kaolinite 0 1
   Quartz  0 1
   Rhodochrosite 0 1
   Sphalerite 0 1
USE solution 2
GAS_PHASE 2
   -fixed_pressure
   -pressure 1
   -volume 1
   -temperature 14
   CO2(g)  0.316
   O2(g)   0.01
SAVE solution 3
```

```
SELECTED_OUTPUT
  -file            selected2.out
  -totals          Al As Cu Fe Mn S
Zn
END
```

SIMULATION 3

```
USE solution 3
EQUILIBRIUM_PHASES 1 Steward
minerals DEEP
  Arsenolite 0 3e-009
  Montmorillonite 0 10
  Pyrite   0 10
  Quartz   0 1
GAS_PHASE 3
  -fixed_pressure
  -pressure 1
  -volume 1
  -temperature 25
  CO2(g)   0.000316
  O2(g)    0.05
SAVE solution 4
END
```

Pyrite is used as the primary deep Steward mineral phases as based on figure 19.

SIMULATION 4

```
USE solution 4
EQUILIBRIUM_PHASES 1 Steward
minerals INTERMEDIATE
  Arsenolite 0 2e-006
  Chalcopyrite 0 10
  Montmorillonite 0 10
  Quartz   0 1
GAS_PHASE 3
  -fixed_pressure
  -pressure 1
  -volume 1
  -temperature 19
  CO2(g)   0.000316
  O2(g)    0.0008
SAVE solution 5
END
```

Chalcopyrite is used as the primary mineral for the intermediate depth of the Steward mine.

SIMULATION 5

```
USE solution 5
EQUILIBRIUM_PHASES 1 Steward
minerals SHALLOW
  Arsenolite 0 3e-009
```

As with the Anselmo, sphalerite is the dominant mineral in the shallow workings of the Steward.

```
   Montmorillonite 0 10
   Quartz   0 1
   Sphalerite 0 10
GAS_PHASE 3
   -fixed_pressure
   -pressure 1
   -volume 1
   -temperature 25
   CO2(g)   0.316
   O2(g)    0.07
SAVE solution 6
END
SIMULATION 6
USE solution 6
EQUILIBRIUM_PHASES 1 Kelley
minerals DEEP
   Arsenolite 0 2e-006
   Montmorillonite 0 3e-005
   Pyrite   0 10
   Quartz   0 1
GAS_PHASE 3
   -fixed_pressure
   -pressure 1
   -volume 1
   -temperature 19
   CO2(g)   0.316
   O2(g)    0.21
SAVE solution 7
END
SIMULATION 7
USE solution 7
GAS_PHASE 4
   -fixed_pressure
   -pressure 1
   -volume 1
   -temperature 25
   CO2(g)   0.316
EQUILIBRIUM_PHASES 2
   Lime     0 0.008
END
```

Conditions similar to that of the Anselmo are assumed for oxygen and carbon dioxide.

This simulation uses the shallow Steward water as inflow to the deep workings. Other simulations use other saved solutions

The deep Kelley mineral phases were assumed to be the same as those of the Steward.

The greater volume of workings above the water table and high observed CO_2 justified high partial pressures for both.

Lime was equilibrated with water in the shaft to demonstrate the potential effects of the cement lined shaft. The high partial pressure for CO_2 was maintaned.